

10-2 PROPERTIES OF REACTOR MATERIALS

BY

H. A. Saller (*deceased*)*

In presenting information on the properties of reactor materials, it has been found desirable to separate the various materials into groups according to their function in the reactor, for example, Fuels and Fertile Materials, Fuel Diluents and Cladding Materials, etc. For the more familiar materials, as aluminum or stainless steel, only that information pertinent to reactors is included. The bibliography gives references to detailed information on mining, fabrication, and related subjects. The lesser known materials such as uranium, thorium, and zirconium, which have been developed for reactor application, are covered in more detail, since information on these materials is not so generally available.

A brief summary of important properties of reactor materials is given in Table 1. More details for each material will be found in the various articles. Summaries of corrosion resistance to liquid metals are given in Figs. 1 and 2.

1 FUELS AND FERTILE MATERIALS

1.1 Reactor Application and Special Requirements

The operation of a reactor is dependent upon fissionable material, and these materials are certainly the most important of all reactor materials. Only slightly less important in the long run are the fertile materials—those elements which can be changed into fissionable material and thus increase our supply of reactor fuel.

Fissionable materials may be incorporated in reactors in various forms: pure metal, alloy, or a compound, that is, UO_2 or UC. The uranium may be in its natural state, or it may be enriched in the fissionable isotope uranium 235. The poor corrosion resistance and relatively low strength of uranium make it necessary to protect and strengthen the basic material in order to overcome these limiting properties. The properties of plutonium parallel those of uranium, and it must be treated similarly.

The fertile materials thorium and uranium 238 are, from a metallurgical point of view, relatively inferior materials and must also be strengthened and protected by cladding or alloying.

As nuclear properties dictate the selection of fuels and fertile materials, their limiting physical and mechanical properties must be enhanced by various techniques. An ideal fuel or fertile material would possess good thermal conductivity, good strength and ductility, radiation stability, and corrosion resistance. Uranium, thorium, and plutonium fall far short of this goal.

1.2 Uranium

1.21 Production. Abundance and Availability. Uranium makes up about 0.0004 per cent of the earth's crust and is actually more abundant than some of the more familiar metals such as cadmium, bismuth, mercury, or silver. Uranium is found in a variety of rock as a large number of minerals. The highest concentrations occur in

* The publishers and the editor-in-chief deeply regret the untimely death of Dr. Saller. They wish to thank Mr. Donald Lozier of Battelle Memorial Institute for reviewing Dr. Saller's contribution.

Table 1. General Properties of Reactor Materials*

Materials	Density, g/cm ³	Melting point, °C	Specific heat, cal/(mole)(°C)†	Thermal conductivity, cal/(sec)(cm)(°C)	Coefficient of thermal expansion, 10 ⁻⁶ per °C	Tensile strength		Modulus of elasticity 10 ⁶ psi
						Yield‡ 10 ³ psi	Ultimate 10 ³ psi	
Fuels and Fertile Materials								
Uranium.....	19.3	1133 ± 1	6.649	100°C, 0.063	25-125°C, 45.8	28	(As cast) 56	24
Thorium.....	11.71	1690 ± 10	100°C, 6.59	100°C, 0.090	30-100°C, 11.5	22.4	(As cast) 30.6	10.6
Plutonium.....	19.60	632 ± 7	See Table 2	75	(Compressive strength) 125	13-16
Uranium Oxide (UO ₂).....	10.96	2500-2600	15.38	100°C, 0.022	22-363°C, 9.3-10.8	21
Al-16 weight % U alloy.....	~650	200°C, 0.42	20-100°C, 20	8.07	17.7	10.6
Zr-4 weight % U alloy.....	6.72	1840 ± 25	100°C, 0.033	190-300°C, 6.66	50	63	14.4
Diluents and Cladding Materials								
Zirconium.....	6.50	1845 ± 25	6.31	50°C, 0.05	5.82	10-18	30-38	13.8
Zircaloy 2.....	6.55	1820 ± 25	< 0.04	20-100°C, 5.2 ± 0.6	45	65	14
Aluminum (2S).....	2.694	660.2	100°C, 6.07	0.53	20-100°C, 23.8	5	13	10.3
Beryllium.....	1.847	1315	100°C, 13.69	100°C, 0.34	25-100°C, 11.54	23	29	44
Magnesium.....	1.74	650	25°C, 6.08	18°C, 0.376	40°C, 26	Annealed, 14	Annealed, 27	Annealed, 6.5
Sintered BeO†.....	2.2-2.8	2550 ± 25	100°C, 7.7	200°C, 0.19	25-100°C, 5.5	400°C, 15	400°C, 39
Be ₂ C.....	6.24	1870	30°C, 0.02	25-200°C, 7.7	400°C, 23
SiC.....	3.21	Decomposes at 2500°C	327°C, 10.06	400°C, 0.060	0-1700°C, 4.4	1700°C, 50
MoSi ₂	6.24	1870	370°C, 0.088	0-1500°C, 5.1	27°C, 22

10-18

Solid Moderators

Graphite.....	2.27	Sublimes at 3650 ± 25°C	2.066	100°C, 0.37-0.48	20-250°C, 1.9-4.0	0.500-2.4	0.5-1.2
---------------	------	----------------------------	-------	------------------	----------------------	-------	-----------	---------

Structural Materials

Stainless steel (347).....	8.027	1427	100°C, 0.12‡	100°C, 0.037	20-100°C, 16.5	35	85	29
Inconel X.....	8.51	1395-1425	25-100°C, 0.109‡	0-100°C, 0.036	20-100°C, 11.5	Annealed, 100-120	
Molybdenum.....	10.2	2622 + 10	100°C, 6.24	0°C, 0.32	5.1	40	67	48
Titanium (commercial purity)....	4.507	1690	0-500°C, 6.61	25°C, 0.41	25°C, 8.5	70-85	85-100	15.5
Niobium.....	8.57	2415	0°C, 6.01	1200°C, 14.7	

Control Materials

10-19	Boron steel (SAE 4140 + 1.25 w/o B, annealed).....	67.3	86.4	32.5
	Cadmium.....	8.694	321	25-321°C, 6.19	0.22	20-100°C, 31.8	10.3	7.1-10
	Boron stainless steel (17-7ss + 1.25 w/o B, annealed).....	58.4	147.6	29.2
Hafnium.....	13.36	2130 ± 15	25-2227°C, 6.16	0-100°C, 5.9	40.8	67.5	14

* Compiled by the author from various sources.

† At room temperature except where temperature specified.

‡ 0.2 per cent offset.

§ Cal/(g)(°C).

¶ Thermal conductivity, strength, and the modulus of elasticity vary directly with the density; however, the coefficient of thermal expansion appears unaffected.

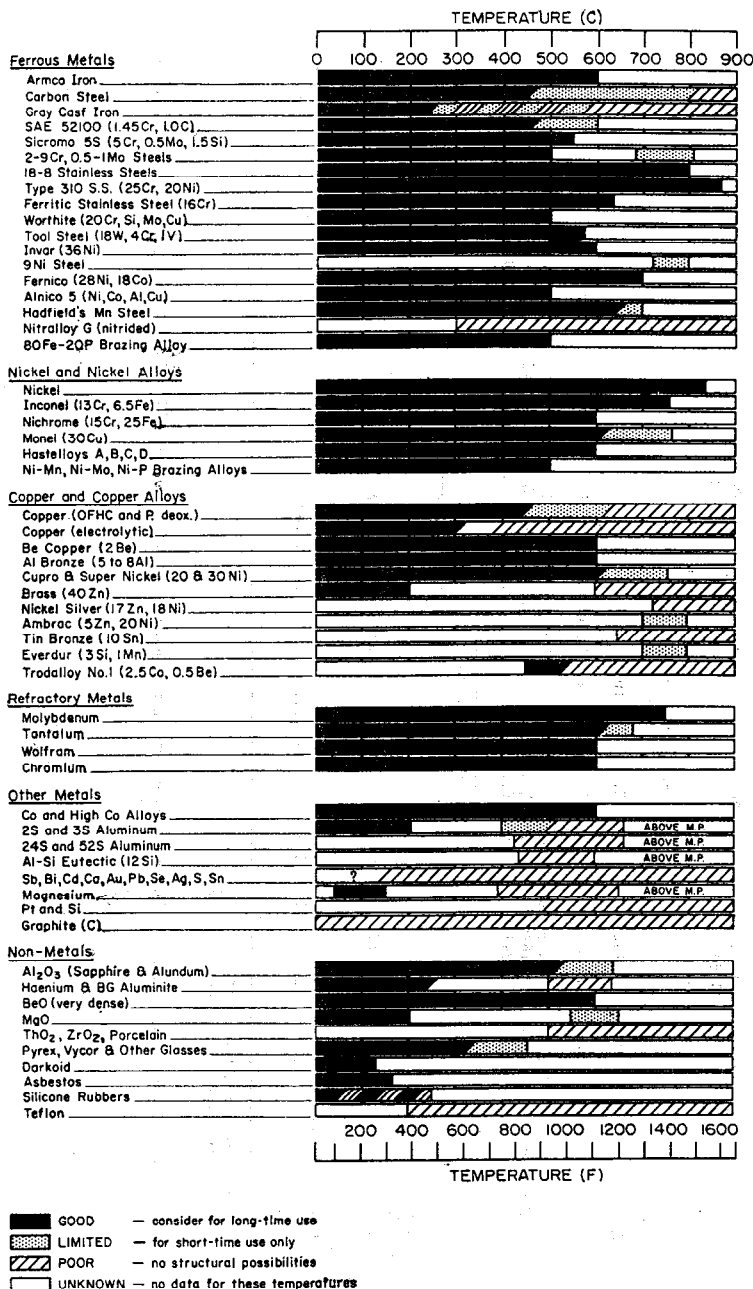


FIG. 1. Resistance of materials to attack by sodium and sodium-potassium alloys. [“Liquid Metal Handbook,” NAVEXOS P-733 (rev.), 2d ed. (revised), U.S. Atomic Energy Commission and Department of the Navy, January, 1954.]

LIQUID METAL →	MATERIAL	Hg	Nb	Ge	Bi	Bi	Sn	Bi	Pb	In	Li	Ti	Cd	Zn	Sb	Mg	Al
		°C	m.p.	m.p.	m.p.	m.p.	m.p.	m.p.	m.p.	m.p.	m.p.	m.p.	m.p.	m.p.	m.p.	m.p.	m.p.
		38.8	22.3	29.8	97	125	231.8	271.3	327	156	180.5	303	321	420	430	631	660
FERROUS METALS		97.9															
	Pure Iron	600	GOOD	GOOD	GOOD	GOOD	GOOD	GOOD	GOOD	GOOD	GOOD	GOOD	GOOD	GOOD	GOOD	GOOD	GOOD
	Carbon Steel (Low-C & Mild-C)	600	GOOD	GOOD	GOOD	GOOD	GOOD	GOOD	GOOD	GOOD	GOOD	GOOD	GOOD	GOOD	GOOD	GOOD	GOOD
	Gray Cast Iron	600	GOOD	GOOD	GOOD	GOOD	GOOD	GOOD	GOOD	GOOD	GOOD	GOOD	GOOD	GOOD	GOOD	GOOD	GOOD
	High-Cr Steel (12 to 20 Cr)	600	GOOD	GOOD	GOOD	GOOD	GOOD	GOOD	GOOD	GOOD	GOOD	GOOD	GOOD	GOOD	GOOD	GOOD	GOOD
	2-9 Cr Steel (with Ti, Mo & Si as required)	600	GOOD	GOOD	GOOD	GOOD	GOOD	GOOD	GOOD	GOOD	GOOD	GOOD	GOOD	GOOD	GOOD	GOOD	GOOD
	Low-Cr Steel (with V or Mo & Si as required)	600	GOOD	GOOD	GOOD	GOOD	GOOD	GOOD	GOOD	GOOD	GOOD	GOOD	GOOD	GOOD	GOOD	GOOD	GOOD
	Cr-Ni Austenitic Stainless (with Nb or Mo as req.)	600	GOOD	GOOD	GOOD	GOOD	GOOD	GOOD	GOOD	GOOD	GOOD	GOOD	GOOD	GOOD	GOOD	GOOD	GOOD
	High-Speed High-W Tool Steel (with Cr, Mo and V)	600	GOOD	GOOD	GOOD	GOOD	GOOD	GOOD	GOOD	GOOD	GOOD	GOOD	GOOD	GOOD	GOOD	GOOD	GOOD
	High-Nickel Steel	600	GOOD	GOOD	GOOD	GOOD	GOOD	GOOD	GOOD	GOOD	GOOD	GOOD	GOOD	GOOD	GOOD	GOOD	GOOD
NON-FERROUS METALS																	
	Aluminum	600	GOOD	GOOD	GOOD	GOOD	GOOD	GOOD	GOOD	GOOD	GOOD	GOOD	GOOD	GOOD	GOOD	GOOD	GOOD
	Bi, Ca, Cd, Pb, Sb, Sn	600	GOOD	GOOD	GOOD	GOOD	GOOD	GOOD	GOOD	GOOD	GOOD	GOOD	GOOD	GOOD	GOOD	GOOD	GOOD
	Beryllium	600	GOOD	GOOD	GOOD	GOOD	GOOD	GOOD	GOOD	GOOD	GOOD	GOOD	GOOD	GOOD	GOOD	GOOD	GOOD
	Chromium	600	GOOD	GOOD	GOOD	GOOD	GOOD	GOOD	GOOD	GOOD	GOOD	GOOD	GOOD	GOOD	GOOD	GOOD	GOOD
	Copper (with Si or Be as required)	600	GOOD	GOOD	GOOD	GOOD	GOOD	GOOD	GOOD	GOOD	GOOD	GOOD	GOOD	GOOD	GOOD	GOOD	GOOD
	Al Bronze	600	GOOD	GOOD	GOOD	GOOD	GOOD	GOOD	GOOD	GOOD	GOOD	GOOD	GOOD	GOOD	GOOD	GOOD	GOOD
	Brass, Tin, Bronze, Etc.	600	GOOD	GOOD	GOOD	GOOD	GOOD	GOOD	GOOD	GOOD	GOOD	GOOD	GOOD	GOOD	GOOD	GOOD	GOOD
	Manganese	600	GOOD	GOOD	GOOD	GOOD	GOOD	GOOD	GOOD	GOOD	GOOD	GOOD	GOOD	GOOD	GOOD	GOOD	GOOD
	Molybdenum	600	GOOD	GOOD	GOOD	GOOD	GOOD	GOOD	GOOD	GOOD	GOOD	GOOD	GOOD	GOOD	GOOD	GOOD	GOOD
	Nickel	600	GOOD	GOOD	GOOD	GOOD	GOOD	GOOD	GOOD	GOOD	GOOD	GOOD	GOOD	GOOD	GOOD	GOOD	GOOD
	Hastelloys A, B & C	600	GOOD	GOOD	GOOD	GOOD	GOOD	GOOD	GOOD	GOOD	GOOD	GOOD	GOOD	GOOD	GOOD	GOOD	GOOD
	Inconel, Nichrome and Chromel	600	GOOD	GOOD	GOOD	GOOD	GOOD	GOOD	GOOD	GOOD	GOOD	GOOD	GOOD	GOOD	GOOD	GOOD	GOOD
	Monel Metal and other Ni-Cu Alloys	600	GOOD	GOOD	GOOD	GOOD	GOOD	GOOD	GOOD	GOOD	GOOD	GOOD	GOOD	GOOD	GOOD	GOOD	GOOD
	Niobium	600	GOOD	GOOD	GOOD	GOOD	GOOD	GOOD	GOOD	GOOD	GOOD	GOOD	GOOD	GOOD	GOOD	GOOD	GOOD
	Platinum, Gold & Silver	600	GOOD	GOOD	GOOD	GOOD	GOOD	GOOD	GOOD	GOOD	GOOD	GOOD	GOOD	GOOD	GOOD	GOOD	GOOD
	Silicon	600	GOOD	GOOD	GOOD	GOOD	GOOD	GOOD	GOOD	GOOD	GOOD	GOOD	GOOD	GOOD	GOOD	GOOD	GOOD
	Stellite & Other Co-Cu Alloys with W or Mo	600	GOOD	GOOD	GOOD	GOOD	GOOD	GOOD	GOOD	GOOD	GOOD	GOOD	GOOD	GOOD	GOOD	GOOD	GOOD
	Tantalum	600	GOOD	GOOD	GOOD	GOOD	GOOD	GOOD	GOOD	GOOD	GOOD	GOOD	GOOD	GOOD	GOOD	GOOD	GOOD
	Titanium	600	GOOD	GOOD	GOOD	GOOD	GOOD	GOOD	GOOD	GOOD	GOOD	GOOD	GOOD	GOOD	GOOD	GOOD	GOOD
	Wolfram	600	GOOD	GOOD	GOOD	GOOD	GOOD	GOOD	GOOD	GOOD	GOOD	GOOD	GOOD	GOOD	GOOD	GOOD	GOOD
	Zirconium	600	GOOD	GOOD	GOOD	GOOD	GOOD	GOOD	GOOD	GOOD	GOOD	GOOD	GOOD	GOOD	GOOD	GOOD	GOOD
NON-METALS																	
	Al ₂ O ₃ & BeO (dense)	600	GOOD	GOOD	GOOD	GOOD	GOOD	GOOD	GOOD	GOOD	GOOD	GOOD	GOOD	GOOD	GOOD	GOOD	GOOD
	Graphite	600	GOOD	GOOD	GOOD	GOOD	GOOD	GOOD	GOOD	GOOD	GOOD	GOOD	GOOD	GOOD	GOOD	GOOD	GOOD
	MgO (porous)	600	GOOD	GOOD	GOOD	GOOD	GOOD	GOOD	GOOD	GOOD	GOOD	GOOD	GOOD	GOOD	GOOD	GOOD	GOOD
	Porcelain & Other Silicate Refractories	600	GOOD	GOOD	GOOD	GOOD	GOOD	GOOD	GOOD	GOOD	GOOD	GOOD	GOOD	GOOD	GOOD	GOOD	GOOD
	Pyrex Glass	600	GOOD	GOOD	GOOD	GOOD	GOOD	GOOD	GOOD	GOOD	GOOD	GOOD	GOOD	GOOD	GOOD	GOOD	GOOD
	TiO ₂ & ZrO ₂	600	GOOD	GOOD	GOOD	GOOD	GOOD	GOOD	GOOD	GOOD	GOOD	GOOD	GOOD	GOOD	GOOD	GOOD	GOOD
	Quartz (fused SiO ₂)	600	GOOD	GOOD	GOOD	GOOD	GOOD	GOOD	GOOD	GOOD	GOOD	GOOD	GOOD	GOOD	GOOD	GOOD	GOOD
LIQUID METAL →																	
		Hg	Nb	Ge	Bi	Bi	Sn	Bi	Pb	In	Li	Ti	Cd	Zn	Sb	Mg	Al
		°C	m.p.	m.p.	m.p.	m.p.	m.p.	m.p.	m.p.	m.p.	m.p.	m.p.	m.p.	m.p.	m.p.	m.p.	m.p.

DEGREE OF RESISTANCE
 ■ GOOD - Consider for long-time use
 ■ LIMITED - For short-time use only
 ■ POOR - No structural possibilities
 ■ UNKNOWN - No data for these temperature

*Materials were tested at the melting points of these metals

FIG. 2. Corrosion resistance of various materials to liquid metals. ("Liquid Metal Handbook," NAVeoz P-733 (rev.), 2d ed., U.S. Atomic Energy Commission and Department of the Navy, January, 1954.)

Table 2. Physical Constants of Uranium, Uranium Oxide, Thorium, and Plutonium*

	Uranium	Uranium oxide, UO ₂	Plutonium	Thorium
Density, g/cm ³	Theoretical α 19.3 γ 18.04	Theoretical 10.96	25°C, α 19.8 β 17.8	Theoretical α 11.71
Density, g/cm ³	Wrought material 18.5-19.0	Reduction of UO ₂ by H ₂ 500°C 10.86	Liquid, 665°C, 16.54 ± 0.08	β ~ 11.1 at 1400°C Cast 11.55-11.63
Density, g/cm ³	Pressed and sin- tered powder 18.9	Mallinckrodt powder, tapped 10.28	Arc-melted iodide 11.66
Melting point, °C...	1133 ± 1	2500-2600	632 ± 7	1690 ± 10
Boiling point, °C.....	3900	>3000
Heat of fusion, kcal/mole.....	2.5-3.0	4.6
Heat of vaporization, kcal/mole.....	93	137	80.46 ± 0.34	130
Specific heat, cal/(mole)(°C)	-249, 28°C, 1.211 -201.61°C, 4.657 -149.70°C, 5.639 -99.57°C, 6.053 -0.16°C, 6.524 27°C, 6.649 227°C, 7.606 427°C, 8.952 627°C, 11.107 774(β)°C, 10.147 774(α)°C, 9.177 827°C, 9.147 727°C, 8.337 827°C, 10.430	-258°C, 0.378 -253°C, 0.968 -248°C, 2.270 -243°C, 5.150 -238°C, 2.425 -233°C, 2.637 -223°C, 3.365 -173°C, 6.958 -123°C, 10.07 -73°C, 12.47 -23°C, 14.17 +27°C, 15.38 H _T -H _{298.15} 400°C, 1.680 600°C, 5.340 800°C, 9.250 1000°C, 13.280 1200°C, 17.420 1400°C, 21.620	99.3°C, 6.59 198.7°C, 6.61
Enthalpy (H _T).....
Entropy	27°C, 12.052 127°C, 13.941 227°C, 15.601 327°C, 17.056 427°C, 18.387 527°C, 19.646 627°C, 20.882 727°C, 22.760 827°C, 24.761	25°C, 13.6 ± 0.8
Electrical resistivity, μohm-cm	20°C, 29.4 × 10 ⁶ 100°C, 35.1 × 10 ⁶ 200°C, 41.4 × 10 ⁶ 300°C, 46.7 × 10 ⁶ 400°C, 50.8 × 10 ⁶ 500°C, 54.1 × 10 ⁶ 600°C, 56.3 × 10 ⁶	20°C, 12.7 × 10 ³ ohm-cm	25°C, 150 200°C, 116 300°C, 110 400°C, 102 500°C, 120	20°C, 18
Thermal conduc- tivity, cal/(sec) (cm)(°C)	20°C, 0.057 100°C, 0.061 200°C, 0.066 300°C, 0.071 400°C, 0.077 500°C, 0.082 600°C, 0.088 700°C, 0.094 725°C, 0.096	Density 10.9 g/cm ³ 100°C, 0.022 200°C, 0.019 400°C, 0.014 600°C, 0.011 800°C, 0.009 1000°C, 0.008	100°C, 0.090 650°C, 0.108
Thermal expansion, 10 ⁻⁴ /°C	(See Table 3)	22-363°C, 9.3-10.8	Alpha Pu, α55 β35	30-100°C, 11.5 30-500°C, 11.9 30-1000°C, 12.5

* Compiled by the author from various sources.

igneous rocks with much lesser amounts found in sedimentary rocks (sandstones). Uranium has been found in sea water, river water, and living organisms.

Pitchblende (UO_2) is the richest of the uranium ores but accounts for a relatively small amount of the uranium production. The bulk of the uranium now produced comes from ores containing relatively low amounts (about 0.25 per cent U_3O_8) of uranium. The uranium occurs in these deposits as uraninite (UO_2) or in combination with vanadium in a mixture of carnotite [$\text{K}(\text{UO}_2)_2(\text{VO}_4)_2 \cdot 3\text{H}_2\text{O}$] and roscoelite [$\text{H}_8\text{K}_2(\text{Mg},\text{Fe})(\text{Al},\text{V})_4(\text{SiO}_3)_{12}$].

Most of the foreign production of uranium comes from the pitchblende deposits at Great Bear Lake in Canada or the Belgian Congo in Africa and from low-grade uraninite deposits at El Dorado in Canada and in South Africa. The South African ore represents tailings from a gold-recovery operation involving the cyanide process.

Domestically, uranium occurs as low-grade carnotite and roscoelite in Colorado and Utah. Less extensive deposits of uraninite occur in several other states.

Extraction and Purification. The relatively high-grade pitchblende is frequently concentrated by mechanical processes prior to extraction of the uranium by chemical methods. Low-grade ores are treated directly by either an acid leach or an alkaline leach process. The final product of any of these methods is U_3O_8 of varying degrees of purity.

Metal Preparation. The production of metallic uranium is made difficult by its extreme chemical activity with the atmosphere, most of the ceramic materials, and other metals. Historically a number of techniques involving reduction of the oxides or halides with aluminum, carbon, and the alkali metals were investigated. Efforts are now concentrated on the reduction of the halides by the alkali metals. For some applications requiring metal of unusual purity an electrolytic process involving uranium halides is used.

1.22 Physical Constants. A number of the physical constants for uranium, uranium oxide (UO_2), plutonium, and thorium are listed in Tables 2 and 3. More complete data on uranium may be found in the volume "Chemistry of Uranium," by Katz and Rabinowitz.^{1,*}

Table 3. Thermal Expansion of Uranium*

From X-ray data, parallel to axis	Linear thermal expansion, $10^{-6}/^\circ\text{C}$		
	25-125°C	25-325°C	25-650°C
(100)	21.7	26.5	36.7
(010)	-1.5	-2.4	-9.3
(001)	23.2	23.9	34.2
Volume	45.8	48.6	61.5
(100) $l_t = l_{27^\circ\text{C}} (1 + 17.2 \times 10^{-6}t + 30.8 \times 10^{-9}t^2)$			
(010) $l_t = l_{27^\circ\text{C}} (1 - 9.2 \times 10^{-6}t + 40.4 \times 10^{-9}t^2 - 67.5 \times 10^{-12}t^3)$			
(001) $l_t = l_{27^\circ\text{C}} (1 + 25.1 \times 10^{-6}t - 21.3 \times 10^{-9}t^2 + 57.5 \times 10^{-12}t^3)$			
Volume $V_t = V_{27^\circ\text{C}} (1 + 45.0 \times 10^{-6}t - 3.4 \times 10^{-9}t^2 + 5.0 \times 10^{-12}t^3)$			

* Based on data of C. M. Schwartz and D. A. Vaughn, Battelle Memorial Institute.

There is another type of material that is fissionable about which much less is known. This type includes compounds of uranium other than the oxide. Such elements are potentially useful in reactors as uranium-bearing material in a matrix of a strong, corrosion-resistant metal such as zirconium or stainless steel. Some properties of these compounds are listed in Table 4.

1.23 Transformations and Crystallography. Uranium metal exhibits three crystalline forms. The α phase, which exists up to 640°C , is orthorhombic with 30 atoms per unit; cell dimensions are $a_0 = 2.854 \text{ \AA}$, $b_0 = 5.867 \text{ \AA}$, and $c_0 = 4.957 \text{ \AA}$. The β phase exists between 660 and 760°C . Its crystal structure is tetragonal with 30 atoms per cell. Cell dimensions are $a_0 = b_0 = 10.590 \text{ \AA}$ and $c_0 = 5.634 \text{ \AA}$. The

* Superscript numbers refer to References at end of subsection.

γ phase, which is tetragonal, exists from 760°C up to the melting point. Its structure is body-centered cubic with $a_0 = 3.474$ Å.

1.24 Health Hazards. Uranium constitutes a health hazard both from whole body radiation and from inhalation of its dusts. Health-physics groups of the various laboratories and the Atomic Energy Commission are in a position to give competent advice on this problem.

1.25 Mechanical Properties. Values for a number of mechanical properties of uranium are given in Tables 5 through 13. It will be noted that many of the results are based on a single experiment. The technology of uranium is not sufficiently mature to have built up a large number of accepted average values for the various properties.

Table 4. Properties of Uranium Compounds*

Compound	Structure	Density, g/cm ³	Decomposition temperature, °C
UO ₂	Cubic	10.96	~2175
UC	fcc	13.63	~2250
UC ₂	bc tetragonal	11.68	2480
UN	fcc	14.32	~2630 ± 50
UAl ₂	fcc	8.14-8.38	1590
UAl ₃	Simple cubic	6.8	1350
UAl ₄	Orthorhombic	5.7 ± 0.3	730
U ₃ Si ₂ †	Tetragonal	12.20	1665
USi	Orthorhombic	10.4	1575
USi ₂	Hexagonal	9.25 β	1700
U ²³⁸ Si ₂ †	Tetragonal	8.98 α	1610
USi ₃	Simple cubic	8.15	1510
U ₃ Fe	bct	17.7	815
UFe ₂	fcc	13.21	1235
UCu ₅	fcc	10.60	1052
U ₆ Ni	bct	17.6	780
UNi	Too complex for present identification	810
UNi ₂	Hexagonal	13.46	985
UNi ₃	fcc	11.31	1295
UBe ₁₃	fcc	4.37	~2027
U ₂ Ti	Hexagonal	15.22	~870
U ₆ Mn	bct	17.8	726
UMn ₂	fcc	12.57	1120

* Compiled from H. A. Saller and F. A. Rough (eds.), "Compilation of U.S. and U.K. Uranium and Thorium Constitutional Diagrams," Battelle Memorial Institute, June 1, 1955.

† These formulas have been identified by X-ray study but are frequently still referred to on constitutional diagrams as U₃Si₂ and U₂Si₃, respectively.

Table 5. The Effect of Carbon Content on the Tensile Properties of Uranium*†

Carbon content, ppm	Total impurities, ppm	0.2% offset yield strength, 10 ³ psi	Ultimate strength, 10 ³ psi	Elongation in 2 in., %	Modulus, 10 ⁶ psi
60	260	20	52	8	23
210	410	22	53	8	24
360	525	28	59	8	23
550	650	29	72	11	25
630	815	28	75	17	24
710	1,000	28	70	12	23
820	925	25	62	9	30
1,250	1,800	25	74	10	24

* Based on data from Los Alamos Scientific Laboratory.

† All specimens cut from cast plates and pulled in as-cast condition; specimens were standard 0.505-in. rounds.

Table 6. Tensile Properties of Uranium at Elevated Temperatures*

Specimen†	Test temperature, °F	0.2% offset yield strength, psi	Ultimate strength, psi	Elongation, %
570°F rolled:				
α-annealed‡	Room	43,300	111,100	6.8
β-annealed¶	Room	24,550	63,800	8.5
1110°F rolled:				
α-annealed	Room	26,000	88,400	13.5
β-annealed	Room	24,600	61,700	6.0
570°F rolled:				
α-annealed	570	17,500	35,200	49.0
1110°F rolled:				
α-annealed	570	18,800	31,570	43.0
β-annealed	570	15,300	26,900	33.0
570°F rolled:				
α-annealed	930	5,100	11,130	61.0
β-annealed	930	7,100	10,500	44.0
1110°F rolled:				
α-annealed	930	5,450	10,450	57.0

* Compiled from data of G. T. Muehlenkamp and A. D. Schwobe, Battelle Memorial Institute, unpublished information.

† All specimens were standard 0.505-in. rounds.

‡ Alpha anneal is 12 hr at 1110°F, slow-cooled.

¶ Beta anneal is 12 hr at 1290°F, slow-cooled.

Table 7. Low-temperature Tensile Properties of Commercial Uranium* in Various States of Heat Treatment†

Heat treatment	Test temperature, °F	0.2% offset yield strength, 10 ³ psi	Ultimate strength, 10 ³ psi	Reduction in area, %	Elongation in 2 in., %	Modulus of elasticity, 10 ⁸ psi	Poisson's ratio
As cast	75	28	56	10	4	24	0.21
	-50	28	47	4	3	26	
	-100	27	42	3	3	26	
As α-rolled (1020°F)	75	31	96	10	11	25	0.22
	-50	40	109	4	4	24	
	-100	37	87	4	3	23	
α-rolled and γ-annealed (1560°F)	75	26	57	10	5	21	0.18
	-50	27	43	4	3	31	
	-100	17	36	5	3	26	
α-rolled and β-quenched (1335°F)	75	36	84	12	9	24	0.24
	-50	40	92	6	5	27	
	-100	42	88	5	4	30	
α-rolled, β-quenched (1335°F), and α-annealed (1020°F)	75	32	90	12	12	22	0.19
	-50	33	83	5	5	31	
	-100	37	89	6	6	27	

* All specimens were standard 0.505-in. rounds.

† Based on unpublished data of S. J. Paprocki, Battelle Memorial Institute.

1.26 Manufacture. Melting and Casting. The chemical activity of uranium with the atmosphere makes melting and casting by ordinary techniques impractical. In induction melting, the use of vacuum, inert atmosphere, or protective flux or slag with graphite crucibles yields ingots of good quality of almost any size and shape.

For special applications where high purity is desirable or for some alloys, arc melting

Table 8. Young's Modulus, Shear Modulus, and Poisson's Ratio for Uranium in Various Conditions of Fabrication*

Condition	Young's modulus, 10 ⁶ psi†	Shear modulus, 10 ⁶ psi	Poisson's ratio
Swaged and annealed.....	29.1	11.9	0.22
γ-extruded.....	29.3	12.0	0.21
γ-extruded.....	30.3	12.1	0.25
Cast.....	29.5	12.1	0.22
Cast.....	30.0	12.1	0.24
Average.....	29.7	12.1	0.23

* Data by Henry L. Laquer, Los Alamos Scientific Laboratory, unpublished information.

Table 9. Compression Tests on Uranium*

Material	Test temperature, °F	0.5% offset yield strength, 10 ² psi	Deforma- tion at propor- tional limit, in.	Deforma- tion at yield strength, in.	Deforma- tion at 120,000 psi, in.	Modulus in comp- ression, 10 ⁶ psi
Normal uranium, as cast (500 ppm carbon, 700 ppm total impurities)	-5	85	0.016	0.080	0.174	2.6
	75	111	0.044	0.070	0.083	5.3
	300	86	0.034	0.080	0.153	3.0
	390	81	0.017	0.084	0.176	2.2
	480	60	0.018	0.086	0.290	1.7
570	48	0.022	0.092	0.364	1.2	
Normal uranium, α-rolled (600 ppm carbon, 1,000 ppm total impurities)	-5	90	0.036	0.133	0.205	1.1
	300	87	0.034	0.081	0.142	3.0
	390	63	0.013	0.077	0.205	2.2
	480	67	0.018	0.089	0.264	1.7
	570	42	0.023	0.110	0.427	0.7

* Data from Los Alamos Scientific Laboratory, unpublished information.

Table 10. Hardness of Alpha-rolled Uranium*†

Scale	Transverse specimen	Longitudinal specimen
Rockwell B.....	97	98
Rockwell G.....	80.5	83
Vickers diamond (10- to 15-kg load).....	220	240
Vickers diamond (30- to 45-kg load).....		250
Brinell (calculated from <i>R_B</i>).....	240	260
Brinell (calculated from <i>R_α</i>).....	250	280
Knoop (200-g load).....	260	320
Knoop (500-g load).....	250	300
Knoop (1,000-g load).....	240	320
Eberbach (263-g load).....	270	300
Eberbach (645.6-g load).....	260	290

* From J. J. Katz and E. Rabinowitz, "The Chemistry of Uranium," part I. NNES, Div. VIII, vol. 5, McGraw-Hill Book Company, Inc., New York, 1951.

† All readings taken on the same sample.

is used successfully. Either an inert electrode (graphite, tungsten, or molybdenum) or a consumable uranium electrode can be utilized. This latter technique produces metal of unusual purity.

Forming and Fabrication. Uranium metal is reasonably ductile and can be fabricated by standard metallurgical techniques. Hot fabrication is normally carried out at α-range temperatures. Fabrication in the β phase is possible but very difficult

because of the close temperature control required. Gamma-phase uranium is too soft and plastic for fabrication by techniques other than extrusion. In the α range fabrication by extrusion, forging, rolling, pressing, and swaging is accomplished readily. Because of the reactivity of uranium with air, heating is performed in an inert atmosphere or other protective media. Uranium can be fabricated at room

Table 11. Charpy Impact Strength of Uranium*

Temperature, °F	Impact strength, ft-lb					
	α -rolled†	Forged‡	As cast†	β -quenched†	β -quenched, α -annealed†	γ -annealed†
-290	5	4				
-100	6	...	8	5	6	8
-75	8	...	10	6	7	8
-50	10	...	12	7	7	10
-25	10	...	12	7	8	11
0	12	...	12	8	9	13
50	14	...	13	9	10	16
75	14	6	14	11	12	16
100	15	...	15	12	14	17
150	18	...	17	15	20	22
200	25	...	23	18	27	28
300	32	11	27	29	52	50
390	...	18				
480	57	36				
570	76	70				
610	...	85				
615	85					
645	...	102				
750	109					

* Compiled from data of Eric Jette, Los Alamos Scientific Laboratory, and S. J. Paprocki, Battelle Memorial Institute, unpublished information.

† Normal purity.

‡ High-purity material: 240 ppm carbon, 333 ppm total impurities.

Table 12. The Shear Strength of Uranium*†

Condition‡	Shear strength, 10 ³ psi		
	1/8-in. diam	1/4-in. diam	3/8-in. diam
As cast.....	85	84	75
Cold-swaged¶.....	127	114	95
Cold-swaged as above and annealed at 1100°F.....	83	88	80
Rolled at 1110°F.....	80	79	77
Rolled 62½% at 1110°F and rolled 68% at 615°F.....	113	95	
Rolled as above and annealed at 1110°F.....	83	88	81

* Data of Eric Jette, Los Alamos Scientific Laboratory, unpublished information.

† Normal uranium 430 ppm carbon, 613 ppm total impurities.

‡ All samples tested at room temperature.

¶ 1/8-in. specimen, 94 per cent; 1/4-in. specimen, 75 per cent; 3/8-in. specimen, 44 per cent.

temperature by drawing, rolling, swaging, or pressing. Frequent annealing during cold fabrication is desirable.

Powder Metallurgy. Uranium is amenable to powder-metallurgical techniques. A good grade of uranium powder is produced by first treating the metal in hydrogen at about 450°F to produce the hydride. This hydride is then decomposed by heating in vacuum at around 900°F. Metal compacts of the desired shape can be produced either by cold pressing and sintering or by hot pressing. Uranium compacts of good

quality can also be produced directly from the hydride by cold pressing and vacuum sintering or hot pressing in a vacuum.

Joining. Uranium can be welded using the Heliarc process and the shielded-arc consumable-electrode process. Again, the principal problem lies in the reactivity of uranium with the atmosphere. Brazing is made difficult both by the reaction with the atmosphere and by the formation of brittle intermetallics between uranium and brazing alloys. It is possible to join uranium by first plating the uranium with silver or nickel and then joining the silver or nickel by conventional brazing methods.

Table 13. Creep of Uranium at 930°F*

Annealing history	Stress, psi	Time, hr	Total deformation, %	Minimum secondary creep rate, %/hr	Grain size after test, mm
Rolled at 1100°F, 10 hr at 1290°F, and 10 hr at 1110°F	2,750	1,530	3.72	0.0025	0.12-0.13 0.10-0.11
	2,220	1,200	2.20	0.0013	
	1,720	1,700	0.82	0.0003	
	1,500	1,515	0.85	0.00035	
Rolled at 1100°F, 10 hr at 1110°F...	2,220	1,200	4.72	0.0018	0.045-0.05
	1,720	1,350	1.92	0.0009	0.05-0.055

* Data of G. T. Muehlenkamp and F. R. Shober, Battelle Memorial Institute, unpublished information.

Machining. Uranium can be machined by most of the conventional methods provided some special precautions are taken. It is advisable to use heavy cuts and high speeds. A coolant must be used both as a health measure and in order to prevent burning of the chips or even the machined piece.

1.27 Corrosion Behavior. Uranium has very poor corrosion resistance in either air or water and thus must be protected by means of cladding or plating for reactor application. Figures 3 through 6 show corrosion rates in air, steam, hydrogen-saturated water, and distilled water.

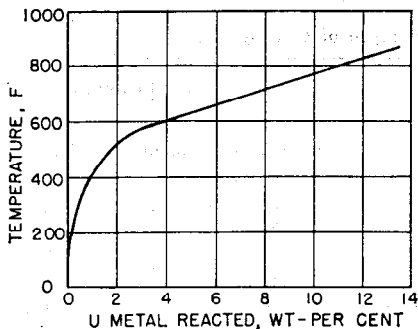


FIG. 3. The oxidation of uranium in air for 4-hr periods from 68 to 930°F.*

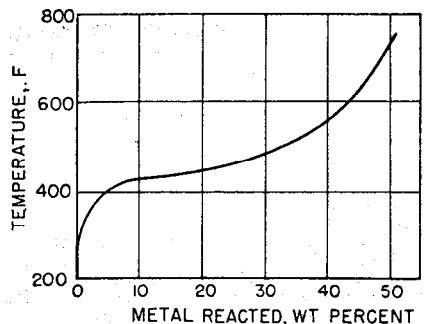


FIG. 4. The action of steam on uranium at various temperatures.*

Uranium and sodium in contact for long periods of time at 550°C show no evidence of reaction; however, uranium must be protected by means of cladding or plating when in contact with either air or water in reactor application.

Protective Techniques. The poor corrosion resistance of uranium in reactor coolants has encouraged the development of protective techniques. After the use of extensive cleaning procedures, uranium can be electroplated with a number of metals, using conventional plating baths; however, protection by plating is often precarious. Uranium has been clad with a number of metals by means of roll cladding.

* Reprinted from T. Wathen, Corrosion of Uranium Metal in Air and Steam at Various Temperatures, BR-223-A, May 13, 1943.

1.28 Alloys. The need to improve corrosion resistance and strength of uranium has led to considerable interest in alloying. A large number of binary systems have been investigated in some detail.²

Uranium alloys might be grouped as systems containing several intermetallic compounds and those having no true compounds. This latter group may be subdivided further into systems showing limited solid solubility and those showing considerable solid solubility.

Many elements form one or more compounds with uranium. Such systems have limited solid solubility in the terminal phases. Compound-forming elements whose diagrams are well defined include aluminum, beryllium, bismuth, carbon, cobalt, copper, gold, iron, lead, manganese, mercury, nickel, silicon, and tin. Other elements, including boron, hydrogen, oxygen, and nitrogen, form compounds, but their constitutional diagrams are not completely defined.

Several elements when alloyed with uranium do not produce intermetallic compounds or show any appreciable solid solubility in the terminal phases. Such systems contain eutectic, peritectic, or monotectic reactions. Uranium-chromium and uranium-vanadium follow the simple eutectic system. A peritectoid reaction characterizes the uranium-tantalum and uranium-tungsten systems. Thorium, silver, magnesium, and cerium form monotectics with uranium. Elements of another group when added to uranium produce alloys with extensive solid solubility at elevated temperatures but no true intermetallic compound. Both zirconium and titanium form this type of alloy. Molybdenum behaves similarly except that solid solubility is not complete at elevated

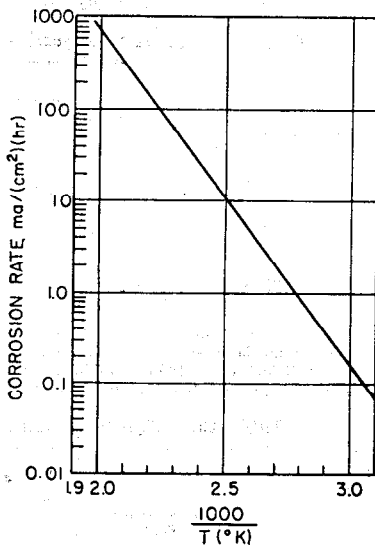


FIG. 5. The corrosion rate of uranium in hydrogen-saturated water versus $1/T$.*

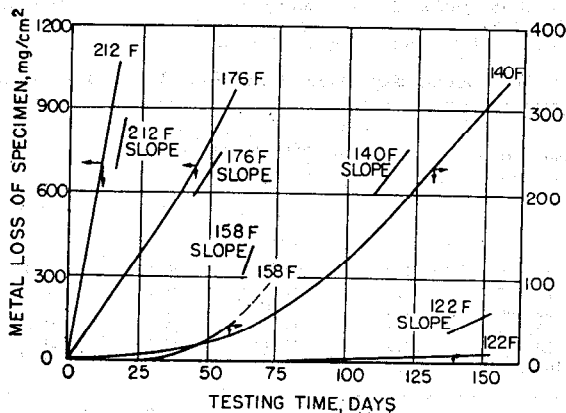


FIG. 6. Corrosion of uranium in aerated distilled water.*

temperatures. The uranium-niobium system is similar but contains no intermediate phase as found in the others. The intermediate phase found in uranium-zirconium, uranium-molybdenum, and uranium-titanium systems is formed from a metastable γ phase. Since it is ductile, it is not considered a true intermetallic compound.

* Reprinted from W. A. Mollison, et al., Corrosion of Tuballoy in Distilled Water, University of Chicago, CT-3055, June 23, 1945.

A number of the compound-forming elements are useful in improving the mechanical properties of uranium when added in small quantities. Large additions of such elements merely form brittle compounds. The greatest improvements in high-temperature mechanical properties are likely in the solid-solution systems. These would include alloys with molybdenum, niobium, titanium, and chromium.

Table 14. Tensile Properties of Forged Uranium-Aluminum Alloys*

Uranium content, weight %	Average modulus of elasticity, † 10 ⁶ psi	Tensile strength, 10 ³ psi	0.2% offset yield strength, 10 ³ psi	Elongation, %	Reduction of area, %
0	10.0	13.0	5.0	45	
12.5	10.4	22.5	10.8	20	34
22.7	10.9	18.6	11.6	4	7
22.7	11.3	23.5	14.5	13	14
30.5	11.3	26.1	14.9	10.5	11.5

* From H. A. Saller, "Preparation, Properties, and Cladding of Aluminum-Uranium Alloys," Battelle Memorial Institute, published at the International Conference on Peaceful Uses of Atomic Energy, UN-562, USA, 1955. Single specimens were used except in the 22.7 per cent uranium alloy.

† Estimated to be correct within ± 3 per cent.

Table 15. Thermal Conductivity of Uranium-Aluminum Alloys*

Temperature, °C	Thermal conductivity, cal/(sec)(cm)(°C), † of indicated uranium content, weight %		
	12.5	22.7	30.5
200	0.44	0.40	0.36
300	0.43	0.39	0.36
400	0.43	0.38	0.35

* From H. A. Saller, "Preparation, Properties, and Cladding of Aluminum-Uranium Alloys," Battelle Memorial Institute, published at the International Conference on Peaceful Uses of Atomic Energy, UN-562, USA, 1955.

† $\text{Cal}/(\text{sec})(\text{cm})(^\circ\text{C}) \times (2.419 \times 10^3) = \text{Btu}/(\text{hr})(\text{ft})(^\circ\text{F})$.

Table 16. Linear Expansion of Uranium-Aluminum Alloys*

Temperature range, °C	Coefficient of linear thermal expansion, 10 ⁻⁶ /°C uranium content, weight %			
	0†	12.5	22.7	30.5
20-100	23.9	20.0	20.0	19.4
20-200	24.6	21.1	21.2	20.8
20-300	25.5	22.1	21.9	21.3
20-400	26.5	23.1	22.5	21.6
20-500	27.7	23.5	22.7	22.1
100-500	24.4	23.2	22.6

* Compiled by the author from the "ASM Metals Handbook," 1948 edition, and unpublished information of Battelle Memorial Institute, 1952.

† "Metals Handbook," 1948.

The greatest improvement in corrosion properties is found again in the solid-solution-type alloys. Small alloy additions, which produce supersaturated solutions of α uranium, are helpful initially, but these alloys may lose their enhanced corrosion resistance on aging. Somewhat larger alloy additions, which will produce a super-

saturated γ phase, are even more helpful. Unfortunately, such alloys may transform and lose their corrosion resistance. Stable alloys of the intermediate phase may offer the most promise for corrosion resistance.

A few intermetallic compounds such as U_3Si have shown excellent corrosion resistance. The use of such compounds is limited considerably by their lack of fabricability.

Table 17. High-temperature Properties of Uranium-Aluminum Alloys*†

Alloy	Temperature, °F	Tensile strength, 10^3 psi	0.2% offset yield strength, 10^3 psi	Elongation, %	Reduction in area, %
2S-O aluminum.....	Room	13.0	5.0	45‡	
	300	7.5	3.5	65	
	570	2.5	90	
11.3 weight % uranium.....	Room	19.7	11.3	28	
	Room	20.1	11.5	28	
	300	14.1	9.2	31	
	300	14.7	10.0	27	
	570	8.6	31	57
	570	8.8	34	60
17.3 weight % uranium.....	Room	19.0	8.6	30	
	300	14.0	7.2	34	
	300	13.7	7.0	35	
	300	13.3	6.5	35	
	570	8.1	48	59.5
	570	8.2	42	58

* Data compiled by the author from various sources.

† Tests in metal annealed at 700°F for 1 hr; 2S-O values from "Alcoa Aluminum and Its Alloys."

‡ Elongation in 2 in., others in 1 in.

Table 18. Densities of Uranium-Zirconium Alloys*

Uranium content, weight %	Density, g/cm ³	
	Arc-melted and rolled alloys	Pressed and sintered alloys
0	6.54	6.59
2	6.64	
4	6.72	6.76
6	6.83	
8	6.91	
10	6.99	
12	7.07	
14	7.16	7.24
16	7.20	
60	10.40	

* H. A. Saller and F. A. Rough, "The Alloys of Uranium," Battelle Memorial Institute, International Conference on Peaceful Uses of Atomic Energy, UN-558, USA, 1955.

The selection of an alloying element as a diluent for enriched uranium in a power reactor is based principally on nuclear rather than metallurgical reasons. This is shown by the interest in the low-cross-section metals zirconium, aluminum, and beryllium as diluents for thermal reactors. When nuclear properties are about equal, fabricability and physical properties become the important criteria.

Important properties of the fuel-element alloys uranium-aluminum and uranium-zirconium are given in Tables 14 through 20.

Table 19. Tensile Properties of Arc-melted Uranium-Zirconium Alloys at 370°C*

Zirconium content, weight %	0.2% offset yield strength, psi	Tensile strength, psi	Elongation in 2 in., %	Reduction in area, %
0	21,300	31,400	27.0	57.0
2.4	35,100	48,400	17.0	49.0
5.5	50,500	77,000	10.0	25.0
11.5	100,800	122,800	8.0	29.0
20.5	124,000	135,200	8.0	18.0
31.4	112,000	145,200	7.0	7.0
41.7	97,000	115,300	8.0	13.0
50.5	68,100	96,100	22.0	28.0
60.6	63,800	97,800	22.0	20.0
70.4	64,800	86,400	20.0	27.0
80.0	72,000	77,900	5.0	22.0
89.4	53,200	64,200	7.0†	11.0†
100.0	8,500	17,300	42.0	

* H. A. Saller and F. A. Rough, "The Alloys of Uranium," Battelle Memorial Institute, International Conference on Peaceful Uses of Atomic Energy, UN-558, USA, 1955.

† Specimens broke in what appeared to be rolling defects.

Table 20. Thermal Conductivity of Uranium-Zirconium Alloys*

Temperature, °C	Conductivity, watts/(cm)(°C), by composition, weight % uranium†									
	100‡	95	80	60	50	30	22	14	3	0
20	0.260	0.193	0.106	0.068	0.053	0.090	0.097	0.110	0.140	0.208
100	0.270	0.209	0.125	0.077	0.066	0.100	0.106	0.116	0.142	0.198
200	0.285	0.230	0.148	0.096	0.084	0.110	0.117	0.123	0.144	0.188
300	0.306	0.254	0.172	0.118	0.104	0.120	0.130	0.130	0.147	0.182
400	0.330	0.279	0.197	0.139	0.127	0.140	0.144	0.179
500	0.360	0.307	0.224	0.167	0.153	0.160	0.161	0.178
600	0.393	0.338	0.253	0.200	0.183	0.180	0.187	0.178
700	0.431	0.370	0.282	0.240	0.216	0.210	0.220	0.185
800	0.475	0.406	0.313	0.286	0.252	0.250				
900	0.522	0.443	0.344	325	0.290	0.290				

* Compiled from data of H. W. Deem and R. A. Winn, Battelle Memorial Institute, unpublished information, 1955.

† Arc-melted crystal bar zirconium.

‡ 100 per cent uranium heat-treated 24 hr at 575°C. All other compositions were treated 1 hr at 800°C, 1 hr at 500°C, air-cooled.

1.3 Thorium

1.31 Production. *Abundance and Availability.* While thorium makes up 0.0012 per cent of the earth's crust, it is very widely distributed and much of it cannot be mined. Actually, the workable deposits of uranium exceed those of thorium. The common thorium mineral is monazite $(CeLaDi)PO_4 \cdot ThSiO_4$. Large deposits are found in India, Brazil, and Africa. Lesser deposits occur in Oregon, North and South Carolina, and Florida.

Extraction and Purification. Several methods for extraction of thorium compounds from monazite sand are available. The sand may be treated with excess concentrated sulfuric acid to form a thick paste. This paste is slowly stirred into excess water and allowed to settle. The solution contains the bulk of the thorium and rare earths, perhaps as phosphate complexes. The thorium is then separated from this solution by partial neutralization, which causes fractional precipitation of thorium phosphate, or by a carbonate process based on the relative solubilities of the carbonates of thorium

and the rare earths. There is a similar process based on the solubility of thorium oxalate. Still another process involved the digestion of monazite sand with caustic soda and solvent extraction of the thorium.

Preparation of the Metal. Thorium, like uranium, is chemically active with the atmosphere and most ceramic materials. Therefore metal is prepared by reduction of the halides with alkali metals. High-purity thorium is produced either by the electrolysis of its halides or by the thermal decomposition of the iodide in the deBoer process.

1.32 Physical Constants. Physical constants of thorium along with those for uranium and plutonium may be found in Table 2.

1.33 Transformations and Crystallography. Thorium has two crystalline forms. The α phase, which exists up to $1380 \pm 25^\circ\text{C}$, is face-centered cubic with $a_0 = 5.089 \text{ \AA}$. This constant increases to 5.161 \AA at 1200°C . The β phase is face-centered cubic with $a_0 = 4.12 \text{ \AA}$.

1.34 Health Hazards. Thorium, like uranium, is an α emitter and also the parent element of the radioactive thorium series. Considerable quantities of radioactive radon may be released during the grinding of thorium ores. Radioactive products may be released during the reduction and casting of primary metal.

Information on proper techniques for handling thorium may be obtained from the AEC.

1.35 Mechanical Properties. The mechanical properties of thorium are influenced greatly by minor amounts of impurities. The effects of deliberate additions of carbon, oxygen, and nitrogen are shown in Table 21.

Table 21. Effect of Carbon, Oxygen, and Nitrogen on Tensile Strength of Iodide Th*

Analysis, weight %			Ultimate strength, 10^5 psi	Reduction of area, %
Carbon	Oxygen	Nitrogen		
			20	60
0.06	36	46
0.10	46	51
0.24	60	25
		0.16	30	55
		0.40	35	50
	0.37	25	47

* Compiled from data of R. M. Goldhoff, H. R. Ogden, and R. I. Jaffee, "A Study of the Strengthening of Thorium by Alloying, Cold Work and Aging," BMI-776, November, 1952.

Room-temperature properties of thorium are affected considerably by variations in strain rate and cold work. Orientation in sheet material has only a slight effect. These data are summarized in Table 22.

The variations of properties both in tension and compression with temperature are shown in Tables 23, 24, and 25.

The Charpy impact strength of cast thorium varies from 1.5 to 10.5 depending on the amount of impurities present. While the relationship between tensile properties and impurity content is not fully established, the impact strength at room temperature tends to decrease with decreasing purity. Wrought thorium exhibits a transition from ductile to brittle fracture in the range from 210 to 390°F . Impact strength (foot-pounds) increases gradually from a value of 12 at -100°F to 33 at 210°F . It then rises sharply to 84 at 390°F . This rise continues to a value of 95 at 450°F .

The dynamic shear modulus of wrought and annealed thorium at room temperature is 4.62×10^6 psi. This value decreases gradually to 3.8×10^6 psi at 570°F . It then drops off sharply.

Only exploratory-type tests have been run on the fatigue strength of thorium. Rotating-beam-type tests at room temperature on cast material gave an endurance limit of 12,000 to 12,500 psi for 5×10^8 cycles. Cold rolling increased this limit to

Table 22. The Effect of Cold Work on the Room-temperature Tensile Properties of Thorium*

Test direction†	Strain rate, in./in. (min)	Proportional limit, psi	0.2% offset yield strength, psi	Ultimate strength, psi	Reduction of area, %	Elongation, %
Perpendicular to RD.....	0.007	25,500	45,500	48,800	36	
Parallel to RD.....	0.007	26,500	42,500	43,600	33.9	
Perpendicular to RD‡.....	0.007	17,300	24,500	33,850	41.2	
Parallel to RD‡.....	0.007	15,000	24,700	33,200	48.5	
Parallel to RD.....	0.007	27,500	42,900	44,200	28	6.3
Parallel to RD‡.....	0.007	20,500	23,000	32,500	50	26
Perpendicular to RD‡.....	0.007	20,100	23,100	32,600	49.0	26
Perpendicular to RD‡.....	39.6¶	47,000	44,000	55.0	37
Parallel to RD‡.....	6¶	37,000	37,200	43	35
Parallel to RD‡.....	39.6¶	47,000	44,000	43.0	35

* Compiled from data of A. D. Schwope and L. L. Marsh, Jr., Battelle Memorial Institute.

† The first four specimens listed were given 25 per cent cold work reduction; the remaining six 50 per cent.

‡ Annealed 3 hr at 1350°F; grain size 0.010 mm.

¶ At these strain rates, a yield phenomenon was noticed. The tensile data were obtained by the use of test specimens 3½ in. long with a reduced section 1½ in. long, 0.250 in. wide, with a gauge length of 1 in.

Table 23. Compression Properties of Hot-rolled and Annealed Thorium*

Temperature, °F	Strain rate, in./in. (min)	Proportional limit, psi	0.2% offset yield strength, psi	Young's modulus, 10 ⁶ psi	Poisson's ratio
75‡	0.005	17,000¶	23,900	9.7 ± 0.2	0.25 ± 0.03
75‡	0.01	15,000¶	26,200	9.7 ± 0.2	0.27 ± 0.01
75‡	0.01	18,000¶	30,500	9.7	
75‡	0.025	15,000¶	26,000	10.0 ± 0.2	
570‡	0.01	9,200§	13,800	9.0 ± 0.2	
570‡	0.025	12,000§	17,000	8.9 ± 0.2	

* Compiled from data of A. D. Schwope and L. L. Marsh, Jr., Battelle Memorial Institute.

† Tests conducted in air.

‡ Tests conducted in argon.

¶ Sensitivity of strain measurement was 5 μ in./in.

§ Sensitivity of strain measurement was 60 μ in./in.

Table 24. The Tensile Properties of As-cast Thorium*†

Test temperature, °F	Proportional limit, 10 ³ psi	Yield strength, 10 ³ psi	Modulus of elasticity, 10 ⁶ psi
Room	17	25	22
200	10	17	21
400	6	12	19
600	5	10	17
800	3.5	8	15
1000	3	6	14
1100	3	5	13

* From G. C. Danielson *et al.*, Progress Report on an Investigation of Properties of Th and Some of Its Alloys, *Ames Laboratory Rept. 24*, vol. 1, 1951.

† These data are points taken from a line graph.

15,000 psi. Bending fatigue tests on hot-rolled and annealed metal gave values of 22,000 psi for unnotched and 18,000 psi for notched samples at 10^7 cycles.

There is a limited amount of information available on creep properties of thorium. It is summarized in Table 26.

Table 25. The Tensile Properties of Hot-rolled Annealed Thorium*

Test temperature, °F	Proportional limit, 10^3 psi	0.2% offset yield strength, 10^3 psi	Ultimate strength, 10^3 psi	Modulus of elasticity, 10^6 psi	Elongation, %	Diamond pyramid hardness
Room	22	27	37	10	40	90
400	8	12	23	...	32	78
590	7	11	22	9	38	66
800	60
930	6	9	17	8	50	40

* Compiled from data of A. D. Schwobe and L. L. Marsh, Jr., Battelle Memorial Institute.

Table 26. Creep Properties of Thorium*

Temperature, °F	Stress, psi	Time, hr	Total deformation, %	Min creep rate, %/hr
200	20,000	1,660	15.4	0.002†
400	14,000	1,500	1.55	Nil
600	10,000	1,300	1.4	0.0001

* Compiled from data of A. D. Schwobe and L. L. Marsh, Jr., Battelle Memorial Institute.

† Third-stage creep started after 1,100 hr.

1.36 Manufacture. Melting and Casting. The melting and casting problem for thorium is quite similar to that for uranium except it is made even more difficult by the higher melting point of thorium. Techniques described for uranium are applicable. The selection of crucible material is somewhat more limited than in the case of uranium. Again arc melting, particularly with a consumable electrode, will produce a very high quality product.

Forming and Fabrication. Thorium is an extremely ductile material that can be fabricated by any conventional method to produce a wide variety of shapes. Hot working at about 600°C is generally recommended for the primary breakdown of cast ingots. The precautions suggested for the heating of uranium also apply to thorium. Fabrication to final size is easily done at room temperature. Annealing is not essential but may permit larger rates of reduction.

Powder Metallurgy. Thorium powder of good quality is easily made by reacting the metal with hydrogen to produce the hydride. This hydride is then reduced by heating in a vacuum. Powder metal objects can be made either by cold pressing and sintering or by hot pressing.

Joining. The welding characteristics of thorium are very erratic, probably as a result of variations in metal purity or welding conditions. Single-pass welds are easily made by the shielded-tungsten-arc process. Attempts to make a second pass over this weld invariably cause cracking. The addition of 2.5 atomic per cent of molybdenum, tungsten, or niobium greatly improves the welding characteristics of the metal.

Thorium cannot be brazed with any of the usual brazes because of the formation of brittle intermetallics. A possible method is joining by first plating with silver or nickel and then brazing the silver or nickel.

Machining. Thorium has machining characteristics similar to those of mild steel. It can be turned at rates of 150 to 175 fpm with high-speed tools. Coolants are

desirable but not essential. The scale resulting from hot working is hard and likely to dull the cutting edge of tools. Scale removal prior to machining is recommended. Thorium chips are pyrophoric and should be removed frequently during machining.

1.37 Corrosion Behavior. Thorium, like uranium, has relatively poor corrosion resistance in air and water. Figure 7 shows the weight gain of thorium sheet in air at various temperatures. In boiling distilled water, thorium becomes covered with

Table 27. The Effect of Alloying Additions on Yield-strength Increment for Arc-melted Binary Thorium Alloys*

Alloy additions, atomic %	Heat treatment†	0.2% offset yield strength, psi	Ultimate strength, psi	Elongation, % in 1 in.	Reduction of area, %	VHN	
						Room temp.	300°C
0	1	29,000	39,000	32	46	106	60
0	2	19,400	31,750	46	49	79	45
2.5 Ag	2	21,200	37,000	...	31	91	51
1 Al	2	24,600	40,800	34	43	99	57
2.5 Au	2	20,700	37,400	...	37	88	54
5 B	2	20,200	34,200	34	38	85	47
5 Ba	2	21,000	32,900	...	50	84	44
2.5 Bi	2	24,800	44,200	19	32	97	65
1 C	2	27,200	38,800	44	48	104	57
2.5 C	1	57,600	58,600	...	19	175	94
5 C	1	52,100	57,700	...	27	175	119
5 C	2	29,400	42,000	35	36	106	59
5 Ca	2	19,600	30,400	37	38	111	41
5 Ce	1	31,000	46,000	36	41	118	72
1 Co	1	28,800	33,300	3	10	115	70
5 Cr	1	32,800	44,000	38	44	105	64
5 Cu	2	23,100	41,000	46	43	104	54
2.5 Fe	2	23,800	36,600	...	37	85	50
1 Ga	2	20,300	34,800	33	48	86	55
1 In	2	22,500	36,100	31	38	87	58
5 In	2	35,600	49,800	23	40	116	83
5 Mg	2	19,400	29,800	42	51	113	87
5 Mn	1	30,800	41,500	107	64
5 Mo	2	23,000	37,600	31	50	81	45
5 N	2	23,600	37,600	42	48	89	52
5 Nb	2	14,700	29,000	21	45	61	44
2.5 Ni	2	23,800	37,300	20	37	85	47
5 P	2	21,500	35,800	...	42	88	52
2.5 Pb	2	24,000	42,700	19	42	91	64
5 S	2	14,000	26,600	42	47	68	38
5 Se	2	12,600	25,200	6	24	57	42
5 Si	2	20,500	32,200	39	50	79	46
2.5 Sn	2	23,000	41,000	18	35	88	60
5 Sr	2	22,100	34,200	38	50	83	53
1 Ta	1	31,800	42,600	...	54	105	62
5 Ti	1	10,900	23,600	33	50	53	44
2.5 Tl	2	24,200	36,000	18	48	88	48
5 V	1	20,900	33,400	30	56	80	51
5 W	1	31,800	43,000	33	31	107	66
1 Zr	2	23,500	37,200	...	31	80	63
1 Zr	1	45,000	56,000	12	25	93	86
5 Zr	1	18,000	34,000	23	43	78	59

* Compiled from R. M. Goldhoff, H. R. Ogden, and R. I. Jaffee, "A Study of Thorium-base Alloys," BMI-720, Dec. 26, 1951 (unpublished information).

† Heat treatment 1, 1 hr at 750°C; heat treatment 2, 2 hr at 850°C.

an oxide but may lose or gain weight. Rates of +0.03 to -0.006 mg/(cm²)(hr) have been reported.

The corrosion resistance of thorium in eutectic sodium-potassium alloy is excellent. At 1100°F, the corrosion rate during a 6-day static test in sodium-potassium was 0.006 mg/(cm²)(hr). The corrosion rate increased with increasing oxygen content in the sodium-potassium. Thorium is not attacked by lithium in 6 days at 1100°F

but is completely disintegrated by gallium at 1100°F. In pure bismuth at 1650°F, severe attack occurs in 1 hr. Under the same conditions, pure lead produces only slight attack in 1 hr. Lead at 1830°F dissolved a sample completely in 40 hr.

Protective Techniques. Thorium can be electroplated with most of the common metals. Again, chemical pretreatment prior to plating is most important.

1.38 Alloys. Interest in alloying of thorium has been considerable, though not so great as that shown for uranium. A number of binary diagrams have been developed and are found in the compilation by Saller and Rough.²

The effect of various alloying elements on the yield strength and hardness of thorium is shown in Table 27.

1.4 Plutonium

Plutonium offers another source of fissionable material for reactor operation. While it has been considered primarily as a weapon material, its advancing technology will eventually make it available for use in reactors. Although minute amounts of plutonium have been found in uranium ores, its source is limited to that produced from uranium 238 in a reactor.

Some of the physical constants of plutonium are listed in Table 2. Additional information on the allotropic forms of plutonium is given in Table 28.

Plutonium is an α emitter and offers a very serious health hazard. The major danger arises from the fact that plutonium entering the body is deposited primarily in the marrow of the bones and is then excreted very slowly. While plutonium may enter the body by ingestion, inhalation, or absorption through the skin, the principal path is through inhalation. Extreme precautions must be taken in handling the material in order to prevent the formation and inhalation of fine particles. Plutonium

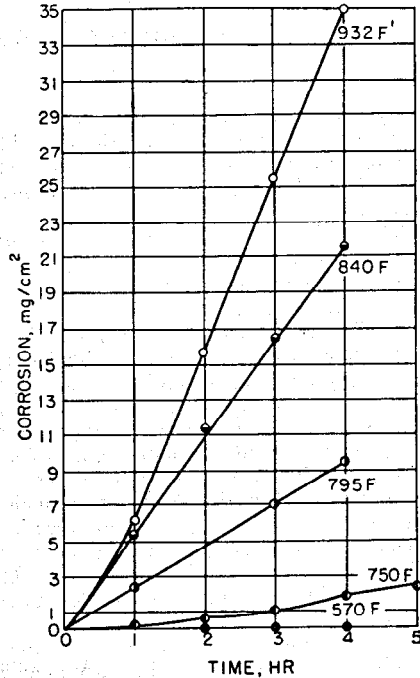


FIG. 7. Corrosion of thorium in air at various temperatures. (Compiled from data of M. W. Mallett, Battelle Memorial Institute, unpublished information.)

Table 28. Properties of Plutonium Metal*

Phase	Temperature range of stability, °C	Crystal structure	Density at 25°C, g/cm³	Average linear expansion coefficient, 10 ⁻⁴ /°C	Electrical resistivity, μ ohm-cm	Temperature coefficient of resistivity†
Alpha.....	Below 117	Orthorhombic like uranium (doubtful)	19.8	55	150 at 25°C	-29.7 × 10 ⁻⁴
Beta.....	117-200	Unknown (complex)	17.8	35	110 at 200°C	Zero (approx)
Gamma....	200-300	Unknown (complex)	36	110 at 300°C	Zero (approx)
Delta.....	300-475	Fcc	16.0	-21	102 at 400°C	+1.5 × 10 ⁻⁴
Epsilon....	475-637	Bcc	16.4	4	120 at 500°C	Zero (approx)

* From Cyril Stanley Smith, Properties of Plutonium Metal, *Phys. Rev.*, **94** (4) (May 15, 1954).
 † Values are in arbitrary units.

metal also emits low-energy γ radiation. Certain alloys of plutonium produce neutrons and must be treated accordingly. Health-physics groups of the various laboratories and the AEC are in a position to give competent advice on these problems.

2 FUEL DILUENTS AND CLADDING MATERIALS

2.1 General Requirements

Even if uranium and thorium were completely satisfactory from the viewpoint of corrosion resistance and strength, it would be necessary to clad or otherwise coat the fuel to prevent the entrance of fission products into the reactor coolant. Also, in the case of enriched reactors, it may be desirable to dilute the fuel with some low-cross-section material.

These cladding and diluent materials must meet very severe requirements. These are as follows:

1. These materials must have adequate strength even under the adverse conditions of temperature and irradiation.
2. They must be corrosion resistant in the reactor coolant.
3. They must be compatible with fuel materials.
4. They must be physically stable under irradiation.
5. They must possess good heat-transfer characteristics.
6. They must have good nuclear properties such as low-capture cross section.
7. They must be reasonably fabricable.
8. They should be reasonable in cost.

From a consideration of cross section alone, only aluminum, beryllium, magnesium, and zirconium, with a thermal cross section of less than 0.5 barn per atom, are attractive for thermal reactors. Of these four, magnesium is usually ruled out on the basis of strength and corrosion resistance. The remaining three, aluminum, beryllium, and zirconium, are the leading cladding and diluent materials for thermal reactors and are discussed in some detail. Some consideration is also given to the ceramic materials BeO , Be_2C , SiC , and MoSi_2 . In fast reactors, a number of other materials become quite attractive. Primary among these is stainless steel, which is discussed in detail as a structural material. Stainless steel may also be considered for special-purpose enriched thermal reactors.

2.2 Zirconium

The low thermal cross section, excellent corrosion resistance, reasonable strength, and good fabricability of zirconium cause it to be a leading cladding and diluent material for thermal reactors. Its position is further improved by the fact that corrosion resistance and strength can be improved by alloying. The only real short-coming possessed by zirconium is its high cost. This situation should improve as production increases.

2.21 Production. Abundance and Availability. Zirconium minerals are widespread over the earth's surface. It ranks ninth among the metals in abundance. The principal zirconium minerals are zircon (ZrSiO_4), zircite (ZrO_2), and baddeleyite (ZrO_2). Commercial sources occur in the United States (Florida and North Carolina), Brazil, Ceylon, India, and Australia. All zirconium ores contain hafnium in amounts from $\frac{1}{2}$ to 3 weight per cent. Some ores contain as much as 20 per cent.

Extraction and Purification. The removal of hafnium with its high cross section from zirconium is essential before the metal can be used in nuclear reactors. This is accomplished by means of solvent extraction, which produces a pure hydrated zirconium oxide. A modified Kroll process is used to produce metal. The oxide is chlorinated either with carbon tetrachloride or by mixing with carbon, pelletizing, and treating with chlorine at elevated temperatures. The chloride is purified by distillation and then reduced by molten magnesium in a closed container. The product is a slightly porous sponge.

Sponge zirconium can be further refined using the de Boer iodide process. In this

process, the sponge is converted to zirconium tetraiodide, which is then thermally decomposed on a heated zirconium filament. Oxygen, nitrogen, and magnesium are the significant elements removed in this process.

2.22 Physical Constants. Physical constants are given in Table 29, together with those of aluminum and beryllium for comparison.

Table 29. Physical Constants of Aluminum, Beryllium, and Zirconium*

	Aluminum	Beryllium	Zirconium
Thermal-neutron cross section:			
Barns/atom.....	0.215 ± 0.008	0.0090 ± 0.0005	0.18 ± 0.02
Cm ² /g.....	0.0048	0.00060	0.00119
Density, g/c.....	Calculated 2.694, measured 2.699	X-ray (25°C) 1.8477 ± 0.0007	α, room temperature, 6.50 α, 863°C, estimated 6.36 β, above 863°C, 6.40
Melting point, °C.....	660.2	1315	1845 ± 25°C
Boiling point, °C.....	2327	2970	
Heat of fusion, cal/mole	2550	2334	5500
Heat of vaporization, kcal/mole.....	67.9	75.528	125
Specific heat, cal/(g)(°C)	-150°C, 0.1367 0°C, 0.2079 100°C, 0.225 300°C, 0.248 600°C, 0.277	-200°C, 0.02 -100°C, 0.20 0°C, 0.42 100°C, 0.51 200°C, 0.57 400°C, 0.64 600°C, 0.69 800°C, 0.74	Room, 0.0692 127°C, 0.0739 427°C, 0.0815 727°C, 0.0862 862°C, α, 0.0880 862°C, β, 0.0797 1127°C, 0.0797
Coefficient of linear expansion per °C	20-100°C, 23.8 × 10 ⁻⁶ 20-200°C, 24.7 × 10 ⁻⁶ 20-400°C, 26.7 × 10 ⁻⁶ 20-600°C, 28.7 × 10 ⁻⁶	(99.28% extruded Be) 25-100°C, 11.54 × 10 ⁻⁶ 25-300°C, 14.44 × 10 ⁻⁶ 25-500°C, 15.95 × 10 ⁻⁶ 25-700°C, 17.23 × 10 ⁻⁶ 25-1000°C, 18.77 × 10 ⁻⁶	25°C c axis, 6.15 × 10 ⁻⁶ α axis, 5.69 × 10 ⁻⁶ Worked and α-annealed: thickness, 6.7 to 10.1 × 10 ⁻⁶ transverse, 4.8 to 6.3 × 10 ⁻⁶ longitudinal, 4.6 to 5.9 × 10 ⁻⁶
Electrical resistivity, μohm-cm	-189°C, 0.64 -100°C, 1.53 0°C, 2.63 20°C, 2.66 100°C, 3.86 400°C, 8.0	Hot-pressed, 4.525 Extruded, 4.076	(0.04% Hf) -200°C, 7 -100°C, 23 0°C, 40 100°C, 58 200°C, 73 300°C, 87 400°C, 100 500°C, 110 600°C, 119 700°C, 125 800°C, 128
Thermal conductivity, cal/(sec)(cm)(°C)	Room, 0.503 100°C, 0.503 200°C, 0.530 400°C, 0.546	Vacuum-cast- extruded 0°C, 0.36 100°C, 0.34 200°C, 0.32 300°C, 0.30 400°C, 0.28 500°C, 0.26 600°C, 0.24	Flake- extruded 0.355 0.33 0.305 0.28 0.26 0.235 0.21
			50°C, 0.05 100°C, 0.049 150°C, 0.048 200°C, 0.047 250°C, 0.046

* Compiled by the author from U.S. Atomic Energy Commission, "Reactor Handbook," vol. 3: General Properties of Materials, AECD-3647, McGraw-Hill Book Company, Inc., New York, 1955.

2.23 Mechanical Properties. Mechanical properties of zirconium and some of its alloys are given in Tables 30 to 33 and Figs. 8 to 12. It will be noted that the physical properties of zirconium, like those of uranium, reflect the lack of years of experience to give single acceptable values.

Table 30. Tensile Strength of Various Types of Zirconium*

Type of zirconium and melting method	Fabrication history	Grain size, mm	0.2% offset yield strength, psi	Tensile strength, psi	Elongation in 2 in., %	Vickers hardness
Sponge, induction-melted in graphite crucibles	Rolled at 1560°F, baked 30 min, air-cooled	0.035-0.045	37,600	61,500	21	180
Sponge, induction-melted in graphite crucibles	Forged and rolled at 1830°F, cold-rolled 30%, annealed 1 hr at 1300°F	0.025	35,800	56,400	24	155
Sponge, arc-melted	Forged and rolled at 1830°F, cold-rolled 30%, annealed 1 hr at 1300°F	0.035	37,600	63,300	30	180
Iodide, arc-melted (0.004 weight % nitrogen)	Forged and rolled at 1450°F, cold-rolled 30%, annealed 1 hr at 1300°F	0.035	16,400	35,500	36	104
Iodide, arc-melted (0.002 weight % nitrogen)	Forged and rolled at 1450°F, cold-rolled 30%, annealed 1 hr at 1300°F	0.065	13,600	29,000	29	74
Iodide, arc-melted	Hot-rolled at 1400°F, cold-rolled 66%, annealed ½ hr at 1110°F	0.02	9,400	34,800	47	
Iodide, arc-melted	Hot-rolled at 1400°F, cold-rolled 10%, annealed 20 hr at 1380°F	0.05	7,700	24,800	40 (in 3 in.)	73

* From B. Lustmann and Frank Kerze, Jr. (eds.), "The Metallurgy of Zirconium," NNES, Div. VII, vol. 4, McGraw-Hill Book Company, Inc., New York, 1955

Table 31. Tensile Properties of Zirconium-Tin Alloys at Room Temperature*

Tin analysis, weight %	0.2% offset yield strength, psi	Ultimate tensile strength, psi	Elongation to max load, %	Total elongation in 2 in., %	Reduction of area, %
0	37,600	63,300	13	30	49
1.1	47,800	68,800	14	34	55
1.6	51,800	69,400	12	32	54
2.0	57,000	72,200	12	34	56
2.5†	50,400	61,200	...	30	57
2.8	57,800	67,800	10	34	56

* From A. D. Schwope and W. Chubb, "Mechanical Properties of Zirconium-Tin Alloys," BMI-817, Apr. 14, 1953 (unpublished information).

† Specimens taken transverse to rolling direction.

2.24 Manufacture. Melting and Casting. With improved quality of zirconium sponge and an increased interest in zirconium alloys, greater emphasis has been placed on the direct melting of sponge. This is accomplished quite successfully by pressing the sponge to form an electrode. This electrode is then melted in a conventional

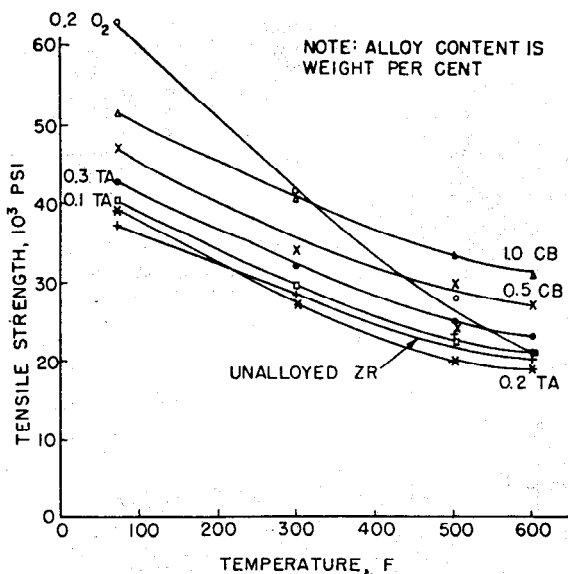


FIG. 8. Tensile strength vs. temperature for unalloyed high hafnium zirconium and alloys with high hafnium zirconium base. [Benjamin Lustman and Frank Kerze, Jr. (eds.), "The Metallurgy of Zirconium," NNEs, Div. VII, vol. 4, McGraw-Hill Book Company, Inc. New York, 1955.]

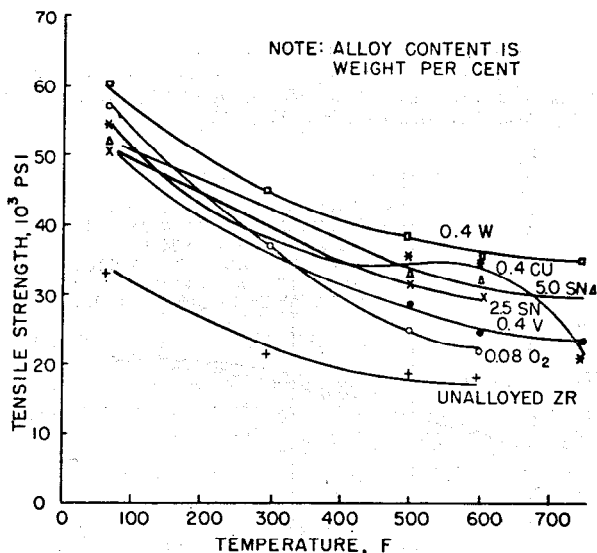


FIG. 9. Tensile strength vs. temperature for unalloyed low hafnium zirconium and alloys with low hafnium zirconium. [Benjamin Lustman and Frank Kerze, Jr. (eds.), "The Metallurgy of Zirconium," NNEs, Div. VII, vol. 4, McGraw-Hill Book Company, Inc. New York, 1955.]

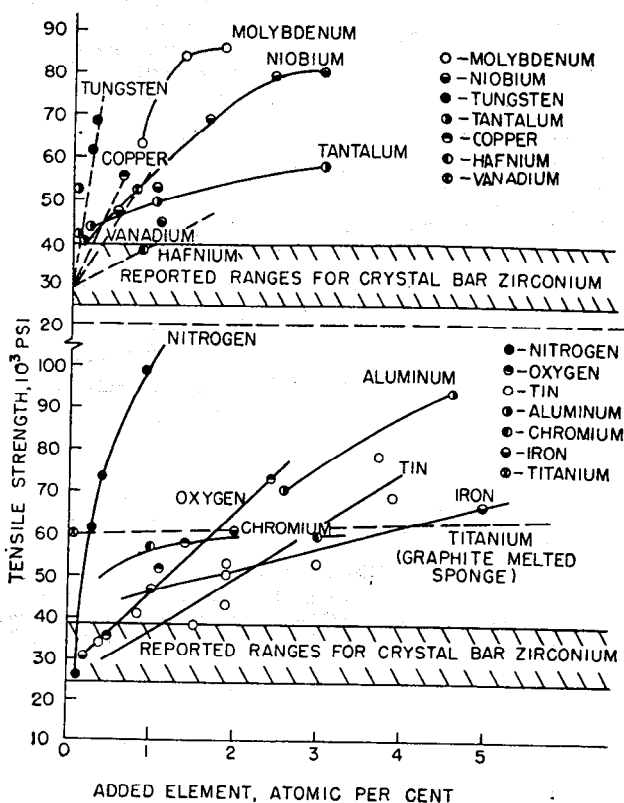


FIG. 10. Room-temperature tensile strengths of various zirconium alloys. [Benjamin Lustman and Frank Kerze, Jr. (eds.), "The Metallurgy of Zirconium," NNES, Div. VII, vol. 4, McGraw-Hill Book Company, Inc., New York, 1955.]

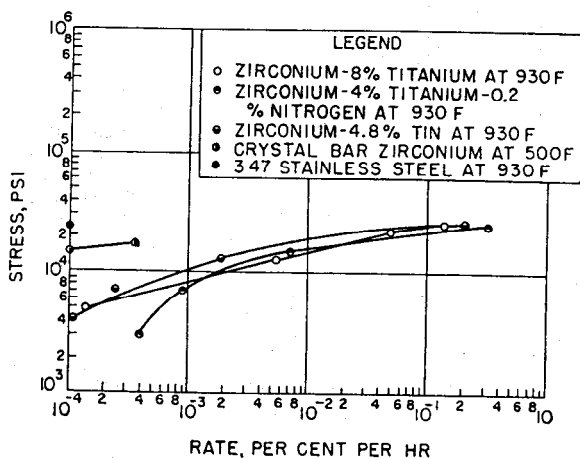


Fig. 11. The creep properties of zirconium and some zirconium alloys compared with type 347 stainless steel. (Prepared by R. W. Dayton et al. from data of BMI Progress Reports for months of October, 1951, and August, 1952, BMI-710 and BMI-769, Nov. 1, 1951, and Sept. 1, 1952.)

water-cooled arc-melting furnace. The resulting ingot is of high quality. For alloys, a second melting is frequently used to ensure homogeneity.

Forming and Fabrication. Zirconium is a very soft, ductile metal that can be fabricated by any conventional method to produce a variety of sizes and shapes. Hot fabrication is usually done at about 1450°F. There is some tendency for oxidation during heating. This is troublesome if it is desired to fabricate to finished size.

Table 32. Tensile Properties of Zirconium-Tin Alloys at 260°C*

Tin analysis, weight %	0.2% offset yield strength, psi	Ultimate tensile strength, psi	Elongation to max load, %	Total elongation in 2 in., %	Reduction of area, %
0	10,800	26,800	20	52	70
1.1	19,200	34,800	22	46	76
1.6	22,300	35,600	19	45	76
2.0	23,600	35,000	18	46	73
2.5†	23,800	31,600	16	44	73
2.8	28,400	36,600	17	42	73

* From A. D. Schwobe and W. Chubb, "Mechanical Properties of Zirconium-Tin Alloys," BMI-817, Apr. 14, 1953 (unpublished information).

† Specimens taken transverse to rolling direction.

Table 33. Fatigue Properties of Zirconium and Some of Its Alloys*

Composition, weight %	Test temperature, °C	Flexure tensile strength, psi	Fatigue limit, psi†		Fatigue ratio‡
			Unnotched	Notched	
Unalloyed iodide Zr.....	Room	33,300	21,000	8,000	0.63
Unalloyed iodide Zr.....	400	12,800	10,500	6,500	0.82
Iodide Zr + 0.34 O ₂	Room	93,700	56,000	12,000	0.60
Iodide Zr + 0.34 O ₂	400	22,400	15,000	6,000	0.67
Iodide Zr + 2.02/2.2 Sn.....	400	21,100	18,000	8,000	0.85
Iodide Zr + 2.1/2.7 Sn.....	400	21,800	20,000	8,000	0.92
Sponge Zr + 2.5 Sn + 0.14 O ₂	400	31,500	24,000	8,000	0.76
Iodide Zr + 2.5 Sn.....	260	27,600¶	21,500	19,000	0.78

* From Benjamin Lustman and Frank Kerze, Jr. (eds.), "The Metallurgy of Zirconium," NNES Div. VII, vol. 4, McGraw-Hill Book Company, Inc., New York, 1955.

† The fatigue limit is the stress below which a material can be cycled indefinitely without failure (endurance limit). Because of the exceedingly long time required to obtain the true fatigue limit, in this report the fatigue limit is based on a minimum of 1.5×10^7 cycles.

‡ Fatigue ratio = (unnotched fatigue limit)/(tensile strength).

¶ Axial-load.

Light machining removes this contamination readily. Protective atmospheres during heating are also helpful.

Some of the alloys, particularly those containing more than 3 per cent tin, are quite hard at elevated temperatures, and fabrication is difficult.

Powder Metallurgy. The high ductility of zirconium metal makes it difficult to produce a powder by crushing. A good grade of powder can be produced, however, by heating zirconium metal at 1470°F in purified hydrogen. The hydride thus formed can be readily crushed to a fine powder. The powdered hydride is reduced to metal by heating in a vacuum. Powder compacts can be made by pressing at 20 to 60 psi and sintering at 2200 to 2370°F.

Joining. Zirconium can be furnace brazed using either copper or silver provided a suitable inert atmosphere or vacuum is maintained. Although these brazed joints are strong, they are not corrosion resistant in water at elevated temperatures.

In most respects, zirconium is welded very easily. The only problem lies in its

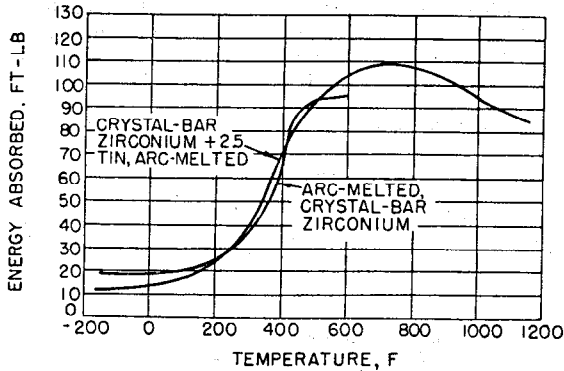


FIG. 12. V-notch Charpy impact tests on arc-melted zirconium and zirconium-2.5 weight per cent tin alloy. (Reprinted from R. W. Dayton, et al., *Hydrogen Embrittlement of Zirconium*, BMI-767, August 22, 1952.)

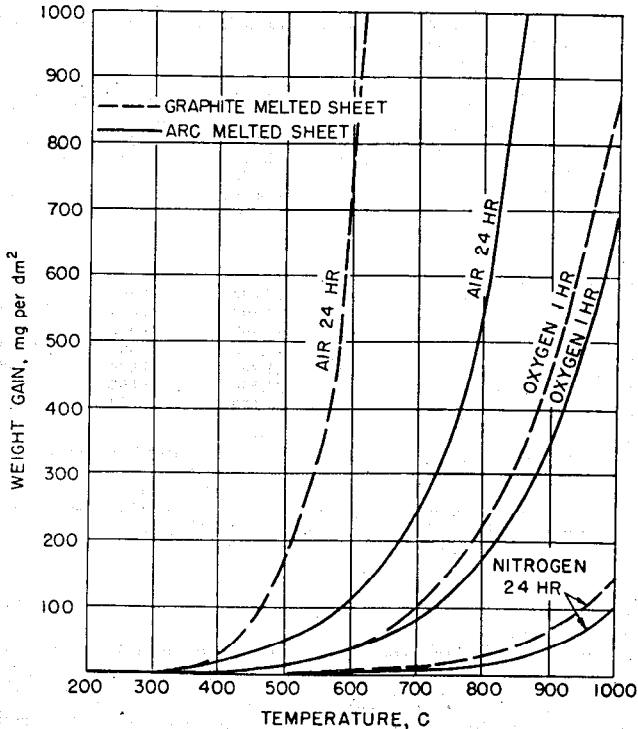


FIG. 13. Heat resistance of zirconium in air, oxygen, and nitrogen. [Benjamin Lustman and Frank Kerze, Jr. (eds.), "The Metallurgy of Zirconium," NNES, Div. VII, vol. 4, McGraw-Hill Book Company, Inc., New York, 1955.]

affinity for nitrogen. This makes it necessary to weld in an atmosphere of helium. Welding is accomplished by a variety of methods including heliarc, resistance, seam, flash, or spot techniques.

Zirconium alloys such as Zircaloy 2 (1.5 weight per cent tin, 0.10 to 0.15 weight per cent iron, 0.08 to 0.12 weight per cent chromium, and 0.04 to 0.06 weight per cent

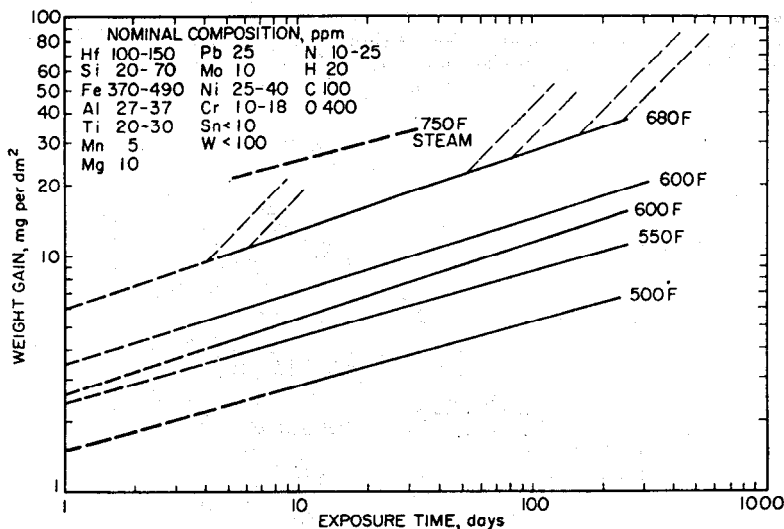


Fig. 14. Weight-gain time curves for the corrosion of crystal-bar zirconium in high-temperature water. [Benjamin Lustman and Frank Kerze, Jr. (eds.), "The Metallurgy of Zirconium," NNES, Div. VII, vol. 4, McGraw-Hill Book Company, Inc., New York, 1955.]

nitrogen) are much less sensitive to nitrogen pickup and can be welded under less exacting conditions than those required for the pure metal.

Machining. The machining characteristics of zirconium resemble those of aluminum. Zirconium is soft and very ductile and galls readily with materials rubbed against it. Some care must be taken to avoid overheating in order to prevent turnings from igniting. This may be accomplished by use of generous clearance angles and sharp tools.

2.25 Corrosion. The corrosion behavior of zirconium in air, oxygen, and nitrogen is shown in Fig. 13. The behavior of zirconium, Zircaloy 2, and other tin-base alloys in hot water and steam is shown in Figs. 14 through 17.

The corrosion behavior of zirconium in various liquid metals is as follows:

Gallium—840°F, bad attack

Mercury—200°F, good: 400°F, fair resistance

Lithium—1830°F, ZrN tarnish film, 4 hr [the nitrogen probably resulted from contamination of the lithium (ORNL-583)]

Sodium potassium—1110°F, negligible weight gain, 6 days

Lead—1830°F, Sn—930°F, Pb-Bi-Sn—930°F, resistant

Bismuth—1830°F, severe attack

Magnesium—1200°F, bad attack

Calcium—2370°F, resistant

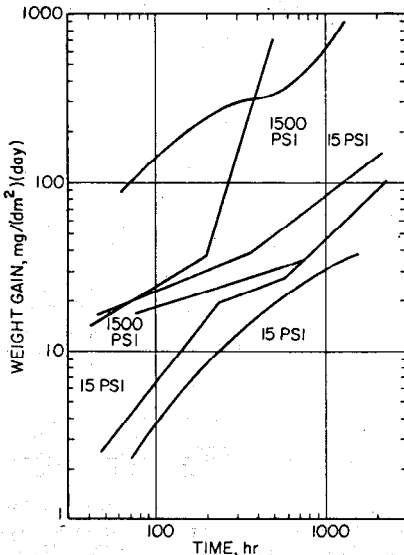


Fig. 15. Corrosion of arc-melted zirconium sponge in steam at 750°F at 15- and 1,500-psi pressure. [Benjamin Lustman and Frank Kerze, Jr. (eds.), "The Metallurgy of Zirconium," NNES, Div. VII, vol. 4, McGraw-Hill Book Company, Inc., New York, 1955.]

Protective Techniques. Although the properties of zirconium are generally very good, there are special applications where a thin coating of some other metal might be useful. Zirconium can be roll clad only with titanium. Other metals form brittle intermetallic compounds at the bond line. It is possible to electroplate zirconium

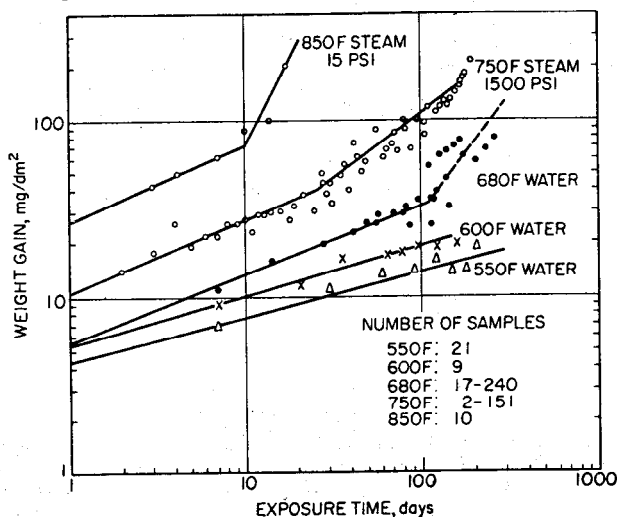


FIG. 16. Weight-gain time curves for the corrosion of Zircaloy 2 in high-temperature water and steam. [Benjamin Lustman and Frank Kerze, Jr. (eds.), "The Metallurgy of Zirconium," NNES, Div. VII, vol. 4, McGraw-Hill Book Company, Inc., New York, 1955.]

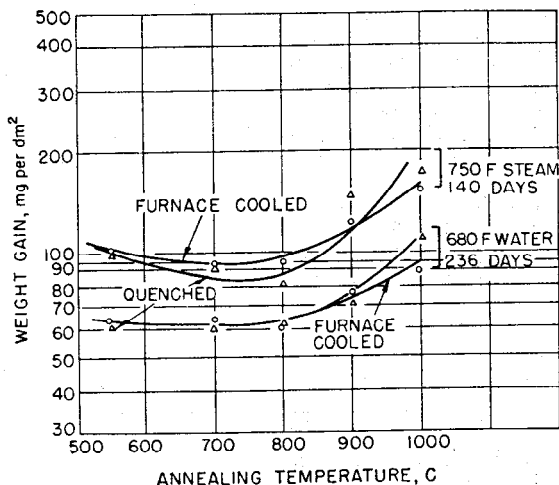


FIG. 17. Effect of heat treatment on corrosion resistance of Zircaloy 2. [Benjamin Lustman and Frank Kerze, Jr. (eds.), "The Metallurgy of Zirconium," NNES, Div. VII, vol. 4, McGraw-Hill Book Company, Inc., New York, 1955.]

with either nickel or iron. Such as-plated deposits are not strong but are much improved by a short diffusion anneal.

2.26 Alloys. There has been an interest in zirconium alloys for two principal reasons. One is the need to alloy in order to improve corrosion resistance in water. The other is the need to alloy in order to improve the high-temperature strength.

Alloys for corrosion resistance were first based on the zirconium-tin binary system.

Additions of 2.5 to 5 weight per cent tin were found very helpful in this regard. Eventually, it was found that alloys containing small amounts of iron, chromium, and nickel in addition to tin were even better behaved. These latter additions also permitted the tin content to be reduced markedly and thus improved fabricability.

It has been found that additions of small amounts of tin, molybdenum, niobium, titanium, and aluminum greatly increase the short-time tensile strength at elevated temperatures. Such alloys have strengths comparable to stainless steel at 930°F. The creep strength of such alloys at this temperature is only about one-fourth that of stainless steel.

A complete compilation of zirconium binary alloys may be found in "Zirconium and Its Alloys."²

2.3 Aluminum

The low thermal-neutron absorption cross section, low cost, ease of fabricability, and good corrosion resistance of aluminum make it a favored diluent and cladding material for low-temperature operations. Its broad usefulness is limited by a low melting point and a decrease in corrosion resistance and strength at moderately elevated temperatures.

Since aluminum is a well-known metal, details of its production and fabrication will not be discussed. In general, it is available as a large number of alloys in a wide

Table 34. Chemical-composition Limits of Selected Aluminum Casting Alloys*

Alloy	ASTM designation	Cu		Fe, max	Si		Mn, max	Mg		Zn, max	Cr, max	Ti, max	Ni		Sn, max	Others [§]	
		Min	Max		Min	Max		Min	Max				Min	Max		Each max	Total max
13†	S12A	...	0.6	0.8	11.0	13.0	0.3	...	0.1	0.3	0.05	0.1	...	0.2
43†, ‡	S5A	...	0.1	0.8	4.5	6.0	0.3	...	0.05	0.2	...	0.2	0.5	0.15
122†, ¶	CG100A	9.2	10.8	1.5	1.0	3.0	0.5	0.15	0.35	0.5	...	0.2	...	0.3	0.3
A132¶	SN122A	0.5	1.5	1.0	11.0	13.0	0.1	0.9	1.3	0.1	...	0.2	2.0	3.0	...	0.05	...
142†, ¶	CN42A	3.5	4.5	0.8	...	0.6	0.1	1.2	1.8	0.1	0.2	0.2	1.7	2.3	...	0.05	0.15
214†	G4A	...	0.1	0.4	...	0.3	0.3	3.5	4.5	0.1	...	0.2	0.05	0.15
218†	G8A	...	0.2	0.8	...	0.3	0.3	7.5	8.5	0.1	0.1	0.1	...	0.2
220†	G10A	...	0.2	0.3	...	0.2	0.1	9.5	10.6	0.1	...	0.2	0.05	0.15
356‡, ¶	SG70A	...	0.2	0.5	6.5	7.5	0.1	0.2	0.4	0.2	...	0.2	0.05	0.15	
360†	SG100A	...	0.6	0.8	9.0	10.0	0.3	0.4	0.6	0.5	0.5	0.1	...	0.2

* Compiled from aluminum producers' data by C. M. Craighead, Battelle Memorial Institute.

† Die-casting alloy.

‡ Sand-casting alloy.

¶ Permanent-mold alloy.

§ The remainder of the alloy is aluminum.

Table 35. Chemical-composition Limits of Selected Wrought Aluminum Alloys*

Alloy	Si		Fe, max	Cu		Mn		Mg		Cr		Zn, max	Ti, max	Others		Al, min
	Min	Max		Min	Max	Min	Max	Min	Max	Min	Max			Each max	Total max	
1100	...	†	†	...	0.20	...	0.05	0.10	0.05	0.15	99.0
3003	...	0.60	0.70	...	0.20	1.0	1.5	0.10	0.05	0.15	Remainder
2017	...	0.80	1.0	3.5	4.5	0.40	1.0	0.20	0.80	...	0.10	0.25	...	0.05	0.15	Remainder
2024	...	0.50	0.50	3.8	4.9	0.30	0.90	1.2	1.8	...	0.10	0.25	...	0.05	0.15	Remainder
5052	...	†	†	...	0.10	...	0.10	2.2	2.8	0.15	0.35	0.10	...	0.05	0.15	Remainder
6061	0.40	0.80	0.70	0.15	0.40	...	0.15	0.80	1.2	0.15	0.35	0.25	0.15	0.05	0.15	Remainder
6063	0.20	0.60	0.35	...	0.10	...	0.10	0.45	0.90	...	0.10	0.10	0.10	0.05	0.15	Remainder

* Compiled from aluminum producers' data by C. M. Craighead, Battelle Memorial Institute.

† 1.0 Si + Fe.
‡ 0.45 Si + Fe.

Table 36. Physical Constants for Selected Aluminum Casting Alloys*

Alloy	Density, g/cm ³	Approximate melting range, °C	Electrical conductivity at 20°C, % IACS†	Thermal conductivity at 20°C, cal/(sec)(cm)(°C)	Coefficient of thermal expansion (20–300°C), 10 ⁻⁶ /°C
13‡	2.69	570–585	39	0.37	21.6
43	2.69	570–620	37	0.35	23.9
43¶	2.69	570–620	42	0.39	
122-T2	2.88	490–620	41	0.38	
122-T61	2.95	490–620	33	0.31	
122‡	2.76	490–620	34	0.32	23.4
142-T21	2.81	530–630	44	0.40	
142-T571‡	2.81	530–630	34	0.32	24.5
142-T77	2.81	530–630	38	0.35	
142-T61‡	2.81	530–630	38	0.31	24.5
214	2.65	580–640	35	0.33	23.9
214¶	2.65	580–640	35	0.33	
218‡	2.60	530–615	24	0.24	24.1
220-T4	2.57	450–620	21	0.21	24.5
356-T51	2.68	570–615	43	0.40	21.4
356-T6	2.68	570–615	39	0.36	21.4
356-T7	2.68	570–615	40	0.37	
356-T6‡	2.68	570–615	41	0.38	
360‡	2.68	555–595	37	0.35	

* Compiled from aluminum producers' data by C. M. Craighead, Battelle Memorial Institute.

† IACS—International Annealed Copper Standard.

‡ Chill-cast samples, all others cast in green-sand molds.

¶ Annealed; while castings are not commonly annealed, similar effects on conductivities may result from the slower rate of cooling of thick sections as compared with thin ones and other variables in foundry practices; comparison of the values for as-cast and annealed specimens will show the extent to which variations may be expected, depending upon the differences in the production of different types of castings.

Table 37. Physical Constants for Selected Wrought Aluminum Alloys*

Alloy	Density, g/cm ³	Approximate melting range, °C	Electrical conductivity at 20°C, % IACS†	Thermal conductivity at 25°C, cal/(sec)(cm)(°C)	Coefficient of thermal expansion, (20–300°C) 10 ⁻⁶ /°C
EC-O	2.70	650–660	62	0.56	23.8‡
EC-H19	2.70	650–660	62	0.56	23.8‡
1100-O	2.71	640–660	59	0.53	25.6
1100-H18	2.71	640–660	57	0.52	25.6
3003-O	2.73	640–655	50	0.46	25.0
3003-H12	2.73	640–655	42	0.39	25.0
3003-H14	2.73	640–655	41	0.38	25.0
3003-H18	2.73	640–655	40	0.37	25.0
2017-O	2.79	510–585	45	0.41	25.0
2017-T4	2.79	510–585	30	0.29	25.0
2024-O	2.77	500–635	50	0.45	24.7
2024-T3	2.77	500–635	30	0.29	24.7
5052-O	2.68	590–650	35	0.33	25.7
5052-H38	2.68	590–650	35	0.33	25.7
6061-O	2.70	580–650	45	0.41	25.4
6061-T4	2.70	580–650	40	0.37	25.4
6061-T6	2.70	580–650	40	0.37	25.4
6063-T42	2.70	615–650	50	0.46	25.2
6063-T5	2.70	615–650	55	0.50	25.2
6063-T6	2.70	615–650	55	0.50	25.2

* Compiled from aluminum producers' data by C. M. Craighead, Battelle Memorial Institute.

† IACS—International Annealed Copper Standard.

‡ 20 to 100°C only.

Table 38. Tensile and Yield Strengths of Cast Aluminum Alloys*

Alloy	Yield strength, 10 ³ psi			Tensile strength, 10 ³ psi		
	Room	400°F	600°F	Room	400°F	600°F
13	20	35		
43	15	28		
43†	8	18		
43‡	8	23		
122-T2†	19	13	4	25	21	8
122-T52‡	36	32		
122-T61†	29	16	4	36	23	8
122-T65‡	35	43		
122-T551‡	34	19	6	34	24	10
A132-T551†	...	13	5	...	22	11
142-T21†	19	13	3	25	21	8
142-T61‡	40	42		
142-T77†	24	18	3	27	22	8
142-T571†	28	29		
142-T571‡	33	22	5	36	28	9
214†	11	11	3	24	18	9
218	27	40		
220-T4†	24	41		
356-T6†	23	8	2	30	13	4
356-T6‡	27	36		
356-T7†	29	31		
356-T7‡	23	30		
356-T51†	19	24		
356-T71†	20	27		
360	27	38		

* Compiled by the author from aluminum producers' data.

† Sand casting.

‡ Permanent-mold casting.

variety of shapes. Compositions of typical cast and wrought alloys are given in Tables 34 and 35. Detailed information can be obtained in handbooks prepared by the principal producers: Alcoa, Kaiser, and Reynolds.

2.31 Physical Constants. Pertinent physical constants of pure aluminum are listed in Table 29 along with those of zirconium and beryllium. Selected physical constants of alloys favorable for reactor use are given in Tables 36 and 37.

2.32 Mechanical Properties. Mechanical properties of selected aluminum alloys are given in Tables 38, 39, and 40 and in Figs. 18 and 19.

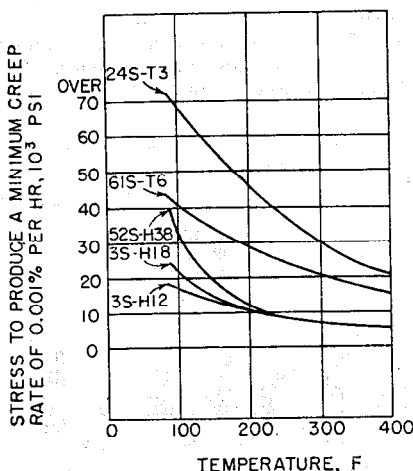


FIG. 18. Effect of temperature on stress to produce a creep rate of 0.001 per cent/hr for several 0.065-in.-thick wrought alloys. (Constructed from aluminum producers' data by C. M. Craighead et al., Battelle Memorial Institute, Aug. 1, 1952.)

Table 39. Tensile and Yield Strengths of Wrought Aluminum Alloys*

Alloy	Yield strength, 10 ³ psi			Tensile strength, 10 ³ psi		
	Room	400°F	600°F	Room	400°F	600°F
EC-O	5	13		
EC-H19	24	27		
1100-O	5	3	1	13	7	3
1100-H12	13	15		
1100-H14	14	6	1	17	9	3
1100-H16	17	20		
1100-H18	21	3	1	24	7	3
3003-O	6	4	2	16	8	4
3003-H12	15	18		
3003-H14	18	9	3	21	14	6
3003-H16	21	25		
3003-H18	25	8	3	29	17	4-5
2017-O	11	27		
2017-T4	46	11	4	68	17	6
2024-O	10	25		
2024-T3	50	20-23	4-5	70	23-28	8-9
2024-T4	50	20-23	4-5	70	23-28	8-9
2024-T36	56	75		
5052-O	14	11	4	29	18	7
5052-H32	27	35		
5052-H34	30	35		
5052-H36	34	11	4	39	25	8
6061-O	8	6	2	18		
6061-T4	20	15	2	35	18	
6061-T6	40	15	2	45	19	3
6063-T5	25	30		
6063-T6	30	35		
6063-T42	14	20		
6063-T83	35	40		
6063-T831	30	30		
6063-T832	40	45		

* Compiled by the author from aluminum producers' data.

2.33 Corrosion. Aluminum possesses good corrosion resistance in water up to temperatures slightly above the boiling point of water.

Recent work by Draley of ANL has shown that the addition of small amounts of acid to the water improves corrosion resistance markedly. Good corrosion behavior at temperatures around 200°C has been observed. This improvement in corrosion

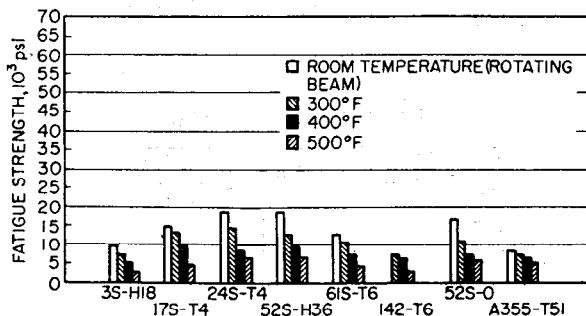


Fig. 19. Comparison of the fatigue strengths of various aluminum alloys at 5×10^8 cycles as affected by temperature. Tested after stabilization periods of 0.5 to 2 hr at testing temperature. (Constructed from aluminum producers' data by C. M. Craighead et al., Battelle Memorial Institute, Aug. 1, 1952.)

Table 40. Modulus of Elasticity of Aluminum Alloys in Tension*

Alloy	Average modulus, 10 ⁶ psi†		
	75°F	300°F	500°F
1100, 3003, 6061, and 6063.....	10.0	9.5	8.0
5052.....	10.2	9.7	8.15
2017.....	10.5	10.0	8.4
2014 and 2024.....	10.6	10.1	8.5
Aluminum casting alloys.....	10.3	9.8	8.25

* Compiled from aluminum producers' data by C. M. Craighead, Battelle Memorial Institute.
 † The modulus of elasticity is about 2 per cent higher in compression than in tension. For most calculations, a value of 10,300,000 psi can be used for all alloys in both tension and compression. The modulus of rigidity is approximately 3,900,000 psi, and Poisson's ratio is about one-third.

resistance in the pH range 5.5 to 6.5 makes aluminum quite attractive for power reactor applications.

2.4 Beryllium

The very low cross section, high melting point, and good strength of beryllium make it appear to be an excellent diluent or cladding material. However, in spite of a considerable amount of research, beryllium has not gained the important position it was once assumed to merit. Its favorable properties have been more than offset by its high cost, low ductility, poor corrosion resistance, and extreme toxicity.

While beryllium is a relatively new and unusual metal, its importance as a reactor material does not warrant any extended discussion on its abundance, melting fabrication, and the like.

In general, beryllium shapes are made by powder metallurgy or a combination of

Table 41. Directional Effects on Beryllium Mechanical Properties*

Test temperature, °C	Direction of test	No. of tests	Ultimate strength, psi	Elongation, %	Reduction, %	No. of tests	Ultimate strength, psi	Elongation, %	Reduction, %
Room	Longitudinal†	4	46,600	0.55	...	3	32,730	0.36	
	Transverse†	2	29,125	0.3	...	2	19,400	0.30	
	Longitudinal‡	2	63,650	5.0	6.1	3	39,970	1.82	
	Transverse‡	1	25,500	0.3	...	2	16,550	0.18	
	Longitudinal¶	2	68,450	6.6	5.7	0			
	Transverse¶	1	26,700	0.3	...	0			
	Longitudinal†	0	3	39,870	13.2	8.0
	Transverse†	0	2	16,600	1.1	
200	Longitudinal‡	0	3	37,870	13.4	8.6
	Transverse‡	0	2	14,250	1.1	1.7
400	Longitudinal†	2	30,590	14.8	9.6	3	27,670	13.4	32.8
	Transverse†	2	22,840	1.9	0.3	2	14,500	1.4	1.7
600	Longitudinal†	2	13,570	10.6	7.2	2	25,850	20.8	23.2
	Transverse†	1	11,200	2.5	0.6	2	15,980	1.2	0.3
800	Longitudinal†	2	4,760	9.1	4.2	3	9,270	25.6	24.0
	Transverse†	1	5,860	0.3	...	2	6,900	9.6	8.9

* From D. W. White and J. Burke (eds.), "The Metal Beryllium," The American Society for Metals, 1955.

† As extruded.

‡ Annealed at 800°C for 1 hr.

¶ Annealed at 800°C for 1 hr plus 1000°C for 1 hr.

powder metallurgy and conventional fabrication. By these techniques, a rather large assortment of sizes and shapes are available:

Considerable information on beryllium is available in the book "The Metal Beryllium," edited by D. W. White and J. Burke and published by the American Society for Metals.

2.41 Physical Constants. Physical constants of beryllium are listed in Table 29.

2.42 Mechanical Properties. Mechanical properties of beryllium are given in Tables 41 through 43.

Table 42. The Effect of Extrusion Temperature and Machining Stresses on the Tensile Properties of Beryllium*

Extrusion temperature, °C	As extruded and machined		As extruded, machined, and annealed at 800°C		As extruded, machined, and etched	
	Ultimate, psi	Elongation, %	Ultimate, psi	Elongation, %	Ultimate, psi	Elongation, %
500	73,100	0.28	51,550	3.35	72,200	0.31
700	60,150	0.31	47,550	2.74	59,750	0.31
900	44,500	0.45	45,050	2.47	51,150	1.45
1060	36,500	0.39	52,133	3.38	49,600	2.57
1105	36,900	0.64	54,300	3.82
1208	34,800	0.44	50,200	3.80	51,300	3.76

* From D. W. White and J. Burke (eds.), "The Metal Beryllium," The American Society for Metals, 1955.

Table 43. Impact Strength of Beryllium*

Temperature, °F	Impact strength, ft-lb	
	Extruded	Powder
Room	0.122	0.118
212 (100°C)	0.132	0.132
392 (200°C)	0.249	0.180
572 (300°C)	0.255	0.218
752 (400°C)	1.212	0.185
932 (500°C)	0.222	0.296
1112 (600°C)	1.357	0.189
1292 (700°C)	>2	0.310
1472 (800°C)	>2	0.278

* From M. C. Udy, H. L. Shaw, and F. W. Boulger, "The Properties of Beryllium," BMI-T-14 (unpublished information).

2.43 Corrosion. Beryllium is reasonably corrosion resistant in air at temperatures up to 750°F. At 1290°F, results are erratic, but some data show beryllium about equal to 18-8 stainless steel.

The corrosion resistance of beryllium in hot water varies widely, depending upon the grade of metal tested. In boiling water, extruded ingot appears superior to extruded flake or powder process material. Several grades of beryllium showed some resistance at 525°F but were badly attacked at 600°F. In general, the corrosion resistance has been too erratic to warrant use of the metal in hot water.

Cladding. Improvement in corrosion resistance can be achieved by cladding with aluminum, using conventional roll-cladding techniques. Although cladding with zirconium would be desirable for high-temperature water application, it does not

appear feasible, since a brittle-compound layer is formed between beryllium and zirconium.

The resistance of various types of beryllium to sodium and its alloys is shown in Table 31.

2.5 Other Materials

Stainless steel is recently gaining prominence as a fuel diluent and cladding material in spite of its cross section. Its high strength and corrosion resistance tend to offset a cross section higher than that of zirconium, aluminum, or beryllium. Stainless steels are particularly attractive as a matrix material containing fuel in the form of a powdered uranium compound.

Table 44. Physical Properties of BeO, Be₂C, SiC, and MoSi₂*

	BeO	Be ₂ C	SiC	MoSi ₂	
Density, g/cm ³	Single-crystal, 3.025 Hot-pressed, 2.6-2.95 Slip castings after firing, 2.2-2.8	X-ray, 2.44 Crystals from BeO-C reaction, 2.30-2.40	Calculated 3.210 Green at 30°C, 3.218 Average values at 20°C, 3.10-3.30	X-ray, 6.24 Powder, hot-pressed at 2,400 psi and 1700°C: 6.20	
Melting point, °C	2550 ± 25	No true melting point at atmospheric pressure—some melting observed above 2200	Decomposes at about 2500	1870	
Specific heat, cal/(g)(°C)	100°C, 0.308 400°C, 0.420 800°C, 0.492	30-100°C (98% Be ₂ C), 0.334 ± 0.013	327°C, 0.251 627°C, 0.280 927°C, 0.299 1227°C, 0.316		
Electrical resistivity, ohm-cm	Sintered beryllia density 2.25 g/cm ³ 1000°C, 80,000,000 1200°C, 4,000,000 1400°C, 250,000 1600°C, 35,000 1800°C, 6,500 2000°C, 1,600	Impure in sintered shapes 30°C, 0.063 425°C, 0.047	Recrystallized, no bond 30°C, 0.063 800°C, 6.5 1200°C, 2.5 1400°C, 1.7	Bonded 10% fireclay 12,500 4,200 1,400	Hot-pressed† 25°C, 21.5 400°C, 70 600°C, 103 900°C, 160 1100°C, 193
Thermal conductivity, cal/(sec)(cm)(°C)	Density 2.87 g/cm ³ 200°C, 0.19 400°C, 0.13 600°C, 0.095 1000°C, 0.055 1400°C, 0.038	30°C, 0.0215	Recrystallized 400°C, 0.060 600°C, 0.052 800°C, 0.044 1000°C, 0.0385 1200°C, 0.032	370.6°C, 0.0886 566.6°C, 0.0803 683.9°C, 0.0764 710.0°C, 0.0767 800.6°C, 0.0757 823.8°C, 0.0757	
Coefficient of linear thermal expansion, per°C × 10 ⁻⁶	25-100 (5.5 ± 1) 25-300 (8.0 ± 0.6) 25-600 (9.6 ± 0.8) 25-800 (10.3 ± 0.9) 25-1000 (10.8 ± 1.0)	25-50°C, 5.6 25-200°C, 7.7 25-400°C, 9.5 25-600°C, 10.5	0-1700°C, 4.3-4.5	0-1500°C, 5.1	

* Compiled by the author from various sources.

† Values in microhm-centimeters.

Since stainless steel has long been popular as a structural material, its properties are covered in that section.

Ceramic materials offer a type of diluent or cladding material with some very attractive properties. They possess very low cross sections and extremely good high-temperature properties and are relatively inexpensive. They suffer from lack of thermal-shock resistance. Physical and chemical constants and selected mechanical properties of BeO, Be₂S, SiC, and MoSi₂ are given in Tables 44 and 45.

Table 45. Mechanical Properties of BeO, Be₂C, SiC, and MoSi₂*

	BeO†	Be ₂ C	SiC	MoSi ₂
Strength: Tensile, 10 ³ psi	Density 2.7-2.8 g/cm ³ 400°C, 15.0 800°C, 13.5 1000°C, 10.5 1100°C, 8.0 1200°C, 4.0	Self-bonded brick may be heated to 1700°C under a 50-psi compressive load without perma- nent deformation	27°C, 22.0 980°C, 40.0 1090°C, 42.2 1200°C, 42.8 1315°C, 41.1
Compressive, 10 ³ psi	500°C, 71.0 800°C, 64.0 1000°C, 36.0 1232°C, 24.0 1600°C, 7.1	800°C, 5.93 1000°C, 8.16 1300°C, 2.09 1350°C, 1.82 1500°C, 0.99	100-350
Hardness	Dense pure beryllia Moh value 9	Knoop values: 50-kg load, 2550 25-kg load, 2740	Knoop values 2100-2700	Rockwell A-80 to A-90 Knoop, 1-kg load, 850-870 25°C, 59
Modulus of elas- ticity, 10 ³ psi	400°C, 39 1000°C, 38 1100°C, 28 1200°C, 10	400°C, 23 500°C, 23.8 700°C, 24.3 1000°C, 24.8	25°C, 59
Modulus of rup- ture, 10 ³ psi	Minus 325 mesh, pressed and sin- tered, 1700°C: room temp. 4.6	25°C, 8-10 1370°C, 7-14	25°C, 50.7 1090°C, 35.7 1315°C, 20.7

* Compiled by the author from various sources.

† Tensile strength and elasticity specimens fabricated from slip castings; compressive strength and rupture specimens pressed; other properties for sintered beryllia.

3 SOLID MODERATORS

3.1 Special Requirements

Moderating materials for thermal reactors must be capable of reducing neutron energy very rapidly. This requires a low atomic weight to give a large average logarithmic neutron energy loss per collision; moderators must also have a low absorption cross section and a high scattering cross section.

Desirable properties other than nuclear would include reasonable cost, fabricability, good strength at operating temperatures, corrosion resistance to reactor coolant,

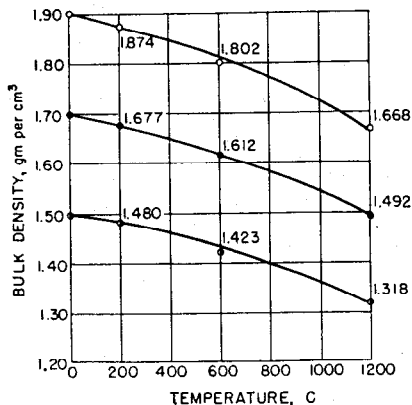


FIG. 20. Variations of graphite bulk density with temperature. (Compiled by J. A. Slyh, Battelle Memorial Institute, from unpublished information, 1952.)

thermal stability, and radiation stability. Such properties are desirable, but they are not obtainable in any single material. Selection of moderator materials is thus based on a compromise between nuclear and physical properties.

From a nuclear consideration, only carbon, beryllium, oxygen, deuterium, and hydrogen show promise among the elements. This, then, limits our selection of solid moderators to graphite, beryllium and its compounds, oxides, carbides, and hydrides. Of these, graphite and beryllium or its compounds have received the most attention.

3.2 Graphite

Graphite has very good nuclear properties as a moderator and, in addition, is abundant, cheap, and easy to fabricate. It has good strength properties up to very high temperatures. Its chief handicap is its lack of corrosion resistance. It is the best known and most widely used solid moderator.

Table 46. Ash and Impurity Contents of Artificial Graphite*

Grade	Ash, ppm	Chemical analysis, ppm					
		B	Al	Ca	Ti	Fe	V
AGX†	1,500	1.3	20	2,000	50	40	70
C-18†	1,200-2,000	1.0	10	1,200	35	100	200
AGHT‡	700-1,700	1.0-1.5	10	500	100	10	14
AGOT‡	350-700	0.2-1.0	...	100-200	20-30	10-20	10-75
CS‡	350-700	0.15	25

* Compiled from data of J. R. Huffman, ANL-4304, June, 1949.

† Typical commercial graphite.

‡ Normal reactor graphite.

The abundance of carbon and the methods of manufacture of graphite are well known and require no discussion here. It might be well to point out, however, that reactor-grade graphite is always an artificial product. The raw materials are carefully selected in order to eliminate any high-cross-section impurities. This is shown in Table 46.

3.21 Physical Constants. Physical constants of several grades of graphite are given in Table 47. Information on the variation of density with temperature, thermal

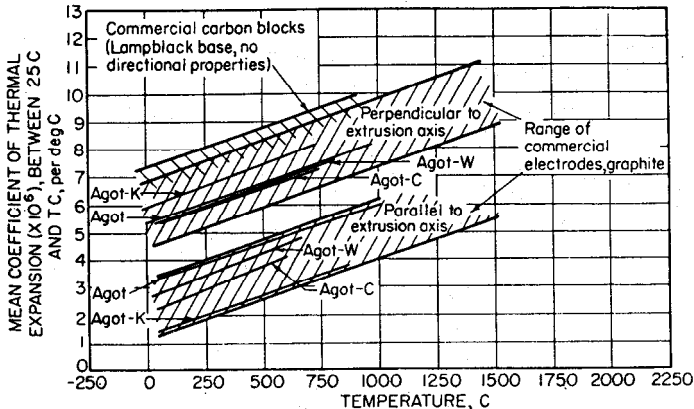


FIG. 21. Thermal-expansion coefficients of various graphites. (Compiled by J. A. Slyh, Battelle Memorial Institute, from unpublished information, 1952.)

Table 47. Physical Constants of Graphite*

Thermal-neutron-absorption cross section, millibarns/atom:	
AGOT (<0.5 ppm B).....	4.8
Density, g/cm ³	
Calculated from lattice constants:	
Artificial.....	2.27-2.28
Natural.....	2.27-2.28
Helium displacement:†	
Artificial.....	2.10-2.17
Natural.....	2.26
Commercial electrodes.....	1.55-1.90
Commercial blocks.....	1.55-1.75
AGHT.....	1.61-1.65
AGOT.....	1.65-1.72
Sublimation temperature, °C.....	3650 ± 25
Heat of vaporization, kcal/mole.....	143
Heat of sublimation, kcal/mole.....	140-170
Specific heat (C _p), cal/(mole)(°C):	
25°C.....	2.066
127°C.....	2.851
327°C.....	4.03
527°C.....	4.75
727°C.....	5.14
927°C.....	5.42
1127°C.....	5.67
Electrical resistivity (parallel), μohm-cm:	
Commercial electrodes.....	850-1,250
Commercial blocks.....	850-1,100
AGHT.....	800‡
AGOT.....	500-850
CS.....	800
GBF.....	720

* Revised by the author from data compiled by J. A. Slyh, Battelle Memorial Institute, for U.S. Atomic Energy Commission, "Reactor Handbook," vol. 3, General Properties of Materials, AECD-3647, McGraw-Hill Book Company, Inc., New York, 1955.

† An explanation of density measurements by helium displacement is given in R. P. Rassman and W. R. Smith, Density of Carbon Black by Helium Displacement, Godfrey L. Cabot, Inc., Boston, Mass., *Ind. Chem. Eng.*, vol. 35 (1943).

‡ Perpendicular: 1,050 to 1,250 μohm-cm.

expansion coefficients, and thermal conductivities are shown in detail in Figs. 20 through 23.

3.22 Mechanical Properties. Tensile and creep properties of various types of graphite at several temperatures are given in Tables 48, 49, and 50 and Figs. 24 through 26.

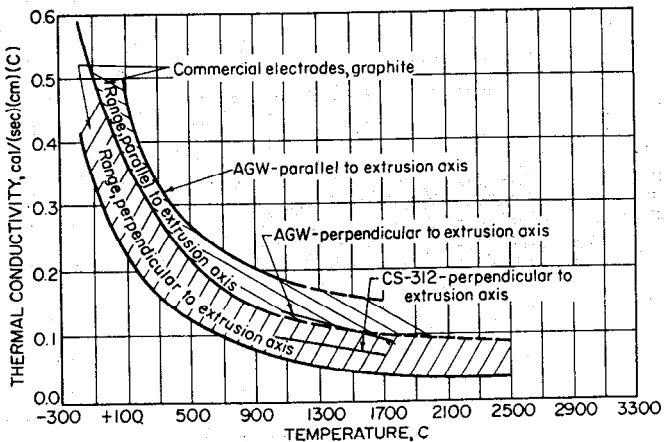


Fig. 22. Typical thermal conductivities of various graphites. (Compiled by J. A. Slyh, Battelle Memorial Institute, from unpublished information, 1952.)

Table 48. Tensile, Compressive, and Transverse Strengths of Carbon and Artificial Graphite at Room Temperature*

Type	Tensile strength, psi		Compressive strength, psi		Transverse strength, psi	
	Longitudinal	Transverse	Longitudinal	Transverse	Longitudinal	Transverse
Commercial electrodes:						
Carbon.....	400-1,200		2,000-10,000		800-6,000	
Porous carbon.....	80-200		3,000-900		200-600	
Graphite.....	500-2,500	900-1,300	3,000-4,000	3,000-5,000	1,000-5,000	
Porous graphite.....	50-100		300-500		150-250	
Commercial blocks:						
Carbon.....	1,000	500-3,000		2,000-8,000		1,000-4,500
Graphite.....	500-2,000	500-3,000		3,000-6,500		1,500-4,000
Commercial tubes:						
Impervious carbon.....	2,000		10,000		4,500	
Impervious graphite.....	2,500		10,000		4,500	
AGOT.....					1,000-2,500	1,000-2,000
AGHT.....	2,200	600				

* Compiled by J. A. Slyh, Battelle Memorial Institute, unpublished information, 1952.

Table 49. Modulus of Elasticity at Room Temperature for Carbon and Artificial Graphite*

Type of product	Modulus of elasticity, 10 ⁶ psi
Commercial electrodes:	
Carbon.....	0.5-1.4
Graphite.....	0.5-1.2
Commercial blocks:	
Carbon.....	1.1
Graphite.....	0.5-0.8
Commercial tubes:	
Carbon.....	1.7-2.1
Carbon, impervious.....	2.6-2.9
Graphite.....	1.3-1.4
Graphite, impervious.....	2.1-2.3
Commercial electrodes and blocks, porous.....	0.12
AGOT.....	1.4-2.1

* Compiled by J. A. Slyh, Battelle Memorial Institute, from various sources.

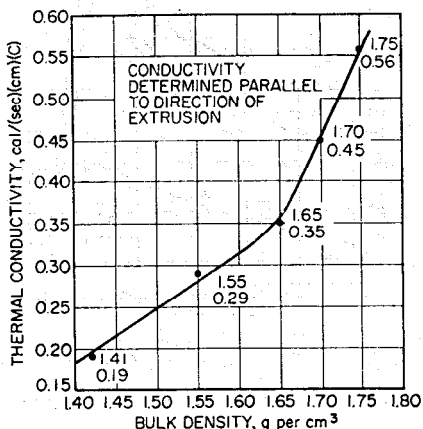


FIG. 23. Thermal conductivity of graphite vs. bulk density at room temperature. (Compiled by J. A. Slyh, Battelle Memorial Institute, from unpublished information, 1952.)

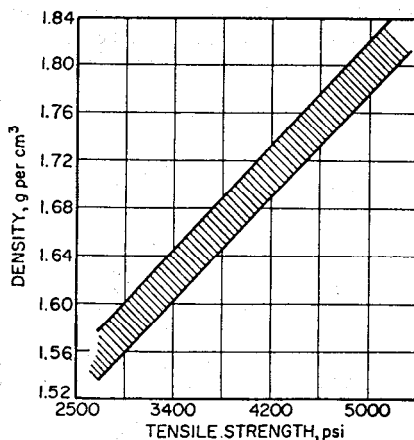


FIG. 24. Variation of room-temperature tensile strength with density for commercial block graphite (EBP). (Reprinted from C. F. Malcolm and A. F. Groton, *Tensile Strength of Type EBP Graphite at Elevated Temperature and Its Relation to Apparent Density at Room Temperature*, NAA-SR-67, March, 1950.)

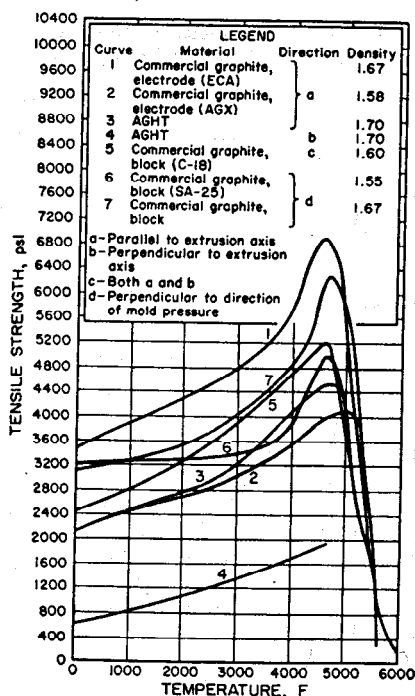


FIG. 25. Effect of temperature on the tensile strength of various graphites. (Reprinted from M. C. Udy and F. W. Boulger, *The Properties of Graphite*, BMI-T-35, June 20, 1950.)

3.23 Corrosion Behavior. The corrosion resistance of graphite in various media is given in Table 51.

3.3 Beryllium and Its Compounds

Beryllium and its compounds, such as the carbide or oxide, possess excellent nuclear properties as moderators. Although the metal itself lacks favorable high-temperature

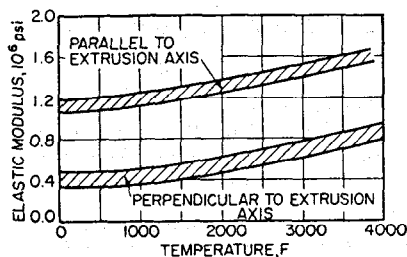


FIG. 26. Effect of temperature on the elastic modulus of commercial electrode graphite. (Adapted from Data of L. Green, Jr., *Measurement of Young's Modulus of Grade AVF Graphite at Elevated Temperatures*, NAA-SR-98, Dec. 7, 1950.)

Table 50. Ductility of Graphite*

Type of graphite	Kind of test	Maximum stress, psi	Temperature, °F	Reduction of area, %	Elongation, (2-in. effective gauge length), %	Increase in volume, %
AGHT†	Tensile	4,380	4800	1.3	7	
AGHT†	Creep	2,200	4800	1.3	9	8
AGHT†	Creep	2,800	4320	0.5	2	1
C-18‡	Creep	2,800	4800	5-7	18	11
C-18‡	Tensile	5,300	4800	0.4-0.5	18	14
C-18‡	Creep	4,000	4300	2.7	11	8
C-18‡	Creep	2,800	4300	1.1	4	3

* From R. E. Adams and H. R. Nelson, NEPA, BMI-N-45, May, 1950.

† Parallel to extrusion direction.

‡ Perpendicular to direction of applied pressure.

Table 51. Reaction of Graphite with Corrosive Agents*

Agent	Temperature, °F	Effect or product
Gases:		
Oxygen.....	840† and higher	Produces carbon oxides
Hydrogen.....	1650-1830	Methane (catalyst necessary)
Fluorine.....	3630 and higher	Acetylene (traces)?
	1650-3450	Produces carbon fluorides
	Room	Interlamellar compounds
Bromine.....	Room	Interlamellar compounds
Potassium vapor.....	Room	Interlamellar compounds
Nitrogen.....	Up to 5430	No effect
Water vapor.....	1470 and lower	Negligible reaction
Chlorine.....	1470 and higher	Increasingly severe attack
	Up to 1470	No effect
Carbon dioxide.....	1470 and lower	Negligible reaction
	1470 and higher	Carbon monoxide
Aqueous solutions:		
Dilute acid or alkali.....	Less than boiling	No attack
Strong acid (HNO ₃ and H ₂ SO ₄).....	570 and higher	Graphitic oxide
KOH (50 per cent solution).....	660 and higher	Reacts with graphite
Solids:		
Alkali hydroxides (inert atmosphere).....	At fusion	No attack
Sodium sulfate.....	At fusion	No attack
Sodium carbonate.....	At fusion	Carbon monoxide
Metals (most).....	2730 and higher	Metal carbide
Metal oxides.....	2730 and higher	Metal carbide and carbon oxides

* Compiled by J. A. Slyh, Battelle Memorial Institute, unpublished information.

† Attack at 660°F is reported; the weight loss is not measurable, but a slight permanent increase in length is noted.

properties, both the oxide and the carbide are very refractory and have excellent high-temperature properties. The high cost and extreme toxicity of beryllium and its compounds are serious handicaps to its widespread usage.

Details on the properties of beryllium and its leading compounds, oxide and carbide, have been covered in detail in Art. 2 under Fuel Diluents and Cladding Materials and will not be repeated here.

4 STRUCTURAL MATERIALS

4.1 Special Requirements

While there is considerable duplication of materials and properties required for Fuel Diluents and Cladding Materials and for Structural Materials, there are important differences between the two. Under Structural Materials are included all those parts which make up the actual reactor core with the exception of fuel elements, control rods,

Table 52. Composition of Wrought Stainless Steels*

AISI type	Composition, %					
	C	Mn (max)	Si (max)	Cr	Ni	Other†
Austenitic Steels						
301	0.08-0.20	2.00	1.00	16.00-18.00	6.00-8.00	
302	0.08-0.20	2.00	1.00	17.00-19.00	8.00-10.00	
302B	0.08-0.20	2.00	2.00-3.00	17.00-19.00	8.00-10.00	
303	0.15 max	2.00	1.00	17.00-19.00	8.00-10.00	‡
304	0.08 max	2.00	1.00	18.00-20.00	8.00-11.00	
304L	0.03 max	2.00	1.00	18.00-20.00	8.00-11.00	
305	0.12 max	2.00	1.00	17.00-19.00	10.00-13.00	
308	0.08 max	2.00	1.00	19.00-21.00	10.00-12.00	
309	0.20 max	2.00	1.00	22.00-24.00	12.00-15.00	
309S	0.08 max	2.00	1.00	22.00-24.00	12.00-15.00	
310	0.25 max	2.00	1.50	24.00-26.00	19.00-22.00	
310S	0.08 max	2.00	1.50	24.00-26.00	19.00-22.00	
314	0.25 max	2.00	1.50-3.00	23.00-26.00	19.00-22.00	
316	0.10 max	2.00	1.00	16.00-18.00	10.00-14.00	Mo 2.00-3.00
316L	0.03 max	2.00	1.00	16.00-18.00	10.00-14.00	Mo 1.75-2.50
317	0.10 max	2.00	1.00	18.00-20.00	11.00-14.00	Mo 3.00-4.00
321	0.08 max	2.00	1.00	17.00-19.00	8.00-11.00	Ti 5xC min
347	0.08 max	2.00	1.00	17.00-19.00	9.00-12.00	Cb 10xC min
Martensitic Steels						
403	0.15 max	1.00	0.50	11.50-13.00		
410	0.15 max	1.00	1.00	11.50-13.50		
416	0.15 max	1.25	1.00	12.00-14.00		¶
420	0.15 min	1.00	1.00	12.00-14.00		
431	0.20 max	1.00	1.00	15.00-17.00	1.25-2.50	
440A	0.60-0.75	1.00	1.00	16.00-18.00		Mo 0.75 max
440B	0.75-0.95	1.00	1.00	16.00-18.00		Mo 0.75 max
440C	0.95-1.20	1.00	1.00	16.00-18.00		Mo 0.75 max
501	0.10 min	1.00	1.00	4.00-6.00		
502	0.10 max	1.00	1.00	4.00-6.00		
Ferritic Steels						
405	0.08 max	1.00	1.00	11.50-13.50		Al 0.10-0.30
430	0.12 max	1.00	1.00	14.00-18.00		
430F	0.12 max	1.25	1.00	14.00-18.00		¶
446	0.35 max	1.50	1.00	23.00-27.00		N 0.25 max

* From Taylor Lyman and Carl H. Gerlach (eds.), "Metals Handbook," 1954 supplement, American Society for Metals.

† Other elements are as follows:

‡ Austenitic steels. Phosphorus is 0.045 per cent maximum and sulfur is 0.030 per cent maximum, except for type 303, in which phosphorus or sulfur or selenium is 0.07 per cent minimum, with zirconium or molybdenum 0.60 per cent maximum.

¶ Martensitic steels. Phosphorus is 0.040 per cent maximum and sulfur is 0.030 per cent maximum, except for types 416 and 430F, in which phosphorus or selenium is 0.07 per cent minimum, with zirconium or molybdenum 0.60 per cent maximum. Type 414 has been omitted from this article because of lack of extensive use.

Table 53. Physical Constants of Various Stainless Steels*

Constant	Austenitic				Martensitic		Ferritic		Range of all types of stainless steel
	Type 310	Type 316	Type 321	Type 347	Type 410	Type 416	Type 430	Type 446	
Density, g/cm ³ †.....	7.92	7.92	7.92	7.98	7.75	7.73	7.70	7.60	{ Cast 7.58-7.75 Wrought 7.60-7.98
Melting range, °C.....	1370-1425	1370-1400	1400-1425	1480-1510	1480-1510	1450-1510	1450-1480	
Electrical resistivity, μohm-cm...	20°C, 90	(76)	72	72	57	57	60	67	
	400°C	100	88	98	
Coefficient of linear thermal expansion, 10 ⁻⁶ /°C	800°C	121	111(700°C)	119	
	100°C, 14.0	16.0	16.5	16.5	10.2	10.1	10.0	8.8	
	600°C, 16.5	17.2	18.0	18.0	11.2	11.5(500°C)	10.5	10.0	
Thermal conductivity, cal/(cm)(sec)(°C)‡	1000°C, 19.5	19.7	20.0	20.0	13.2	12.4(787°C)	12.0	11.2	
	100°C, 0.032	0.035	0.037	0.037	0.060	0.060	0.057	0.050	
Specific heat, cal/(cm)(°C)¶.....	500°C, 0.040	0.050	0.052	0.052	0.065	0.062	0.058	
Magnetism.....	0.12 Nonmagnetic‡				0.11 Ferromagnetic		0.11 Ferromagnetic		

* Compiled from steel producers' data by J. H. Jackson and Erwin Eichen, Battelle Memorial Institute, 1952.

† Gram/cm³ × 62.43 = lb/ft³.

‡ Cal/(sec)(cm)(°C) × (2.419 × 10³) = Btu/(hr)(ft)(°F).

¶ Cal/(g)(°C) × 1 = Btu/(lb)(°F).

§ Can be slightly magnetic after cold working.

and solid moderator. This includes all supporting members, pressure vessel, tubes, valves, pumps, and the like. Although in some cases a single material like stainless steel serves as both cladding and structural material, such cases are not the rule.

The nuclear and physical properties considered desirable for Fuel Diluents and Cladding Materials are, in general, desirable for Structural Materials. In the selection of structural materials, more emphasis is placed on strength and corrosion resistance than on nuclear properties.

Aluminum, zirconium, and stainless steels have been most widely used as structural materials in thermal reactors. Of these, aluminum and zirconium have been described under Fuel Diluents and Cladding Materials.

As less emphasis is placed on low thermal-neutron capture cross section and more emphasis is placed on high-temperature properties, a number of metals and alloys warrant consideration. These include the metals molybdenum, titanium, and niobium and alloys of the so-called "superalloy" type developed for gas-turbine application.

As operating temperatures continue to rise, metals are no longer able to meet the requirements. Ceramics and cermets (ceramets) will be used for such applications.

4.2 Stainless Steels

The good corrosion resistance, reasonable cost, relatively high strength, and fairly low cross section of stainless steel have made it the leading structural material for reactor application. Although much emphasis has been placed on Type 347 stainless

Table 54. Typical Room-temperature Physical Properties of Wrought Stainless Steels*

AISI and ASTM designation, type No.	Tensile strength, 10 ² psi		Yield strength (0.2% offset), 10 ² psi		Elongation in 2 in., %		Reduction of area, %	Izod impact, ft-lb	Rockwell hardness		Modulus of elasticity, 10 ⁶ psi†
	Annealed	Hardened	Annealed	Hardened	Annealed	Hardened			Annealed	Hardened	
301	100.0	40.0	50.0	60.0	85.0	B90	29.0
302	80.0	30.0	50.0	60.0	85.0	B90	29.0
302B	90.0	35.0	40.0	60.0	80.0	B90	29.0
303	75.0	30.0	40.0	50.0	85.0	B90	29.0
304	80.0	30.0	50.0	60.0	60.0	B80	29.0
305	75.0	25.0	50.0	60.0	85.0	B90	29.0
308	80.0	30.0	40.0	50.0	70.0	B95	29.0
309	80.0	30.0	40.0	50.0	80.0	B95	29.0
310	80.0	35.0	40.0	50.0	80.0	B90	30.0
316	75.0	30.0	40.0	50.0	70.0	B95	29.0
317	75.0	30.0	40.0	50.0	70.0	B95	29.0
318	75.0	30.0	40.0	50.0	70.0	B95	29.0
321	85.0	30.0	40.0	50.0	80.0	B95	29.0
330	85.2	40.0	46.0	72.0	98.0	29.0
347	85.0	35.0	40.0	50.0	80.0	B95	29.0
403	65.0	200.0	38.0	165.0	20.0	2.0	50.0	85.0	B95	C45	30.1
405	60.0	32.0	20.0	50.0	25.0	B90	29.0
410	65.0	200.0	38.0	165.0	20.0	2.0	50.0	85.0	B95	C45	29.0
414	100.0	220.0	65.0	175.0	15.0	2.0	50.0	60.0	C30	C45	29.0
416	85.0	200.0	50.0	115.0	15.0	15.0	40.0	B90	C30	29.0
418	75.0	200.0	40.0	180.0	20.0	10.0	50.0	60.0	B96	C40	29.0
420	90.0	270.0	50.0	220.0	15.0	2.0	40.0	B100	C55	29.0
420F	85.0	245.0	50.0	175.0	15.0	5.0	40.0	B100	C50	29.0
430	65.0	35.0	20.0	40.0	B95	29.0
430F	65.0	35.0	15.0	40.0	29.0
431	105.0	220.0	90.0	185.0	20.0	10.0	60.0	70.0	C28	C45	28.0
440A	95.0	275.0	55.0	240.0	20.0	2.0	40.0	B100	C55	31.8
440C	100.0	285.0	60.0	275.0	8.0	1.0	35.0	B105	C58	31.8
440F	100.0	285.0	60.0	275.0	8.0	1.0	35.0	B105	C58	31.8
442	80.0	45.0	20.0	40.0	B95	29.0
446	75.0	45.0	20.0	40.0	B95	29.7
501	60.0	220.0	25.0	175.0	30.0	14.9	70.0	85.0	B85	C40	29.0
502	60.0	220.0	25.0	175.0	30.0	14.9	70.0	85.0	B85	C40	29.0

* Compiled from steel producers' data by J. H. Jackson and Erwin Eichen, Battelle Memorial Institute, 1952.

† Static determination.

steel for many applications, a steel containing less nickel and chromium could be used.

This would, of course, lead to savings both in dollars and in neutrons. Designations, compositions, and cross sections of a number of wrought stainless steels are given in Table 52.

Cast stainless steels find little application in reactors and are therefore not covered here. In those cases where a cast material is desirable, complete information may be found in the ASM "Metals Handbook."

Since availability, melting, fabrication, machining, and the like of stainless steels are covered well in the literature, these items will not be discussed here.

4.21 Physical Constants. Physical constants of typical stainless steels are shown in Table 53.

4.22 Mechanical Properties. Mechanical properties of wrought stainless steels are given in Tables 54 and 55. Additional data are available in *ASTM Special Technical Publication 52-A, 1950*.

4.23 Corrosion. Stainless steels have been used a great deal as reactor containers for water at temperatures around 600°F. Although stainless steels develop a dark-tarnish film and sometimes a powdery red or black oxide under these conditions, they are in general very satisfactory.

The oxidation resistance of stainless steels varies greatly with chromium content. Typical maximum operating temperatures are given in Table 55.

Table 55. Oxidation Resistance of Stainless Steels*

AISI and ASTM designation	Max temp for continuous operation with good resistance to scaling and oxidation, °F	AISI and ASTM designation	Max temp for continuous operation with good resistance to scaling and oxidation, °F
301	1650	410	1200
302	1650	414	1250
303	1650	416	1250
304	1650	418	1300
305	1650	420	1200
308	1700	420F	1200
309	2000	430	1500
310	2100	430F	1550
316	1700	431	1600
317	1700	440A	1400
318	1700	440C	1400
321	1700	440F	1400
347	1700	442	1800
403	1250	446	2050
405	1300		

* Compiled from various sources by J. H. Jackson and W. K. Boyd, Battelle Memorial Institute, 1952.

In general, the chromium-iron and austenitic chromium-nickel alloys are not resistant to molten metals such as zinc, tin, solder, babbitt, copper, brasses, aluminum, bismuth, lithium, bismuth-lead, bismuth-indium, and lead. Molten lead and molten sodium under certain conditions are exceptions. Stainless steels, in general, are corrosion resistant in sodium and sodium-potassium alloys at elevated temperatures provided the oxygen content of the sodium is below 0.02 per cent. The carbon content of the sodium must also be kept low. Types 304, 310, 316, 321, and 347 appear to resist potassium at temperatures of 1400 to 1600°F.

Stainless steels are generally not resistant to molten caustics.

4.3 High-temperature Alloys

A number of so-called superalloys containing nickel, chromium, cobalt, and iron have been developed for gas-turbine applications. Although many of these alloys have relatively high thermal cross sections, some are attractive for thermal reactor application because of their excellent high-temperature strength and oxidation

resistance. For intermediate or fast reactors, many of the alloys are attractive. Nominal compositions of a number of heat-resisting alloys are given in Table 56. Typical stress-rupture values are given in Table 57.

Table 56. Nominal Compositions of Heat-resisting Alloys*

Alloy	C	Mn	Si	Cr	Ni	Co	Mo	W	Cb	Ti	Al	Fe	Other
Iron-Chromium-Nickel Alloys													
Wrought alloys:													
A-286.....	0.08†	1.25	1.0†	14.75	25.5	1.25	2.10	0.35†	Rem	V 0.25
Croloy 15-15N.....	0.15†	2.0†	0.75†	16.0	15.0	1.55	1.40	1.05	Rem	N 0.15†
Discaloy 24.....	0.04	1.38	1.00	13.5	26.2	3.9	1.61	0.11	Rem
H.R. Crown Max.....	0.23	0.65	1.16	23.2	12.3	3.0	Rem
Haynes Alloy 88.....	0.07	1.50	0.50	12.5	15.0	2.0	0.6	0.6	Rem	B 0.15
Incoloy T.....	0.10	1.0	0.4	20.5	32.0	1.0	Rem
S-588.....	0.42	1.5	0.8	18.4	20.0	4.0	4.0	4.0	Rem
Timken 16-25-6.....	0.10	1.35	0.70	16.0	25.0	6.0	Rem	N 0.15
19-9 DL.....	0.30	1.10	0.60	19.0	9.0	1.25	1.2	0.40	0.30	Rem
19-9 DX.....	0.30	1.00	0.55	19.2	9.0	1.50	1.2	0.55	Rem
Cobalt-Nickel-Chromium-Iron Alloys													
Wrought alloys:													
K-42-B.....	0.05	0.7	0.7	18.0	43.0	22.0	2.5	0.2	13.0
N-155.....	0.15	1.5	0.5	21.0	20.0	20.0	3.0	2.5	1.0	Rem	N 0.15
Refractaloy 26.....	0.05	0.7	0.7	18.0	37.0	20.0	3.0	2.8	0.2	18.0
Refractaloy 80.....	0.10	0.6	0.7	20.0	20.0	30.0	10.0	5.0	14.0
S-590.....	0.42	1.25	0.4	20.5	20.0	20.0	4.0	4.0	4.0	24.0
S-816.....	0.38	1.20	0.4	20.0	20.0	43.0	4.0	4.0	4.0	4.0†
V-36.....	0.31	0.9	0.5	25.0	20.0	42.0	4.0	2.6	2.2	3.0
Nickel-base Alloys													
Wrought alloys:													
Hastelloy X.....	0.15	22.0	45.0	9.0	Rem
Inco 700.....	0.10	0.05	0.2	15.0	49.0	28.0	3.0	2.0	3.0	0.5
Inco 739.....	0.07	0.05	0.2	15.0	77.0	1.7	2.7	1.0
Inconel.....	0.04	0.35	0.20	15.5	76.0	1.0
Inconel W.....	0.04	0.60	0.25	15.0	75.0	2.5	0.6	7.0
Inconel X.....	0.03	0.5	0.3	15.0	73.0	0.6	2.3	0.9	6.5
Inconel X, 550.....	0.03	0.5	0.3	15.0	73.0	0.6	2.5	1.1	6.5
M-252.....	0.15	1.0	0.65	19.0	Rem	10.0	10.0	2.5	0.87	5.0†
Nimonic 75.....	0.12	0.4	0.6	20.0	76.0	0.4	0.06	2.4
Nimonic 80A.....	0.05	0.70	0.50	20.0	76.0	2.3	1.0	0.5
Nimonic 90.....	0.08	0.50	0.40	20.0	58.0	16.0	2.3	1.4	0.5
Waspaloy.....	0.10†	1.0†	0.75†	19.5	Rem	13.5	4.25	2.50	1.25	2.0†
Cast alloys:													
Hastelloy B.....	0.10	0.8	0.7	1.0	65.0	28.0	5.0
Hastelloy C.....	0.10	0.8	0.7	16.0	57.0	17.0	4.0	5.0
Cobalt-base Alloys													
Wrought alloy:													
Haynes 25 (L605).....	0.12	1.50	1.0	20.0	10.0	51.0	15.0	1.0
Cast alloys:													
Haynes 21.....	0.25	0.60	0.60	27.0	3.0	62.0	5.0	1.0
Haynes 30 (422-19).....	0.40	0.60	0.60	24.0	17.0	51.0	6.0	1.0
Haynes 31 (X-40).....	0.40	0.60	0.60	25.0	10.0	55.0	8.0	1.0
Haynes 36.....	0.40	1.2	0.50	19.0	10.0	54.0	14.5	1.0	B 0.03

* From Taylor Lyman and Carl H. Gerlach (eds.), "Metals Handbook," 1954 Supplement, American Society for Metals.

† Maximum.

Table 57. Typical Stress-rupture Properties of Heat-resisting Alloys*

Alloy	Stress, 10 ³ psi to rupture in 100 and 1,000 hr									
	1200°F		1350°F		1500°F		1600°F		1800°F	
	100	1,000	100	1,000	100	1,000	100	1,000	100	1,000
Iron-Chromium-Nickel Alloys										
Wrought alloys:										
A-286.....	61.0	48.0	35.0	21.5	13.8	7.7				
Croloy 15-15N.....				18.0		10.0				
Discaloy 24.....	55.0	41.0	32.0	20.0	15.0					
H.R. Crown Max.....	29.5	24.5	18.5	13.5						
Haynes Alloy 88.....	59.0	49.0	42.0	31.0	25.5	16.0	13.5			
Incoloy T.....	33.0	26.1	20.1	14.7	10.8	7.0				
S-588.....	41.0	30.0	25.0	18.0	15.0	10.0				
Timken 16-25-6.....	45.0	34.0	25.0	17.0	13.5	9.0				
19-9 DL.....	52.0	38.0	28.0	19.0	17.0	10.0				
19-9 DX.....	52.5	42.0								
Cobalt-Nickel-Chromium-Iron Alloys										
Wrought alloys:										
K-42-B.....	66.0	40.0	37.0	27.0	17.5	11.0				
N-155.....	50.0	40.0	31.0	24.0	18.0	13.0	12.0	8.0	5.0	2.5
Refractloy 26.....	80.0	63.0	51.0	38.0	27.0	18.0				
S-590.....	48.0	38.0	30.0	22.0	22.0	16.0	12.5	9.0	5.6	3.5
S-816.....	60.0	45.0	36.0	28.0	24.0	17.5	14.0	9.5	5.5	3.0
V-36.....			35.0	26.5	23.0	18.0	15.0	11.0	8.5	5.0
Nickel-base Alloys										
Wrought alloys:										
Hastelloy Alloy X.....	44.5	30.5	26.0	18.5	15.5	10.0				
Inco 700.....			73.0	60.0	42.0	30.0	28.0	18.5	6.5	3.5
Inco 739.....					34.0	20.0	19.0	11.0	5.3	
Inconel.....	22.0	14.5	10.5	6.8	5.7	3.7	4.2	2.7	2.5	1.6
Inconel W.....	74.0	54.0	45.0	30.0	19.0	11.5	7.5	4.8	3.2	
Inconel X.....	80.0	68.0	48.0	38.0	28.0	18.0	18.0	9.0	3.3	2.3
Inconel X, 550.....					34.0	21.0	18.0	10.2	3.3	
M-252.....			52.0	35.0	29.0	18.0	16.0	10.0		
Nimonic 80A.....	67.3	56.0	48.0	36.0	24.0	15.5	14.0	8.5		
Nimonic 90.....	76.1	63.0	50.6	38.0	28.0	17.9				
Waspaloy.....			57.5		31.5	20.0	19.5			
Cast alloys:										
Hastelloy Alloy B.....	51.0	40.5	35.0	25.5	18.5	12.7				
Hastelloy Alloy C.....	49.5	42.5	32.0	25.0	19.0	14.5	13.2	9.2		
Cobalt-base Alloys										
Wrought alloy:										
Haynes Alloy 25 (L605).....	70.0	58.0	43.0	33.0	23.0	17.0	15.5	10.5	7.0	3.8
Cast alloys:										
Haynes Alloy 21.....	51.0	44.2	32.0	2.0	22.0	14.2	16.7	13.2	9.4	7.0
Haynes Alloy 30 (422-19).....			47.0	36.0	28.6	21.7	15.8	14.8	10.0	7.1
Haynes Alloy 31 (X-40).....	55.0	46.0	45.0	33.0	28.4	23.4	21.0	18.0	11.3	9.8
Haynes Alloy 36.....			48.0	41.5	29.0	25.5	23.0	18.5	10.5	7.2

* From Taylor Lyman and Carl H. Gerlach (eds.), "Metals Handbook," 1954 Supplement, American Society for Metals.

Another type of alloy containing iron, chromium, and aluminum has excellent oxidation resistance at temperatures up to 2200°F but is not strong at these temperatures. Such alloys might well serve as oxidation-resistant claddings for stronger, less corrosion-resistant materials. Typical compositions and properties are given in Tables 58 and 59.

Table 58. Mechanical Properties of Iron-Chromium-Aluminum Alloys*

Cr, %	Al, %	C %	Temperature, °C	Density, g/cm ³	Coefficient of thermal expansion, 10 ⁻⁴ /°C	Tensile strength, 10 ⁴ psi	Elongation, %	Brinell hardness
16-18	4.5-18	0.03-0.07	Room	7.0-7.2	20-100°C, 14.5-15.0	85-99	15-25	150-170
23-27	4.5-7	0.03-0.07	Room	6.9-7.2	20-100°C, 14.5-15.0	99-114	15-20	160-180
40-45	7.5-12.0	0.03-0.07	Room	6.8-7.0	20-100°C, 16-17	114-142	2-7	240-260
65-68	7.5-12.5	0.03-0.07	Room	6.75-6.85	20-100°C, 16-17	270-300
17	5.6	0.03	200	85	25
25	5.07	0.03	200	86.5	23.2
17	5.6	0.03	400	79	28.2
25	5.07	0.03	400	81.5	22.4
17	5.6	0.03	800	10	67.1
25	5.7	0.03	800	10.1	67
10	5	Room	0-1000°C, 13.9	128
15	10	Room	0-1000°C, 16.3	230
25	10	Room	0-1000°C, 18.6	255
10	20	Room	0-1000°C, 26.9
11†	6	Room	86	22.5
18†	3	Room	96.5	25.0
11.5†	10	Room	99.8	5.0
25†	10	Room	128
25†	5	1200	0-1000°C, 15.3	100.5	18

* Compiled by the author from various sources.

† Annealed at 700°C.

‡ Arc-melted, hot-rolled.

Table 59. Creep Properties of Iron-Chromium-Aluminum Alloys*

Cr, %	Al, %	Other, %	Temperature, °F	Stress to rupture, psi				Stress to produce minimum creep, psi		
				0.5 hr	1 hr	10 hr	100 hr	1.0%/hr	0.1%/hr	0.01%/hr
25†	5	2200	695	550	270	100
25†	5	5 Ta	2200	1,100	950	500	310	400	330	240
25†	5	10 Ta	2200	1,335	1,160	720	420	550	420	320†
25†	5	2.5 Nb	2200	825	700	350	240
25†	5	5 Nb	2200	1,115	930	460	290	420	300	210
25†	5	5 W	2200	960	730	370	270	320	220
25†	5	5 Mo	2200	800	650	350	>230	290	175‡
25†	5	1 Be	2200	880	775	440	310

* Compiled by the author from various sources.

† Arc-melted, hot-rolled.

‡ Extrapolated.

4.4 Molybdenum, Titanium, and Niobium

Among the elements, molybdenum, titanium, and niobium are promising structural materials of intermediate cross section. Titanium possesses excellent corrosion resistance in hot water and has good strength at moderate temperatures. Molybdenum and niobium have excellent high-temperature strength but are not corrosion resistant. Physical constants of molybdenum, titanium, and niobium are given in Table 60. Mechanical properties of these elements are given in Table 61. High-temperature properties of several molybdenum alloys are given in Table 62.

Table 60. Physical Constants of Molybdenum, Titanium, and Niobium*

	Molybdenum	Titanium	Niobium
Thermal-neutron cross section:			
Barns/atom.....	2.4 ± 0.2	5.6 ± 0.4	1.1 ± 0.1
Cm ² /g.....	0.0151	0.070	0.0071
Density, g/cm ³	Cold-pressed bar, 6.0 Sintered bar, 9.8 Arc-cast, 10.2	4.507	8.57
Melting point, °C.....	2622 ± 10	1690	2415
Specific heat, cal/(gm)(°C).....	0°C, 0.0589 100°C, 0.0650 475°C, 0.0750	0-500°C, 0.1386	0°C, 0.0647
Electrical resistivity, μ ohm-cm.....	27°C, 5.78 727°C, 23.9 1127°C, 35.2 1927°C, 59.5 2622°C, 81.4	20°C, 47.8	18°C, 13.1
Thermal conductivity, cal/(sec)(cm)(°C).....	0°C, 0.32 1473°C, 0.26 2173°C, 0.17	25°C, 0.41	
Coefficient of linear thermal expansion, 10 ⁻⁶ /°C	27°C, 5.1 500°C, 5.1 1000°C, 5.5 1500°C, 6.2 2000°C, 7.2	25°C, 8.5	

* Compiled by the author from data found in U.S. Atomic Energy Commission, "Reactor Handbook," vol. 3, General Properties of Materials, AECD-3647, McGraw-Hill Book Company, Inc., New York, 1955.

Table 61. Mechanical Properties of Molybdenum, Titanium, Niobium, and a Niobium-Titanium Alloy*

	Molybdenum				Titanium†				Niobium	Nb-10 w/o Ti	
	38	93	150	200	93	200	315	538			
Tensile strength:											
Test temperature, °C....	38	93	150	200	93	200	315	538	1200	1200	
Yield strength, 10 ³ psi....	40	24	15	12	90	73	56	17			
Ultimate strength, 10 ³ psi	67	55	52	47	102	84	66	22	14.7	15.6	
Hardness, Vickers.....	Room temp (arc-cast, hot-rolled), 225 Room temp (annealed at 1150°C), 187 100°C, 110 300°C, 69 400°C, 59 500°C, 58 600°C, 56 700°C, 54				Room temp, 200-220 100°C, 210 300°C, 120 500°C, 59 600°C, 39 800°C, 13 900°C, 7				Room temp (arc-melted sheet), 140 Room temp (annealed sheet), 88 870°C (arc-melted), 63.2	Room temp (arc-melted), 187 870°C (arc-melted), 156	
100-hr creep rupture:	Recrystallized, arc-cast, cold worked; tested in vacuum				In sodium with calcium getter						
Temperature, °C.....	870	980‡	1090		425				Recrystallized 980	Cold-rolled 980	Arc-melted 980
Stress, 10 ⁴ psi.....	18.5	12.5	10		.20				15	16.5	12.5
Creep rate, %/hr.....	0.06	0.5	0.11						0.15	0.077	0.07

* Compiled by the author from various sources.

† Commercial grade.

‡ 57-hr rupture time.

Table 62. Maximum Stress-rupture Strengths Shown by Molybdenum-base Alloys at 1600, 1800, and 2000°F*

Alloy	Stress, psi, to produce rupture at		
	1600°F	1800°F	2000°F
In 1,000 Hr			
0.75% Cb	65,000	42,000	12,000
0.092% Zr	58,000	45,000	
0.46% Ti	58,000	43,000	16,000
In 100 Hr			
0.75% Cb	69,000	51,000	22,000
0.092% Zr	64,000	56,000	> 25,000
0.46% Ti	66,000	53,000	> 25,500
0.50% Ti	> 70,000	55,000	> 25,000
In 10 Hr			
0.75% Cb	75,000	60,000	39,000
0.092% Zr	74,000	63,000	
0.46% Ti	76,000	63,000	46,000

* From Howard C. Cross and Ward F. Simmons, "Alloys and Their Properties for Elevated Temperature Service," Battelle Memorial Institute.

NOTE 1: All 1,000-hr rupture strengths are estimated.

NOTE 2: All above values are for materials tested in stress-relieved condition.

4.5 Ceramics and Cermets

For extremely high-temperature operation, it is necessary to depend on materials other than metals. These may be either ceramics or cermets.

Ceramic materials as a class have excellent high-temperature strength and may be oxidation resistant. They suffer from low ductility and poor thermal shock resistance. The leading contenders for nuclear application, BeO , Be_2C , MoSi_2 , and SiC , have been covered in detail in Art. 2 under Fuel Diluents and Cladding Materials.

Cermets, a combination of a refractory ceramic and a metallic binder, attempt to capture the worth-while properties of both metals and ceramics without retaining the poor qualities of either. Such materials have good high-temperature strength and oxidation resistance. Compositions of leading cermets are given in Table 63. Rupture data for cermets are shown in Fig. 27.

A comparison of high-temperature strength of a large number of high-temperature materials is given in Fig. 28.

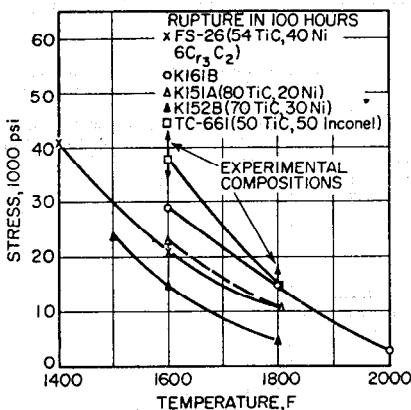


FIG. 27. Rupture-strength curves for cermets. (Reprinted from Howard C. Cross and Ward F. Simmons, *Alloys and Their Properties for Elevated Temperature Service*, Battelle Memorial Institute.)

Table 63. Cermets*

Alloy	Chemical composition, %			
	TiC	Ni	Mo	Cr ₂ C ₃
FS-26	54.3	40.0	...	5.7
FS-27	42.9	50.0	...	7.1
K-151A	80	20		
K-152-B	70	30		
K-162B	70	25	5	
TC-66-I	50	Balance Inconel (infiltrated)		

* From Howard C. Cross and Ward F. Simmons, "Alloys and Their Properties for Elevated Temperature Service," Battelle Memorial Institute.

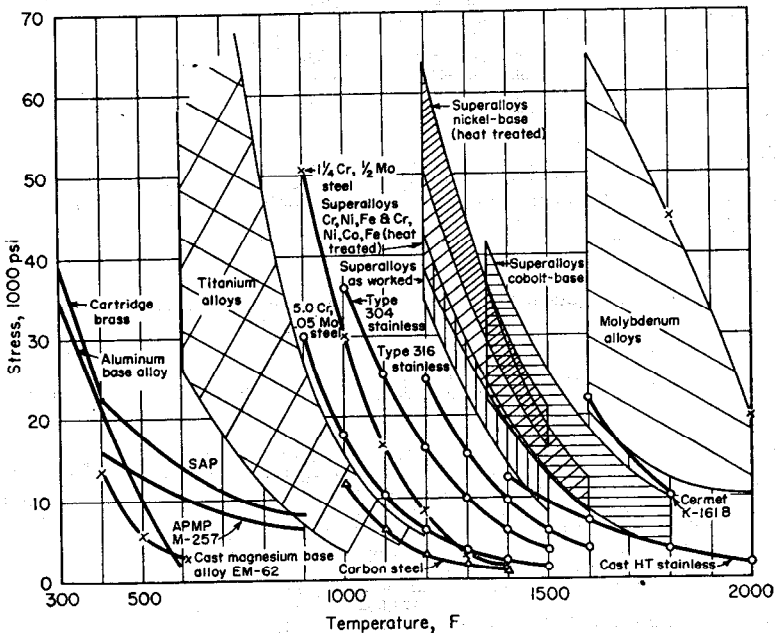


FIG. 28. Stress vs. temperature curves for rupture in 1,000 hr. (Reprinted from Howard C. Cross and Ward F. Simmons, *Alloys and Their Properties for Elevated Temperature Service*, Battelle Memorial Institute.)

5 CONTROL AND ABSORBER MATERIALS

Materials to be used as absorbing controls in reactors need to possess a number of nuclear and metallurgical properties. These include:

1. A high cross section for absorption of neutrons
2. Adequate strength
3. Low mass to permit rapid movement
4. Good corrosion resistance to reactor coolant
5. Chemical and dimensional stability under heat and irradiation
6. Availability, fabricability, and reasonable cost

Boron and cadmium of the better known elements have high absorption cross sections and have been used for control materials. In use, the boron is usually incorpo-

Table 64. Physical Constants of Boron, Cadmium, and Hafnium*

	Boron	Cadmium	Hafnium
Thermal-neutron cross section: Barns/atom.....	750 ± 10	2400 ± 200	115 ± 15
Cm ² /g.....	42	12.9	0.39
Density, g/cm ³	Crystal, 2.33 Amorphous, 2.3	Cast, 8.648 Cold-worked, 8.694	Calculated, 13.36 Measured (crystal bar), 13.36
Melting point, °C.....	2000-2300	321	2130 ± 15
Heat of vaporization (25°C), cal/mole.....	90,000	26,750	
Heat capacity, cal/(mole)(°C) †	1.54 + 440 × 10 ⁻⁷ T	5.31 + 2.94 × 10 ⁻⁷ T	6.00 + 0.524 × 10 ⁻⁷ T
Temperature range, °C.....	25-927	25-321	25-2227
Electrical resistivity, μohm-cm	Pressed powder 100°C, 13.20 320°C, 36 600°C, 0.08	18°C, 7.54 100°C, 9.82 300°C, 16.50	100°C, 47.1 300°C, 75.0 600°C, 106.3
Linear coefficient of thermal ex- pansion, 10 ⁻⁶ /°C	Crystalline 20-750°C, 8.3	20-100°C, 31.8	0-1000°C, 5.9
Thermal conductivity, cal/(sec)(cm)(°C)	B.C. density 2.5 100°C, 0.29 300°C, 0.22 500°C, 0.18 700°C, 0.155	Room temperature, 0.22 435°C, 0.114	

* Compiled by the author from data found in U.S. Atomic Energy Commission, "Reactor Handbook," vol. 3, General Properties of Matter, AECD-3647, McGraw-Hill Book Company, Inc., New York, 1955.

† T in degrees Kelvin.

Table 65. Mechanical Properties of Boron Steel, Boron Stainless Steel, Cadmium, and Hafnium*

	Boron steel †	Boron stainless steel ‡	Cadmium	Hafnium
Tensile strength, psi	Annealed 1550°F, 1 hr F.C. 0.2% yield: 67,300 Ultimate: 86,400 Normalized 1600°F, 1 hr A.C. 0.2% yield: 100,000 Ultimate: 136,000	Annealed 2000°F, 1 hr W.Q. 0.2% yield: 58,400 Ultimate: 147,600 Annealed 2000°F, 1 hr W.Q.; aged 16 hr at 1470°F A.C. 0.2% yield: 136,500 Ultimate: 174,000	99.95% cadmium, chill-cast and aged at room temperature Ultimate: 10,300 99.95% cadmium, cold-worked 70%, aged at room temperature Ultimate: 13,700	Arc-melted crystal bar 0.2% yield: 40,800 Ultimate: 67,500
Modulus of elasticity, 10 ⁶ psi	Annealed 1550°F, 1 hr F.C. 32.5 Normalized 1600°F, 1 hr A.C. 32.5	Annealed 2000°F, 1 hr W.Q. 29.2 Annealed 2000°F, 1 hr W.Q.; aged 16 hr at 1470°F A.C. 29.5	7.1-10	14.0
Hardness	Annealed 1550°F, 1 hr F.C. Rockwell: 21.5 C to 21.8 C Normalized 1600°F, 1 hr A.C. Rockwell: 33 C to 36.2 C	Annealed 2000°F, 1 hr W.Q. Rockwell: 35.4 C Annealed 2000°F, 1 hr W.Q.; aged 16 hr at 1470°F A.C. Rockwell: 36.6 C	1-in. chill casting Brinell: 21-23	Cold-swaged, annealed at 1000°C; cold-swaged 20%

* Compiled by the author from various sources. F.C. = furnace cooled. A.C. = air cooled.

† SAE 4140 + 1.25 per cent boron.

‡ 17-7 stainless steel + 1.25 per cent boron.

rated in steel or otherwise contained. Cadmium may be protected by cladding or may itself be clad to a structural material. Recently hafnium, the high-cross-section material removed from zirconium, has gained prominence as a control material. Hafnium has good strength and excellent corrosion resistance in water. For many applications it is an ideal material. Properties of boron, cadmium, and hafnium are given in Tables 64 and 65.

A number of the rare earths have high cross sections and may eventually be useful as control materials. Some of their properties are given in Table 66.

Table 66. Physical and Chemical Constants of the Rare-earth Metals*

Element	Thermal-neutron-absorption cross section, barns/atom	Density, g/cm ³	Melting point, °C	Boiling point, °K	Heat of vaporization, kcal/mole	Heat of fusion, kcal/mole	Crystal structure at room temperature
Sc	13 ± 2	3.016	1550-1600	2750†	73†	3.8	Hcp
Y	1.38 ± 0.14	4.472	1500	3500†	94†	4.1	Hcp
La†	8.9 ± 0.3	6.162	920	4515	81	2.4	Hcp
Ce	0.70 ± 0.08	6.768	804	3200	79	2.2	Fcc
Pr	11.2 ± 0.6	6.769	935	3290	79	2.4	Hcp
Nd	44 ± 2.0	7.007	1024	3450	69	2.6	Hcp
Pm	1300	3000†	70†	3.0	
Sm‡	6500 ± 1000	7.540	1052	1900†	46†	2.6	Rhom-hcp
Eu	4500 ± 500	5.166	1700†	42†	2.5	Bcc
Gd	44,000 ± 2000	7.868	1350	3000†	72†	3.7	Hcp
Tb	44 ± 4	8.253	1400-1500	2800†	70†	3.9	Hcp
Dy	1100 ± 150	8.556	1400	2600	67	4.1	Hcp
Ho	64 ± 3	8.799	1500	2600†	67†	4.1	Hcp
Er	166 ± 16	9.058	1500-1550	2900†	70†	4.1	Hcp
Tm	118 ± 6	9.318	1550-1650	2400†	51†	4.4	Hcp
Yb	36 ± 4	6.959	824	1800†	32.5†	2.2	Fcc
Lu	108 ± 5	9.849	1650-1750	2200†	59†	4.6	Hcp

* Compiled by the author from U.S. Atomic Energy Commission, "Reactor Handbook," vol. 3, General Properties of Materials, AECD-3647, McGraw-Hill Book Company, Inc., New York, 1955, and unpublished information from Ames Laboratory, Iowa State College.

† Estimated values.

‡ Fcc La has a lattice parameter of $a_0 = 5.302$ Å; density = 6.190 g/cm³. The low-temperature transition occurs between 300 to 350°C.

§ The true structure of Sm is rhombohedral; $a_0 = 8.996$ Å = $23^\circ 13'$.

Boral⁴ is a mixture of 35-50 weight per cent B₄C and aluminum. It is available in sheet form $\frac{1}{8}$ in. and $\frac{1}{4}$ in. over-all thickness, including 0.020-in.-thick aluminum clad. The thermal conductivity is 25 Btu/(hr)(ft)(°F) at 200°F and 19 Btu/(hr)(ft)(°F) at 500°F. The density is 2.53 g/cm³ and specific heat 0.175 cal/g. The heat generation from the (n, α) reaction is 7.4 watts/ft² in a thermal-neutron flux of 10^{10} neutrons/(cm²)(sec)—the heat generation is substantially independent of thickness, since both the $\frac{1}{8}$ - and the $\frac{1}{4}$ -in. sheets are substantially black to thermal neutrons. The cost is \$15 per sq ft for $\frac{1}{8}$ -in. sheet and \$18 for $\frac{1}{4}$ -in. sheet.

REFERENCES

1. Katz, J. J., and Eugene Rabinowitz: "Chemistry of Uranium," NNES, Div. VIII, vol. 5, chap. 4, McGraw-Hill Book Company, Inc., New York, 1951. (Unclassified.)
2. Saller, H. A., and F. A. Rough: "Compilation of U.S. and U.K. Uranium and Thorium Constitutional Diagrams," BMI-1000, June 1, 1955.
3. Lustman, B., and Frank Kerze, Jr. (eds.): "The Metallurgy of Zirconium," NNES, Div. VII, vol. 4, McGraw-Hill Book Company, Inc., New York, 1955.
4. U.S. Atomic Energy Commission: "Reactor Handbook," vol. 1, Physics, p. 750, McGraw-Hill Book Company, Inc., New York, 1955.

BIBLIOGRAPHY

1. U.S. Atomic Energy Commission: "Reactor Handbook," vol. 3, sec. 1, General Properties of Materials, AECD-3647, McGraw-Hill Book Company, Inc., New York, 1955.
2. Lyman, Taylor (ed.): "Metals Handbook," American Society for Metals, 1948 ed.
3. Lyman, Taylor, and Carl H. Gerlach (eds.): "Metals Handbook," 1954 Supplement, American Society for Metals.
4. Saller, H. A.: Metals for Reactor Core Construction, *Science*, **119** (3079): 4 (Jan. 1, 1954).
5. Keeler, John R.: Thorium, in "Engineering Materials Handbook," C. L. Mantell (ed.), McGraw-Hill Book Company, Inc., New York, 1958.
6. "Handbook on Titanium Metal," Titanium Metals Corporation, 4th ed., July 15, 1951.
7. Lyons, R. N., *et al.*: "Liquid Metals Handbook," U.S. Atomic Energy Commission, Department of the Navy, NAVEXos, June 1, 1950.
8. Edwards, J. D., F. C. Frary, and Zay Jefferies: "The Aluminum Industry," McGraw-Hill Book Company, Inc., New York, 1930.
9. White, D. W., and J. Burke (eds.): "The Metal Beryllium," American Society for Metals, 1955.
10. Howe, John P.: The Properties of Graphite, *J. Am. Ceram. Soc.*, **35** (11) (1952).
11. Parke, R. M.: Molybdenum, A High Temperature Metal, *Metal Progr.*, **60** (1): 81-96 (1951).
12. Smith, C. Stanley: Properties of Plutonium Metal, *Phys. Rev.*, **94** (4) (May 15, 1954).
13. "Zirconium and Zirconium Alloys," American Society for Metals, 1953.

10-3 STRUCTURAL MATERIALS IN HIGH-TEMPERATURE WATER REACTOR SYSTEMS

BY

Roger Sutton

The problem of selection of structural materials for use in high-temperature water reactors is more involved than similar selections for conventional use because of unique factors peculiar to nuclear reactors, such as radiation effects, as well as the conditions normally encountered in high-temperature water systems. The choice of materials is, as in conventional systems, based on considerations of corrosion, galling, wear, mechanical properties, and fabricability. Information concerning the two last items is available in Sec. 10-2.

In all cases where trade names and proprietary designations are used, it is to be understood that such nomenclature is used to indicate the material actually tested. There is no implication of superiority of these products over equivalent grades produced by other manufactures.

1 CORROSION

Materials in reactor systems must generally be much more corrosion resistant than in nonnuclear systems, both because of transport of radioactive material to the external system and because of deposition of corrosion products on fuel elements and other heat-transfer surfaces.

1.1 Water Conditions

Several conditions of service must be taken into consideration in the selection of materials for use as guides, bearings, gears, shafts, seals, etc. The major ones are

1. Water temperature
2. Water velocity
3. Gas content of the water
4. Type and amount of dissolved or suspended solid matter in the water
5. pH of the coolant

1.11 Inhibitors. Corrosion inhibitors used in conventional fossil-fuel power-plant systems cannot be used in nuclear systems. Organic inhibitors would be decomposed by irradiation. Inorganic inhibitors would become radioactive and seriously limit accessibility to the system for maintenance and repairs. Inhibitors would also prohibit use of ion-exchange systems.

1.12 Irradiation Effects. Neutron irradiation causes dissociation of water. At elevated temperatures the net rate of dissociation is decreased by an increase in the rate of the back reaction. See Art. 3.1 of Sec. 10-5.

1.13 Dissolved Gases. With continuous degassification the gases resulting from the net radiolytic dissociation of water will achieve a steady-state concentration. An experimental in-pile loop of AISI 347 stainless steel, when operated at 500°F with continuous degassing, maintained an oxygen concentration of 0.02 to 0.5 ml/liter (STP). Similar systems, operated without degassification, reached a state of pseudo-equilibrium with a hydrogen content of several milliliters per liter (STP) as a result of the

intensification of the recombination reaction from the high gamma intensity and the removal of oxygen from the system by corrosion processes prior to equilibrium. The initial corrosion could be almost entirely suppressed by initially pressurizing the system with hydrogen. The pseudo-equilibrium concentration of hydrogen is a function of neutron and γ flux, water temperature, ionic impurities in the water, and, indirectly, the over-all corrosion rate of the system. Furthermore, oxygen gas has been injected into the coolant system up to at least 30 ml/liter (STP), and hydrogen gas has been injected up to over 500 ml/liter (STP). The major effect of these additives on corrosion rate is attained at approximately 3 ml/liter O_2 or 25 ml/liter H_2 . Hence it is possible to operate a high-temperature water reactor either degassed, under steady-state conditions in a closed system, or with the deliberate addition of gases, particularly hydrogen.

1.14 Other Control. In addition, through the use of filters, deionizing columns, and addition agents such as sodium hydroxide and sulfuric acid, it is possible to control, at least partially, the pH and purity of the coolant.

1.2 Selection Criteria

From the corrosion standpoint, tentative criteria for the selection of the materials to be used for the critical components of a high-temperature, high-pressure, water-cooled, and moderated power reactor might be as follows:

1. Satisfactory for unrestricted service: Rate of weight change less than 20 mg/(dm²)(month), no local attack, and thin adherent film.
2. Usable in special applications and limited quantities. Rate of weight change between 20 and 200 mg/(dm²)(month), no local attack, and no evidence of thick or loose films.
3. For use only where other conditions dictate absolute necessity. Rate of weight change over 200 mg/(dm²)(month), minor local attack, and no loose, flaky scale.

1.3 Corrosion Data

Data reported by S. C. Datzko^{1*} are summarized in Table 1. The addition of over 50 ml/liter of hydrogen permits the widest selection of materials under the conditions chosen for presentation in the table. These conditions were:

Temperature, °F.....	500
Pressure, psig.....	2,000
Flow past specimens, fps.....	30
Resistivity of water, ohm-cm.....	>500,000
Ion-exchanger bypass.....	approx 0.1% of total flow

Since the data are from as-tested specimens, a weight loss indicates "sloughing" of the corrosion product, and materials showing significant weight loss are, in general, the least desirable.

2 GALLING AND WEAR

2.1 Galling

Parts subject to relative motion (as in bearings, seals, control drive mechanisms, and other components involving rotary or translatory motion) must function without conventional lubricants and must therefore be resistant to galling as well as to corrosion and wear.

Galling is the physical manifestation of the union of the lattices at the high spots of two contacting surfaces moving relative to one another. If the lattices are widely dissimilar, the effect may be negligible, although John M. Bailey and Douglas Godfrey² propose a mechanism of fretting wherein it is postulated that the occurrence and extent of adhesion or cold welding were indicated during the first few cycles of fretting of practically all material combinations. Copper and iron, for instance, showed significant adhesion or cold welding to glass. If the metals are similar, and particularly if the materials involved are soft, local welding will occur. If motion is to con-

* Superscript numbers refer to References at end of subsection.

tinue, these welds must be broken with resulting surface damage. The resultant "scoring" is termed galling, and the ultimate result will be increasing temperatures and pressures on the high spots, finally causing seizure. From the earliest stages in the development of the nuclear power plant the problem of corrosion was recognized. As a result, early designs made generous use of 18-8 type stainless steels. However, these steels cannot be used for sliding surfaces, since even the very simplest mechanical parts may gall and seize when assembly is attempted or, at best, after a few cycles of operation. Since galling is inevitably related to wear, data available apply to both. Much of the wear encountered in these systems involving boundary lubrication is promoted by incipient galling.

Table 1. Corrosion of Metals in High-temperature Water*

Material	Weight change mg/(dm ²)(month)					
	Hydrogen			Degassed	Oxygen	
	500 ml/ liter	50 ml/ liter	25 ml/ liter		0.3 ml/ liter	3.0 ml/ liter
Zirconium.....	5	14	12	10	1.5
Zirconium - 2.5% Sn.....	-5	6	7	6
Zirconium - 5% Sn.....	8	4	5	10	9
AISI 302.....	0	-1	0	3	2
AISI 303.....	0	2	-4	2	3
AISI 304L.....	0	0	-7	1	1
AISI 304.....	-1	0	-2	2	3
AISI 316.....	2	1	2	-4	1	2
AISI 347.....	0	0	0	-8	2	3
AISI 304 (nitrided).....	-175	-200	-129	-12	16
AISI 347 (nitrided).....	-250	-168	-12	11
AISI 410 (hardened).....	-40	3	-20
AISI 44C (hardened).....	-36	-7	-17
17-4 PH.....	-41	1	-1
17-7 PH.....	-70	-74	1	2
17-7 PH (nitrided).....	92	-49	-12	13
USS-W (nitrided).....	-170	-97	-5	16
Carpenter 20.....	-1	-7	-40	2	-1
Stellite 3.....	-7	-3	-100	-40
Stellite 19.....	-5	-6	-7	-10	-150	-80
Stellite 21.....	-1	-10	-10	-18
Stellite 25.....	-7	-15	-30	-50
A-Nickel.....	3	-300	-6	-25
70-30 cupronickel.....	0	-200	-1300	-400
Inconel.....	0	0	-3	-36	-20
Inconel X.....	-2	-6	-33
Monel.....	-60
K Monel (age-hardened).....	20	-200	-60
K Monel (annealed).....	-50
20% Pd, 30% Cd, 50% Ag.....	2	95	-2100	-6600
15% Pd, 30% Cd, 55% Ag.....	-30	38	-2900	-9000

Temperature, 500°F; Water velocity, 30 fps.

* Summarized from S. C. Datzko, "Corrosion of Metals in High Temperature Water," ANL-5354.

2.2 Wear

Wear is the displacement of material as a consequence of relative motion between surfaces. The result is a change in clearance brought about by surface damage. This interferes with the performance of the device and ultimately progresses to a point where the unit can no longer perform the function for which it was designed.

2.21 Abrasion. When relative motion is introduced, high temperatures are developed at the points of actual contact. At the points where these high tempera-

tures are developed, chemical reactions are accelerated. With air or water present, oxidation is the most usual reaction. Therefore, wear products in the form of oxides are produced. Since metallic oxides are generally abrasive in character, there is an increase in wear rate. Also, general corrosion may interfere with clearances and may also produce products that result in added wear by abrasion and damage of surface finish.

2.22 Fatigue Cracking. Fatigue, i.e., failure of a material by rupture as a result of cyclic stressing, is a function of the degree of stress and the numbers of cycles of operation. Because of other limitations, the stresses in reactor components are usually so low that this mechanism of failure may be neglected.

2.23 Plastic Deformation. This type of failure occurs when soft materials are overloaded with resultant undesirable changes of geometry. If the deformed material is the supporting medium of a harder, more brittle surface, spalling will result. If the material is homogeneous, deformation will eventually result in loss of function.

2.3 Wear Testing

Several factors are influential in determining the extent of wear and galling. The most important are:

1. Environment, i.e., the medium in which the moving elements operate, its temperature, and its pressure
2. Geometry, including surface finish
3. Load
4. Relative surface velocity
5. Materials
6. Service conditions, e.g., whether continuous or intermittent operation is involved

2.31 Piston-cylinder Tests. R. C. Westphal and J. Glatter³ have reported on the wear resistance of a number of materials combinations as determined by split piston-cylinder tests involving linear motion. The experimental data were obtained from tests performed under the following conditions:

Water temperature, °F.....	500
Resistivity of water (min), ohm-cm.....	500,000
Oxygen content, ml/liter STP.....	5-16

The last condition was maintained by pressurizing the system at 500°F (with argon gas containing 5 per cent oxygen) to 100 psi above the saturated steam pressure of 665 psi. The stress was low (3 lb radial load applied to a split piston 0.747-in. diameter) in order to minimize seizure. Test duration was approximately 500,000 cycles.

Table 2 is a partial summary of the results of these tests, arranged in ascending order of wear factor. These particular materials combinations were selected to cover the full range of wear-factor values observed and to illustrate the influence of several variables on the mechanisms of wear. Materials combinations were arbitrarily classified into five groups by the authors: values up to 25, excellent; from 25 to 50, good; from 50 to 100, fair; from 100 to 200, poor; and those over 200 unusable.

It is seen that nitrided surfaces have the lowest wear factor of any observed. Unfortunately, materials in this group may have insufficient corrosion resistance in high-temperature, high-pressure water.

Second in wear resistance is hard industrial chromium plate. It was found that it could be used successfully with a wide variety of mating materials. Corrosion resistance is assured by plating on a corrosion-resistant base of stainless steel, since any porosity in the plate might otherwise cause eventual lifting of the plate. If unit loads are significant, the use of corrosion-resistant base material of more strength and hardness than the usual AISI 300 types is indicated in order to provide a better resistance to deformation and subsequent cracking and spalling of the chromium plate. Precipitation-hardening stainless steels such as 17-4 PH have been used successfully. A danger in the use of chrome plate must be recognized, namely, the

possibility of flaking or scuffing. This can be minimized by careful control of the plating process.

It will also be noted that excellent wear resistance was found with martensitic straight chromium stainless steels, particularly AISI 440 C, as compared with nickel-chromium stainless-steel grades. These straight chromium stainless steels are not

Table 2. Partial Summary of Piston-cylinder Wear Tests*
(First item is the piston)

Materials combinations†	Wear factor
	mg wt loss/(lb. load) (million cycles), oxygenated water
1. Nitrided type 347 ss-nitrided 347 ss	0.0
2. Nitrided chrome-plate-nitrided chromium	0.0
3. As-plated chrome-nitrided titanium	4.7
4. Metamic LT-1-nitrided Armco 17-4 PH	7.0
5. Honed chrome plate-Stellite 3	8.3
6. Type 440-C ss-type 440-C ss	15
7. Type 410 ss-Stellite 3	16
8. Honed chrome plate-Kentanium K-151	16
9. Honed chrome plate-Armco 17-4 PH	20
10. Honed chrome plate-nitrided Armco 17-4 PH	22
11. Stellite 1-type 440 C ss	23
12. Stellite 12-honed chrome plate	25
13. Stellite 6-Stellite 6	27
14. Nitrided Armco 17-4 PH-nitrided titanium	28
15. U.S. Steel type W (SA)-Stellite 3	31
16. Wall Colmonoy 6-Stellite 6	32
17. As-plated chrome-as-plated chrome	34
18. Armco 17-4 PH-honed chrome plate	35
19. Haynes 21 (SA)-Stellite 6	39
20. Carboloy 608 (chrome carbide)-honed chrome plate	41
21. Haynes 21 (SA)-Haynes 21 (SA)	51
22. Stellite 3-honed chrome plate	55
23. Stellite 3-Wall Colmonoy 6	61
24. Armco 17-4 PH-Stellite 6	62
25. Honed chrome plate-Stellite 6	65
26. Stellite 3-Stellite 3	71
27. Armco 17-4 PH-Carboloy 608 (chrome carbide)	72
28. Metamic LT-1-Metamic LT-1	76
29. Stellite 3-Haynes 25 (CW)	77
30. KR-Monel-honed chrome plate	81
31. Stellite 1-Stellite 6	88
32. Haynes 21 (PH)-Haynes 21 (SA)	98
33. Haynes 21 (SA)-honed chrome plate	102
34. Honed chrome plate-Haynes 25 (CW)	105
35. Stellite 3-Armco 17-4 PH	115
36. Haynes 21 (PH)-Haynes 21 (PH)	120
37. U.S. Steel type W-Stellite 3	130
38. Honed chrome plate-honed chrome plate	135
39. Honed chrome plate-Hastelloy D	140
40. Type 304 ss-as-plated chrome	150
41. Armco 17-4 PH-Stellite 3	150
42. KR-Monel-Stellite 3	170
43. Stellite 3-Hastelloy D	300
44. Armco 17-4 PH-Armco 17-4 PH	460
45. Everdur 1012-Haynes 21 (SA)	660
46. Stellite 3-Armco 17-4 (SA)	700
47. Everdur 1012-honed chrome plate	830
48. Type 304 ss-type 304 ss	3,200

* R. C. Westphal and J. Glatzer, WAPD-T-64.

† SA, solution annealed; PH, precipitation hardened; CW, cold-worked.

suitable for use in oxygenated water because of corrosion but are often usable in hydrogenated water.

Metamic LT-1, which is a cermet consisting of chromium and alumina, exhibited excellent wear and corrosion resistance when run in combination with an abrasive resistant mating material (Table 2, No. 4). Against mating materials with slightly less abrasion resistance, the wear factor was found to be high.

The cobalt-base alloys, as represented by the various Stellites, show excellent to very good resistance to wear and galling, both against themselves and in combination

with other types of material. This, coupled with their more than adequate corrosion resistance, makes these alloys among the most useful of those available.

Effect of Hardness. Hardness has a very pronounced yet inconsistent effect on wear. For example, nitrided surfaces, chrome plate, and Stellites have decreasing

Table 3. The Effect of Corrosion on Wear in Piston-cylinder Tests*

Materials combinations†	Wear factor, mg wt loss/(lb load) (million cycles)	
	Oxygenated water	Hydrogenated water
Honed chrome plate-Stellite 3.....	8.3	0.3
Honed chrome plate-Armco 17-4 PH.....	20	13
Armco 17-4 PH-honed chrome plate.....	35	11
Haynes 21 (SA)-Haynes 21 (SA).....	51	19
Stellite 3-Wall Colmonoy 6.....	61	60
Honed chrome plate-Stellite 6.....	65	24
Stellite 3-Stellite 3.....	71	34
Stellite 3-Haynes 25 (CW).....	77	47
KR-Monel-honed chrome plate.....	81	1.1
Haynes 21 (SA)-honed chrome plate.....	102	28
Stellite 3-Armco 17-4 PH.....	115	33
U.S. Steel type W-Stellite 3.....	130	11
Honed chrome plate-Hastelloy D.....	140	45
Armco 17-4 PH-Stellite 3.....	150	25
KR-Monel-Stellite 3.....	170	31
Stellite 3-Hastelloy D.....	300	43
Everdur 1012-Haynes 21 (SA).....	660	18
Everdur 1012-Honed chrome plate.....	830	2.2

* R. C. Westphal and J. Glatter, WAPD T-64.

† SA, solution annealed; PH, precipitation hardened; CW, cold-worked.

hardness values that correspond to decreasing wear resistance. However, many contradicting examples can be cited, for instance,

1a. Armco type 17-4 PH vs. Stellite No. 3 (R_c 54 to 60) had a wear factor almost three times greater than b.

b. Armco type 17-4 PH vs. Stellite No. 6 (R_c 40 to 46) (Table 2, Nos. 41 and 24).

2a. U.S. Steel type W vs. Stellite No. 3 with the type W material at maximum hardness (R_c 42 to 45), had a wear factor of (130).

b. If the hardness was reduced to R_c 39 by overaging or was in the solution-annealed condition (R_c 24), the wear factor was substantially reduced (31).

3a. With Armco type 17-4 PH stainless steel the effect of hardness was directly opposite. The wear factor for fully hardened material (R_c 45) in combination with Stellite No. 3 was 115.

b. When the material was solution-annealed (R_c 32) the wear factor rose to 700.

4a. Stellite No. 21, when run in combination with itself, resulted in the least wear when both elements were solution annealed.

b. More wear when one element was hardened.

c. Most wear when both elements were hardened.

Effect of Surface Finish. Surface finish is another variable that affects the wear resistance and galling tendencies of different materials combinations. When the mating materials differ greatly in hardness, it is important that the harder of the two have a good finish; otherwise wear is accelerated by continuous cutting action on the softer material by the rough surface followed by abrasive wear. Under certain circumstances wear can be reduced by controlling the degree of roughness of at least one of the mating surfaces. As an example, as-plated chromium vs. as-plated chromium, with a surface roughness of 30 to 40 μ in., has a wear factor of 34, whereas the same materials combination with honed surfaces and 1.0- μ in. surface roughness has a wear factor of 135. Light sandblasting of large bolt threads made of 18-8 stainless steel was successful in preventing seizure, and sandblasted journals or

sleeve bearings, made of materials that ordinarily seized would operate, although the wear rates were still very high. The porous structure developed by powder metallurgy techniques also presents an interrupted surface and may result in better anti-galling characteristics.

Effect of Corrosion. The effect of corrosion on wear is illustrated by comparing the wear factors listed in the two columns of Table 3. In the second column are the results of a number of tests, standard in every respect, except that Westphal and Glatter substituted a partial pressure of hydrogen for the oxygen-argon mixture. In almost every case a substantial reduction in wear factor is noted. The greatest change took place with those materials which are most susceptible to oxidation. The combination of Everdur No. 1012 (silicon bronze) and chrome plate has an extremely high wear factor (830) in oxygenated water and a very low wear factor (2.2) in hydrogenated water. There was an 88 per cent reduction in wear for the combination of KR-monel and chrome plate. In contrast, the Stellite combinations, because they are more oxidation resistant, did not show improvements of this magnitude. The reductions ranged from a few up to a maximum of 50 per cent.

Table 4. Coefficients of Friction in Water at Room Temperature*

Materials combination	Static	Kinetic
Armco type 17-4 PH-Armco type 17-4 PH.....	0.45	0.45
Armco type 17-4 PH-Stellite 1.....	0.25	0.23
Armco type 17-4 PH-as-plated chromium:		
Initial.....	0.24	0.17
Final.....	0.50	0.50
Armco type 17-4 PH-ground chrome plate:		
Initial.....	0.16	0.14
Final.....	0.62	0.62
Stellite 1-as-plated chromium.....	0.29	0.22
U.S. Steel type W (SA)-Stellite 1.....	0.35	
U.S. Steel type W (SA)-Haynes 21.....	0.21	0.17
U.S. Steel type W (SA)-as-plated chrome.....	0.27	0.16
U.S. Steel type W (SA)-ground chrome plate.....	0.20	0.13
U.S. Steel type W (SA)-Armco 17-4 PH.....	0.79	0.79
Stellite 6-U.S. Steel type W (SA).....	0.32	0.32
Stellite 6-U.S. Steel type W (SA) sandblasted.....	0.38	0.37
Powder materials applied to sandblasted U.S. Steel type W (SA) vs. Stellite 6:		
Lead.....	0.14	0.13
Copper.....	0.20	0.16
Teflon.....	0.19	0.18
Silver.....	0.25	0.21
Neolube.....	0.27	0.23
Tin.....	0.48	0.44
PbO (litharge).....	0.31	0.22
Pb ₂ O ₄ (red lead).....	0.31	0.25
2 PbCO ₃ ·Pb(OH) ₂ (white lead).....	0.32	0.26
PbO ₂	0.35	0.27
PbCrO ₄ (chrome yellow).....	0.41	0.31
SnO ₂	0.46	0.39

* R. C. Westphal and J. Glatter, WAPD-T-64.

Effect of Friction. Some very interesting observations on friction were made by Westphal and Glatter. These data (Table 4) include measurements of static and kinetic friction of several materials combinations in water. In addition, the effectiveness of various materials as solid-film lubricants is shown. These materials were applied in powdered form to a lightly sandblasted surface, since it was found that this condition promoted greater adherence.

The introduction of lead or lead oxides onto lightly sandblasted surfaces of wear test specimens greatly reduced the wear rate as well as the friction. Neolube, a commercially available product consisting of an alcohol suspension of colloidal graphite, was also effective in this respect, although not to the same degree as were the lead

compounds. The most effective solid film lubricant of all was metallic lead operated in oxygen-free or hydrogenated water.

Wear and friction are closely related phenomena. Any reduction in friction of a given material combination that is accomplished by any of the various methods mentioned is always accompanied by a corresponding reduction in wear rate according to the authors. Nevertheless, it does not necessarily follow that low wear rates will be found for all materials combinations having low coefficients of friction, nor are high friction coefficients always an indication of high wear.

2.32 Fretting Tests. Unpublished work by W. K. Anderson and associates at Argonne National Laboratory yields data on fretting and wear of several materials combinations. Basically, the test consisted of oscillating balls, 0.135-in. diameter, against a face plate having a 2-in. radius of curvature at a speed of 4 cps over a distance of $\frac{1}{16}$ in. Contact between the balls and the face plate was maintained, as was a stress of 100,000 psi (Hertz formula), by spring loading. The tests were conducted with oil lubrication at 250°F. A summary of the results of these tests is presented in Table 5.

Table 5. Fretting Tests*

Material		Result†
Ball	Plate	
410	410	A
	420	D
410 nitrided	410	A
	420	NA
440C	420	D
	440C	NA
440C nitrided	440C	D
	17-4 PH	17-4 PH
17-4 PH	17-7 PH	NA
	17-7 PH	NA
17-7 PH	17-7 PH	D
	Stellite 3	A
322	Stellite 6	NA
	17-4 PH	NA
322 nitrided	322	A
	Stellite 3	D
Stellite 3	17-7 PH	D
	322	A
Stellite 6	Stellite 6	A
	17-7 PH	D
Stellite 6	322	A
	Stellite 3	A
	17-7 PH	NA

* J. Frank, W. Neisz, and D. N. Dunning, unpublished work.

† NA, not acceptable; D, doubtful; A, acceptable.

2.33 Component Wear Tests. Gear and Bearing Wear Tests. A series of tests on gears and associated bearings were run in oxygenated water at 450 to 500°F. Two 3-in.-PD 1-in. face gears were driven on a common shaft at 100 rpm by an external motor. Mating gears, on a parallel shaft, were spring loaded. The reaction stresses also produced calculable bearing loads. Results of the tests are summarized in Table 6.

Rack and Pinion Wear Tests. A test of oscillating bearings, guide bearings, and rack and pinion gears was established at Argonne National Laboratory under the direction of M. C. Shaw. A vertical shaft was positioned by two cylindrical guide bearings carrying a rack. The rack meshed with a 3-in.-PD 1-in. face pinion supported by two bearings on a horizontal shaft. The pinion was oscillated through 170° by an external crank and sector. Varying the frequency of cycling between 1 and 5 cps permitted actual load variation. Tests were conducted at 450 to 500°F in oxygenated water. A summary of data is given in Table 7.

In a private communication, W. K. Anderson has compared a list of materials that are acceptable corrosion-wise with the results of simulated component wear tests and selected combinations that were satisfactory from both standpoints. His findings are summarized in Table 8. The general superiority of the cobalt-base alloys, as represented by the Stellites, is evident.

Table 6. Gear and Bearing Wear Tests*

Material drive gear	Driven gear	Tooth load, lb/in.	Results†
Cast iron	AISI 316	26	D
Cast iron	AISI 316	68	D
Cast iron	AISI 316	96	NA
AISI 316	Cast Iron	26	D
AISI 316	Cast Iron	48	D
AISI 316	Cast Iron	96	NA
AISI 316	AISI 316	34	NA
AISI 316	AISI 440C	26	D
AISI 316	AISI 440C	48	D
U.S. Steel type W	U.S. Steel type W	34	NA
U.S. Steel type W	AISI 440C	96	NA
U.S. Steel type W	Stellite 3	20	D
U.S. Steel type W	Stellite 3	10	D
U.S. Steel type W	Stellite 3	30	D
U.S. Steel type W, Cr plated	U.S. Steel type W, Cr plated	20	NA
U.S. Steel type W, nitrided	U.S. Steel type W, nitrided	20	A
AISI 420	AISI 420	20	VG
Stellite 3	Hastelloy C	92	NA
Stellite 3	AISI 440C	20	A
Stellite 3	Stellite 3	20	A
Stellite 3	U.S. Steel type W	10	D
Stellite 3	U.S. Steel type W	20	D
AISI 304 nitrided	AISI 440C	20	NA } Wear O.K.
AISI 304 nitrided	AISI 304 nitrided	20	NA } case chipped
Tantung G	Tantung G	20	A
Hastelloy C	Hastelloy C	92	NA
Hastelloy C	Stellite 3	92	NA
Hastelloy C Cr plated	Hastelloy C Cr plated	20	NA
AISI 440 C	AISI 316	105	A
AISI 440C	U.S. Steel type W	96	A
AISI 440C	Ampco 18	56	G
AISI 440C	Stellite 3	20	VG
AISI 440C	AISI 304 nitrided	20	A
AISI 440C	S Monel	20	A
Ampco 18	440C	56	D
Ampco 18	S Monel	20	NA
Ampco 18	Ampco 18	30	NA
S Monel	440 C	20	A
S Monel	S Monel	20	NA
S Monel	K Monel	20	NA
S Monel	Ampco 18	20	NA
K Monel	S Monel	20	NA

Bearings

Material			Bearing load, lb	Results
Balls	Races	Retainers		
Stellite 3	Stellite 3	AISI 304	20	VG
Stellite 3	Type W	AISI 304	30	NA
Stellite 3	Type W	AISI 304	20	D
17-7 PH	17-4 PH	AISI 304	16	NA

* Data from tests performed at Argonne National Laboratory, under the direction of M. C. Shaw.
 † D, doubtful; NA, not acceptable; VG, very good; A, acceptable; G, good.

Table 7. Rack and Pinion Wear Tests*

Material pinion gear	Rack gear	Tooth load, lb/in.	Rating†
Stellite 3	Stellite 3	260	NA
Stellite 3	Stellite 3	72	G
Stellite 3	Stellite 3	29	G
U.S. Steel W nitrided	U.S. Steel W nitrided	72	VG
U.S. Steel W nitrided	U.S. Steel W nitrided	29	A
AISI 410 nitrided	AISI 410 nitrided	260	VG
AISI 440-C	AISI 440-C	260	G

Pinion Bearings
(Oscillating Type)

Bearing type	Bearing load	Bearing material	Rating
Needle	130	AISI 440-C	D
Needle	130	AISI 440-C Cr plated	NA
Needle	130	SAE 52100	NA
Needle	37	SAE 52100	A
Needle	14.5	SAE 52100	D
Needle	130	Armco 17-4 PH	NA
Needle	14.5	Armco 17-4 PH	NA
Spherical ball	14.5	AISI 410 Nitrided	NA
Sleeve	130	Graphite 40	NA

Guide Bearings
Sliding Type

Sleeve	37.8	Graphite C-18	NA
Sleeve	11.5	Graphite C-18	NA
Sleeve	3.1	Graphite #14	A
Sleeve	1.2	Graphite #14	A
Linear ball	‡	440C	NA
Linear ball	‡	410 Nitrided	NA
Sleeve	37.8	Ampeco 18	NA
Sleeve	37.8	Lead Bronze	NA

* Data from tests performed at Argonne National Laboratory under the direction of M. C. Shaw.

† NA, not acceptable; D, doubtful; A, acceptable; VG, very good.

‡ Bearing load not reported.

Table 8. Materials Combinations Suitable for Use as Bearings
in High-temperature Water Reactors*

17-4 PH vs. 17-4 PH
 U.S. Steel W vs. Stellite 6
 U.S. Steel W vs. Stellite 3
 U.S. Steel W vs. Haynes 25
 Stellite 3 vs. Haynes 25
 Stellite 3 vs. U.S. Steel W
 Stellite 3 vs. 17-7 PH
 Stellite 3 vs. Stellite 3
 Stellite 3 vs. Stellite 6
 Stellite 6 vs. U.S. Steel W
 Stellite 6 vs. 17-4 PH
 Stellite 6 vs. Stellite 6

* W. K. Anderson, private communication.

REFERENCES

1. Datzko, S. C.: "Corrosion of Metals in High Temperature Water," ANL-5354, Oct. 4, 1954.
2. Bailey, John M., and Douglas Godfrey: Coefficient of Friction and Damage to Contact Area during Early Stages of Fretting, part II, Steel, Iron, Iron Oxide, and Glass Combinations, *NACA Tech. Note* 3144, April, 1954.
3. Westphal, R. C., and J. Glatte: WAPD-T-64, Dec. 4, 1953.
4. De Paul, D. J. (ed.): "Corrosion and Wear Handbook for Water Cooled Reactors," Supt. Docs., U.S. Government Printing Office, Washington, D.C., 1958.

10-4 RADIATION DAMAGE TO SOLIDS

BY

John P. Howe and Sidney Siegel

The types of radiation that can affect the macroscopic properties of solids include charged particles, neutrons, and γ rays. The nature, properties, and attenuation characteristics for each of these radiation types are described in Secs. 4 and 7-3. The effect produced by a given type of radiation depends markedly on the nature of the substance being irradiated. Metals are affected by corpuscular radiations, e.g., protons, neutrons, electrons, having energy and momentum high enough to produce atomic displacements. In nonmetallic systems, the ionization and excitation produced in the solid are of primary importance, so that all types of radiation, including γ rays, can produce property changes. The ambient temperature at which the exposure occurs has a marked effect on the magnitude of the changes produced.

The major sources of charged corpuscular radiation are electronuclear machines, e.g., the cyclotron for protons and deuterons, the electrostatic generator for electrons. The major sources of neutrons are nuclear reactors. The most important sources of γ radiation are reactors, materials activated in reactors, or fission products contained in or separated from spent reactor fuel elements.

1 NUCLEAR REACTORS AS SOURCES OF RADIATION

Nearly all reactors that have been constructed to date have been used to some extent for radiation-damage investigations, regardless of their principal purpose. However, the reactors that have been designed primarily for research or test purposes provide the most useful facilities for such investigations and include the Materials Testing Reactor, the Oak Ridge research reactors, the Brookhaven reactor, the Canadian NRX reactor, and the CP-5 reactor at the Argonne National Laboratory. Several additional reactors of advanced design are planned or under construction (see Sec. 13-6). Of these the Engineering Test Reactor (ETR) was placed in operation late in 1957 at somewhat below the design power.

1.1 The Materials Testing Reactor (MTR)

The MTR is a water-moderated and cooled thermal reactor; it uses highly enriched uranium as its fuel. The reactor, when operating at the original design power level of 30 Mw, has an average thermal-neutron flux of 2×10^{14} neutrons/(cm²)(sec). The active core fills a region 40 by 70 by 60 cm and is surrounded by a beryllium reflector that fills the remainder of a cylinder 3 ft high and 5 ft in diameter. The beryllium reflector is, in turn, surrounded by a graphite reflecting region approximately 6 ft thick and 9 ft high. Experimental test facilities are provided within the active core and in both reflecting regions.*

The test positions within the core tank are provided by the insertion of an experimental assembly in one of the *L* lattice positions or by replacing a beryllium reflector element in an *A* position. Tests in *L* positions can be carried out in assemblies that simulate a fuel element, approximately 3 by 3 in. in square cross sections, or in alumi-

* John R. Huffman: The Materials Testing Reactor, *Nucleonics*, 12: 21-26 (April, 1954).

num L pieces having an axial hole 1.375-in. ID. No leads can be brought out from L pieces. Tests in A positions can be carried out in specially constructed substitute assemblies about 3 by 3 in. or within cored beryllium pieces having axial holes up to 1.375-in. ID. Electrical leads and fluid lines can be brought out from tests in A positions. Table 1 gives pertinent data relating to these L and A test positions.

Table 1a. Data on Core Test Positions in MTR at 30-Mw Power

All test positions are vertical and have a usable length of about 20 in. The ambient temperature is about 100°F. The γ -ray flux in all L positions produces heating at a rate of about 14 watts/g.

Facility.....	L-41		L-43		L-45		L-47		L-49	
Max thermal flux.....	1.8×10^{14}		3.0		3.5		3.0		1.8	
Fast flux > 1 Mev.....	6×10^{13}		6		6		6		6	
Facility.....	L-51	L-52	L-53	L-54	L-55	L-57	L-58	L-59		
Max thermal flux.....	1.8×10^{14}	2.0	2.5	2.8	2.8	2.5	2.3	1.8		
Fast flux > 1 Mev.....	1.0×10^{13}	1.3	1.3	1.3	1.0	1.0	1.0	0.8		

Table 1b. Data on Be Reflector Test Positions in MTR at 30-Mw Power

All test positions are vertical and have a useful length of about 2 ft. The ambient temperature is about 100°F, but special cooling can be provided to A pieces. Values are given for one quadrant of the reflector; similar values exist in the other three quadrants.

Facility.....	A-4		A-6		A-7		A-3		A-5		
Max thermal flux.....	1.25×10^{14}		1.4		0.75		0.75		0.6		
Fast flux > 1 Mev.....	5×10^{12}		3		1.5		1.0		0.8		
Gamma-ray heating rate, watts/g.....	2		1.5		1.0		0.9		0.75		
Facility.....	A-38		A-39		A-40		A-43		A-41		A-42
Max thermal flux.....	1.9×10^{14}		1.4		1.0		0.75		0.6		0.5
Fast flux > 1 Mev.....	10×10^{12}		5		0.8		0.8		0.5		0.3
Gamma-ray heating rate, watts/g.....	2.5		1.25		0.9		0.75		0.4		0.5

A large number of test facilities penetrate the shield and the reflector region and provide blind or through thimbles in which irradiations or in-pile tests can be carried out.

Relevant information on these facilities appears in Table 2. The physical location of these facilities and contours of the thermal-neutron flux at the mid-plane of the reactor are shown in Fig. 1.

1.2 The Low-intensity Test Reactor (LITR)

The LITR was constructed at the Oak Ridge National Laboratory as a hydraulic mock-up of the MTR and is in many respects identical in physical configuration with the MTR. It operates at 3 Mw, with an average thermal-neutron flux in the core of 2.2×10^{13} neutrons/(cm²)(sec). The experimental facilities include six beam holes, four low-flux short tubes, and lattice or beryllium reflector positions similar to those in the MTR. The beryllium reflector pieces in the LITR are 2 by 2 in. in cross section. Table 3a gives data on the thermal-neutron flux in these various facilities. Table 3b gives information on the neutron energy spectrum at the inner end of the HB-2 hole; this spectrum is typical for a position near the surface of the active lattice in both the MTR and the LITR.*

1.3 The ORNL Graphite-moderated Reactor (X-10)

The X-10 reactor at the Oak Ridge National Laboratory is graphite moderated and air cooled and uses natural uranium fuel. It operates at a power of 3.5 Mw, with an

* Data on the LITR was compiled by C. D. Cagle and J. A. Cox of the Oak Ridge National Laboratory.

Table 2. MTR Irradiation Facilities

Facility designation	Dimensions		Orientation and penetration	Estimated flux		Max gamma, watts/g	Temp, °F	Cooling facilities	Remarks
	Cross section, in.	Usable length, in.		Max thermal, neutrons/(cm ²)(sec)	Max fast, neutrons/(cm ²)(sec)				
HB-1,2,3	6 ID in Be	5	Horizontal to core	4.5×10^{14}	1×10^{14}	10	≈ 100	Cooling water available in facility cubicle	Beam-hole plugs usually water cooled
HB-4,5,6	6 ID in Be	5	Horizontal to lattice	2.5×10^{14}	3×10^{12}	2.0	≈ 100	Cooling water available in facility cubicle	Beam-hole plugs usually water cooled
DB-1,2,3,4,5,6	6 ID	Inclined down to tank wall	2×10^{13}	No coffin available for removal of shielding plugs
HG-5,6	6 ID	9	Horizontal to tank wall	4×10^{12}	2×10^{13}	0.1	≈ 100	Air-cooled	
HG-9	10 by 16	10	Horizontal to tank wall	4×10^{13}	5×10^{13}	2.5	≈ 100	Air-cooled	
VG-9	10 by 10	~36	Vertical from top to HG-9	8×10^{12}	Not measured	0.008	≈ 100	Air-cooled (all VG's)	
T-2	72 by 72	Horizontal to Pb window	1×10^{11}	Air-cooled	
VG-2,4	4 ID	36	Vertical through graphite	5×10^{12}	Cd ratios 2.4	0.009	≈ 100	Air-cooled	VG used for piping (not available)
HR-1,2	1 ID	12	Horizontal through tank	1.2×10^{14}	6×10^{13}	5	≈ 100	Air-cooled	Pneumatic rabbit facility
HR-3,4	4 ID	24	Horizontal to tank	4×10^{13}	1×10^{10}	0.3	≈ 100	Air-cooled	Water can be provided. These are hydraulic rabbits (standard shuttle sizes, 1 3/8 by 3, 1 3/4 by 3 in.)
VH-1,2,3,4	1 and 1.3 ID	20	Vertical from basement in Be	$2-3 \times 10^{14}$	2.2×10^{12} - 1.9×10^{13}	1.5	≈ 100	Water	
VG-1,3,5,6	4 ID	36	Slant from top into pebble graphite	6×10^{12}	0.009	≈ 100	Air-cooled (all VG's)	
VG-7,10-14,16-20	2 1/2 ID	~36	Slant from top into pebble graphite	2.5×10^{13}	Cd ratio (indium) 22	0.5-0.1	≈ 100	Air-cooled	

Table 2. MTR Irradiation Facilities. (Continued)

Facility designation	Dimensions		Orientation and penetration	Estimated flux		Max gamma, watts/g	Temp, °F	Cooling facilities	Remarks
	Cross section, in.	Usable length, in.		Max thermal, neutrons/(cm ²)(sec)	Max fast, neutrons/(cm ²)(sec)				
VG-23-26, 29-41,43 45-55, 57-62	2 ID	36	Vertical from top into permanent graphite	5×10^{10} - 5×10^{12}	Cd ratio (indium) 2×10^4	0.0001-0.01	≈ 100	Air-cooled	
T-2-H-1,2	4 × 4	N-S horizontal across T-2	2×10^9	Cd ratio (indium) 10^4 - 10^6	5×10^{-9}	≈ 100	Air-cooled	
T-2-H-3,4,5, 6,7,8	4 × 4	9	Horizontal in T-2	1×10^{11}	Cd ratio (indium) 10^2 - 10^5	100	Air-cooled	
T-2-V-1,2	12 × 12	Vertical reactor top to T-2	2×10^{10}	5×10^{-7}	100	Air-cooled	
HT-1	$4\frac{3}{8} \times 4\frac{3}{8}$	12	Horizontal through tank	1.2×10^{14}	1×10^{12}	2.5	100	Water-cooled	
HI-2,3	$10\frac{3}{4}$ ID	E-W horizontal through graphite	1×10^{12}	0.003	100	Used for reactor instruments
HG-1,2	8 ID	~12	N-S horizontal through graphite	1×10^{12}	0.003	100	Air-cooled	
HG-3,4	4 ID	~12	N-S horizontal through graphite	1×10^{12}	0.003	100	Air-cooled	

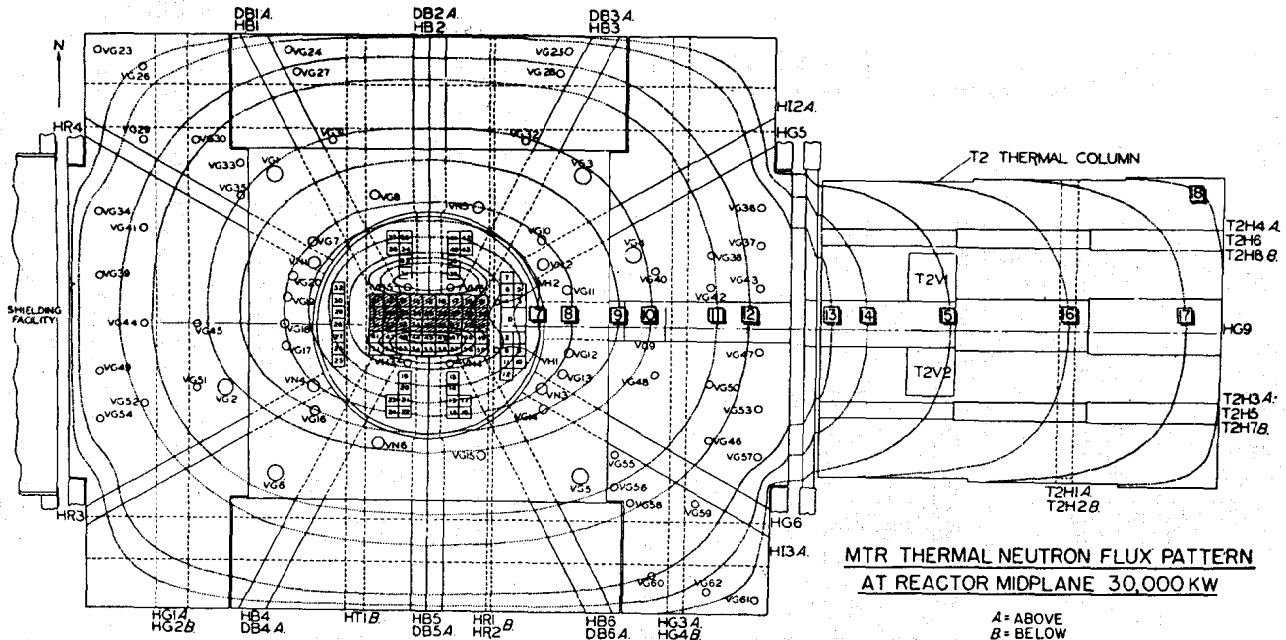
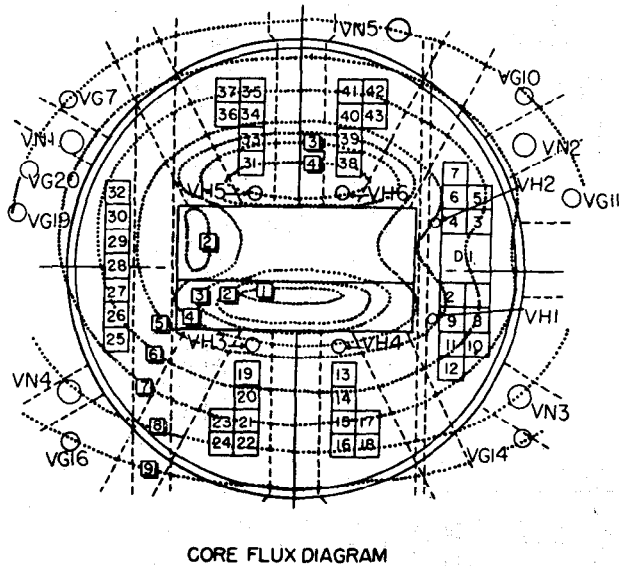


FIG. 1a.



CORE FLUX DIAGRAM

Fig. 1b.

KEY TO CONTOURS OF THERMAL NEUTRON FLUX

1	= 5	$\times 10^4 / \text{cm}^2 \text{sec}$
2	= 4	"
3	= 3	"
4	= 2.5	"
5	= 2	"
6	= 1	"
7	= 0.5	"
8	= 0.25	"
9	= 0.1	"
10	= 0.05	"
11	= 0.01	"
12	= 0.005	"
13	= 10^{-3}	"
14	= 5×10^{-4}	"
15	= 10^{-4}	"
16	= 10^{-5}	"
17	= 10^{-6}	"
18	= 10^{-7}	"

Fig. 1c.

average thermal-neutron flux of 5×10^{11} neutrons/(cm^2)(sec). The moderator stack is nearly a cube 24 ft on edge. There are 1,248 horizontal fuel channels through the graphite, of square cross section large enough to accommodate a cylinder $1\frac{1}{4}$ -in. diameter on an 8-in. lattice spacing. These channels are cooled by air flowing through them.

There are normally about 820 of these channels loaded with fuel, so that an appreciable number of the remainder is available for experimental purposes. Leads can be brought out from the experimental piece to equipment near the reactor face. Three fuel channels contain special hollow fuel slugs that provide a high local fast-neutron flux. These assemblies can accommodate a sample 11 in. long by $\frac{1}{2}$ in. in diameter. The exterior of these elements is cooled by air, but the ambient temperature in the central region is about 100°C . The neutron energy spectrum in these hollow slugs is given in Table 4.

The principal experimental facilities are provided by a group of about 50 horizontal holes, 4 in. square, that penetrate the graphite at right angles to the fuel channels and

Table 3a. Thermal-neutron Flux in LITR Test Facilities at 3-Mw Power Level

Beam tube	HB-2	HB-4	HB-5	V-1	V-2	V-3	V-4
Flux, neutrons/ (cm^2)(sec)	3×10^{13}	7.8×10^{12}	7.6×10^{12}	4×10^{11}	5×10^{11}	2.4×10^{11}	2.6×10^{11}
Core position			C-42	C-44	C-46	C-48	C-38
Flux, neutrons/(cm^2)(sec)			3.1×10^{13}	3.3×10^{13}	3.4×10^{13}	3.4×10^{13}	3×10^{13}

Table 3b. Neutron Spectrum at Inner End of HB-2 in LITR at 1-Mw Power Level

Neutron energy, Mev	Flux, neutrons/(cm^2)(sec)
Thermal	11×10^{12}
> 0.6	7.0×10^{12}
> 2.6	2.0×10^{12}
> 4.0	0.7×10^{12}
> 6.2	0.25×10^{12}
> 8.1	0.07×10^{12}

Table 4. Neutron Energy Spectrum in X-10 Hollow Slugs

Energy, Mev.....	Thermal	>1	>2	>4	>6
Flux, neutrons/(cm ²)(sec).....	3.8×10^{11}	1.6×10^{11}	6.5×10^{10}	1.4×10^{10}	3.5×10^9

lie between them. In all except a few special cases these holes have no special cooling provided and operate at about 135°C. Twenty-two of these holes extend completely through the reactor; the remainder go from the shield to a position near the reactor center.

The maximum thermal flux in these holes depends on their location in the reactor and varies from about 4×10^{11} to 1.1×10^{12} neutrons/(cm²)(sec) from peripheral to central holes. The cadmium ratio is about unity. One of the 4-in.-square holes is provided with a water-cooled, enriched uranium converter cylinder, which can accommodate a sample up to 2 in. in diameter and 10 in. long. The fast flux in this facility is about 10^{12} , and the temperature 25°C.*

1.4 The BNL Research Reactor

The research reactor at the Brookhaven National Laboratory is graphite moderated and air cooled and operates at a power near 25 Mw. The maximum thermal flux produced is 5×10^{12} neutrons/(cm²)(sec). The over-all dimensions of the reactor shield are approximately 60 (length) by 40 (width) by 40 ft (height). One of the 40-ft-square ends is reserved for the operational loading and unloading of the fuel elements. The other five faces of the box are research areas where all the experimental facilities are located.

A pattern of 30 horizontal beam holes extends through the graphite core and the opposite shielding walls in the direction perpendicular to the fuel channels. These holes, 4-in. squares in the graphite, are spaced 3 ft apart horizontally and 4 ft apart vertically. They are used for either neutron-beam or in-pile-irradiation types of experiments.

The bottom face of the reactor is accessible by means of two tunnels built underneath the graphite structure. The larger tunnel is 2 ft square in cross section and has an exposure window 3 by 2 ft in area. The smaller tunnel is 1 ft square in cross section and has a window 3 by 1 ft in area. A small flatcar moves on rails in the bottom of each tunnel and can be loaded through openings in the floor of the building on both sides of the reactor. These tunnels were built to provide for the irradiation of large-size instruments or equipment. Leads can be taken out of the tunnels from the experiments to monitoring or recording meters in the reactor room.

The face opposite the loading and unloading face is used primarily for the production of radioisotopes and to provide service irradiations of special targets. Eleven special tubes, parallel to the fuel channels, terminate at this face; some of them are used to convey samples pneumatically into and out of the core. Others can be used manually to insert samples of special nature, with or without monitoring leads connected to them. The fuel channels are also accessible through this face.

A wide variety of devices is built into the reactor for doing irradiations of specialized character at controlled ambient temperatures. The graphite and air temperatures in the reactor range between 50 and 200°C. Two of the 4-in.-square beam holes have been provided with water-cooled irradiation chambers to yield a controlled temperature of 30°C. These are built so that samples can be inserted or removed while the reactor is in operation. A third such beam hole has a chamber cooled by liquid nitrogen to provide an ambient temperature of -190°C. A fourth beam hole has a furnace installed to provide elevated temperatures up to 500°C.

Detailed information on the flux level, the dimensions, and the temperature of some of these facilities is given in Table 5. The neutron energy spectrum in one of the 4-in. horizontal beam holes is shown in Fig. 2, where the total flux above any given

* Data on the X-10 graphite reactor were compiled by C. D. Cagle and J. A. Cox of the Oak Ridge National Laboratory.

Table 5. Data on Facilities in BNL Reactor

Reactor facility	Max size, in.	Thermal flux	Ambient temperature, °C
Target conveyor.....	Containers are $\frac{3}{4}$ ID, $2\frac{1}{2}$ long	Choice, 10^{11} - 4×10^{12}	150-200
Pneumatic tubes.....	Carriers are $1\frac{1}{4}$ ID, 4 long	Up to 4×10^{12}	60-75
Water-cooled holes.....	$1\frac{1}{4}$ OD \times 4 $2 \times 2 \times 7$	3×10^{12} 1.5×10^{12}	30
Liquid-nitrogen-cooled hole.....	$\frac{3}{8}$ OD, 6 long	4×10^{12}	-190
Tunnels (under reactor).....	$15 \times 24 \times 24$ $6 \times 12 \times 24$	2×10^9	30
South core hole.....	$12 \times 12 \times 24$	10^{12}	175
Experimental holes.....	$3\frac{3}{4} \times 3\frac{3}{4}$ cross section	Up to 5×10^{12}	175 max
Fuel channel.....	$2\frac{1}{2}$ OD	Up to 5×10^{12}	50-175
Air-cooled holes.....	2 OD, 24 long	Up to 4×10^{12}	50-75
High-temperature facility.....	$1\frac{1}{4} \times 7$	1.2×10^{12}	125-500

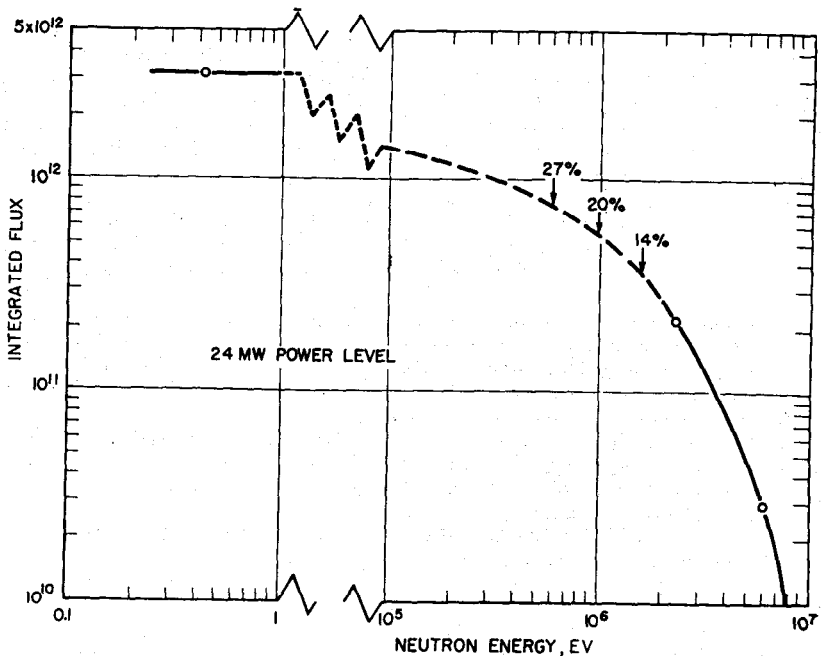


Fig. 2. Neutron flux-energy distribution hole (E-25 Brookhaven reactor).

energy is plotted against that energy. This is probably representative of graphite reactors generally.*

1.5 The NRX Reactor at the Chalk River, Canada, Laboratories

The NRX reactor is D_2O -moderated and uses natural uranium fuel. The power level is near 40 Mw, and the maximum thermal flux is 6×10^{13} neutrons/(cm^2)(sec). The moderator temperature is maintained below 120°F; the graphite reflector temperature below 320°F.

* Data on the BNL graphite reactor were compiled by Marvin Fox of the Brookhaven National Laboratory.

Experimental facilities include a central thimble, lattice positions, tubes at the periphery of the D₂O-moderated core, and horizontal beam holes that penetrate the shield and reflector. Relevant data for these experimental positions are given in Table 6.*

Table 6. Data on Experimental Facilities in NRX Reactor

Facility	Thermal flux, neutrons/(cm ²)(sec)	Useful dimensions	Cooling
Central thimble (vertical).....	6×10^{13}	5' long, 5½" diam	Air or water
Lattice position.....	$\sim 5 \times 10^{13}$	5' long, 2¾" diam	Air or water
Lattice position with converter.....	$\sim 5 \times 10^{13}$ (fast flux)	½" diam or less	Water
Reflector position.....	$\sim 1 \times 10^{13}$	5' long, 1¾" diam	Air or water
"Self-serve" positions.....	2×10^{12} to 2×10^{13}	1.6" long, 0.62" diam	Air
Horizontal holes.....	$< 1 \times 10^{13}$	Twelve 4" diam, three 12" diam	Air or water

1.6 The CP5 Research Reactor at Argonne National Laboratory

The CP5 reactor is D₂O-moderated and uses enriched uranium fuel. The reactor tank is about 6½ ft in diameter, and the reactor is a right cylinder about 4 ft in height and diameter. The tank is pierced by a large number of horizontal beam holes, and vertical thimbles extend downward through the tank cover. The reactor operates at 1-Mw power level and provides a maximum thermal flux within the core of 2×10^{13} neutrons/(cm²)(sec).

Experimental facilities available in the reactor are described in Table 7.

Table 7. Data on Facilities in the CP5 Reactor

Facility	Number provided	Fluxes, neutrons/(cm ²)(sec)		Internal size of hole, in.
		Thermal	Epithermal	
Vertical core thimbles.....	7	2×10^{13}	1×10^{13}	1.4 and 1.0 diam
Fast flux thimbles.....	3	1×10^{13}	2×10^{13}	0.5 diam
Vertical D ₂ O thimbles.....	4	1×10^{13}	5×10^{12}	1.4 and 1.0 diam
Vertical graphite thimbles.....	10	2×10^{12}	1×10^{10}	1.4 and 1.0 diam
Vertical graphite thimbles.....	7	2×10^{12}	1×10^{10}	4.75 diam
Through beam holes.....	2	1×10^{13}	5×10^{12}	5.75 diam
Small rabbit.....	1	2×10^{13}	1×10^{13}	0.5 diam
Sliding gate holes.....	4	1×10^{13}	5×10^{12}	3.75 diam
Rotating gate holes.....	4	1×10^{13}	5×10^{12}	11.0 and 3.75 diam

1.7 Armour Research Reactor

The Armour research reactor was designed and built for the Armour Research Foundation by Atomics International. The maximum thermal-neutron flux at the center of the core is 10^{12} neutrons/(cm²)(sec) at an operating power of 50 kw. It is a homogeneous solution-type (water boiler) reactor and has a graphite reflector. It contains a 5-ft-square thermal column, seven 4-in. beam holes, two 3-in. beam holes, one 2-in. pneumatic tube, one 1½-in. pneumatic tube, one 1½-in. tube passing through the center of the core, and γ exposure facilities in the subpile room that utilize the gaseous fission-product activity. The thermal column has nine 4-in.-square removable graphite stringers. Access to the thermal column is gained through two 6-in.-diameter holes and two 6-in.-square holes and through the 5½-ft square thermal

* Data on the NRX research reactor were compiled by W. B. Lewis, Atomic Energy of Canada, Ltd., Chalk River, Ontario; see also Ref. 1.

column door opening. The γ facilities in the subpile room consist of four 4-in. exposure tubes, two 8-in. exposure tubes, and a 6- by 18-in. rectangular exposure port.

2 EXPERIMENTS USING NUCLEAR REACTORS

Properties of materials and material systems are measured during and after irradiation either to determine their behavior and utility in reactor application or to learn and describe the basic phenomena produced in material systems by irradiation.

In-pile measurements are made (1) to observe those changes which may undergo transients or which obtain a steady state while under irradiation but which may change subsequently, for example, creep and thermal conductivity at elevated temperature, and (2) to determine and control the conditions that prevail around or in the specimens being studied. *Postirradiation* examination and measurements are made for those properties which do not change or recover at the temperatures of handling, storage, and measurement after irradiation.

Reactor positions are selected on the basis of the characteristics given in the foregoing article and the demands of the experiment, for example, (1) fast-neutron flux to produce damage by knock-ons or recoil displacements, (2) slow-neutron flux for damage to fissile materials and other substances having atoms of high-neutron-absorption cross section, and (3) γ -radiation field for damage by ionization or excitation.

2.1 Experimental Conditions

These may be provided, measured, and controlled as follows:

2.11 Dosage may be estimated from standard measurements of flux of each kind of radiation that are made for experimental positions for each reactor presently in use. Values are given for a standard power level, and if the operating data that give power vs. time are used, an integrated flux may be obtained for the experiment in question. More accurate values may be obtained by flux monitors suitably incorporated in an experiment. Procedures for flux monitoring are given later. Total energy input into selected materials placed in selected positions in the X-10 reactor at Oak Ridge has been measured calorimetrically by Richardson.² When the material placed in the calorimeter is varied, the relative energy input due to fast neutrons and γ radiations has been determined. Such devices and measurements may be used as standards for dose in limited applications. The exposure or dose given to materials containing fissile atoms is often determined by quantitative analysis of a standard fission product. Chemical dosimetry³ can also be used but is more adaptable to studies of covalent materials.

2.12 Thermometry may be accomplished most conveniently by means of thermocouples. For proper insulation see Art. 2.31 on electrical resistance. Resistance thermometers appear to be satisfactory, although no extensive calibration of them has been made. Gas thermometers made of quartz or metal and filled with helium have been used but are bulky. Excellent thermal contact of the thermometer with the specimen is required because of radiation heating of the sensing element. Also the generation and flow of heat in the specimen must be taken into account in locating the thermometer and in ascertaining the representative temperature value for the experiment.

Temperature control is carried out using standard laboratory procedures based on signals from thermocouples. Heating to supplement radiation heating is done electrically, and cooling is usually accomplished with flowing gas or water. Whenever possible, the cooling system of the reactor itself is used. The response time and latitude of the control system and of the auxiliary heating and cooling must be designed to fit the expected variation in power level in the reactor used.

2.2 Specimens, Specimen Holders, and Containers

These must be designed not only to fit the reactor position to be used but also to facilitate handling and measuring upon removal from the reactor; for example, speci-

mens for tension tests are often machined prior to insertion in the reactor and used for electrical-resistivity measurements while in the reactor and subsequently, as well as for the determination of stress-strain curves after removal from the reactor. When such preparation is not possible, hot laboratory techniques (see Sec. 7-4) are used for preparation and examination after reactor exposure.

2.3 In-pile Measurements

In-pile measurements in reactors are made as follows.

2.31 Electrical resistance is usually determined by bridge methods, which compensate for the resistance of the leads into the reactor. In all electrical measurements attention must be paid to the insulation. At best, organic insulation is not useful for exposures above about 10^{18} *nt*; however, ceramic-type insulation is generally acceptable. Asbestos properly supported serves well for thermocouples; Fiberglas also serves but is somewhat less reliable. The ceramic materials magnesia or alumina appear to be entirely suitable if properly supported. Braid appears suitable for support in most instances; however, for the most rugged construction, sheathed lines analogous to calorods in construction are desirable. Vacuumtight seals for electrodes present considerable trouble in that glass-to-metal seals can be used only in low flux. Ceramic bushings (e.g., porcelain) soldered to metal by the titanium or zirconium hydride method⁴ are perhaps the most dependable.

2.32 Pressure measurements are accomplished using gas leads made of metal or of fused silica which may be brought out of the reactor to conventional piezometers. When it is necessary to confine gas to small volumes within the reactor, metal diaphragms with electrical contacts to permit null-point determinations have been used. An external pressure which balances that to be measured is read by standard means outside the reactor.

2.33 Measurements of displacement or strain may be made using differential transformers. If they are properly insulated and supported, no change in calibration of the transformer occurs. Resistance strain gauges change their calibration by 5 to 10 per cent at 10^{17} *nt* owing partially to changes in the mounting cement and partially to the changes in the resistivity of the wire used in the gauge. Pneumatic gauges depending on change in pressure drop across an orifice have also been used for measurement of displacement.

2.4 Postirradiation Operations and Measurements

Insertion, removal, and handling of apparatus must be done according to the means specified at each site and according to the reactor position.

2.41 Level of radioactivity to be expected may be estimated if the composition is known in some detail by using tabulated cross sections and decay constants together with neutron flux, exposure time, and cooling time. Since the composition of many commercial materials is not known in detail, it is more convenient to use results of actual exposures such as those given in Table 8. Handling of irradiated materials is always subject to monitoring by a health-physics organization.

2.42 Shielding during operation and upon removal of the apparatus from the reactor is also specified by local practice (see instructions for reactor to be used). The radioactivity to be expected upon removal is estimated beforehand, and precautions are taken to see that shielding during removal, handling, and transport is adequate. Provisions for shielding at various activity levels are described elsewhere. Handling, examination, and measurement of properties after removal from the reactor are accomplished by means of remotely operated equipment. Items specific to radiation-damage studies are as follows (more general techniques are given in Sec. 7-4).

2.43 Metallography is done by carrying out the standard steps remotely in a hot cell. *Sectioning* is usually accomplished with an abrasive saw, shear, or machine tool, depending on the shape, size, and nature of the material. Normally these are standard tools whose controls are extended through the cell wall, motorized, or operated with the general-purpose manipulator. *Mounting* may be performed in a standard mount-

Table 8. The Gamma Radioactivity of Commercial Materials Exposed in a Reactor*

The following tabulated component activities determined by exposing the commercial material listed in the ORNL graphite-moderated reactor permit the estimation of the γ radioactivity of the material. The procedure for estimation is:

1. Compute the value of each component activity for the material from the relation

$$A_j(t_i) = A_{j_s} \left[1 - \exp \left(\frac{-0.693t_i}{t_{j\frac{1}{2}}} \right) \right]$$

where A_{j_s} = saturated value of component activity given in table

t_i = irradiation time

$t_{j\frac{1}{2}}$ = half-life for component activity j

2. Plot each component activity on semilog paper by drawing a straight line with slope $(-0.693/t_{j\frac{1}{2}})$ and intercept $A_j(t_i)$.

3. Add the components (sum over j) as selected points on the time axis and plot the composite curve.

4. Read off values of the total activity at the desired cooling time.

Saturation Values of the Component Activities A_{j_s} , † Equivalent CO^{60} Photons ‡/(sec)(g), Neutron Flux = 10^{12}

Material	Irradiation time, hr	$t_{\frac{1}{2}}$	A_s	$t_{\frac{1}{2}}$	A_s	$t_{\frac{1}{2}}$	A_s	$t_{\frac{1}{2}}$	A_s	$t_{\frac{1}{2}}$	A_s
Armco iron.....	4,870	2.5 hr	9×10^7	45 days	3.5×10^7	5.3 years	5.7×10^7				
1015 steel.....	4,700	2.5 hr	1.5×10^8	45 days	3.7×10^7	5.3 years	5.3×10^7				
Inconel.....	1,850	2.5 hr	3.5×10^8	25 days	1.5×10^7	60 days	4.9×10^7	5.3 years	8.5×10^8		
Inconel X.....	1,850	2.5 hr	7×10^8	25 days	2×10^7	60 days	5×10^7	115 days	1.1×10^8	5.3 years	8×10^8
Steel:											
304.....	4,380	2.5 hr	9×10^8	25 days	2.0×10^7	45 days	4.0×10^7	5.3 years	5.7×10^8		
347.....	4,500	2.5 hr	3.1×10^8	25 days	3.7×10^7	45 days	3×10^7	120 days	3.3×10^7	5.3 years	7×10^8
430.....	4,280	2.5 hr	8×10^8	25 days	2.8×10^7	45 days	2.8×10^7	5.3 years	2.4×10^8		
Al:											
2S.....	15,380	2.5 hr	2×10^8	15 hr	1.2×10^7	130 days	1.3×10^8	5.3 years	5.7×10^8		
52S.....	4,510	2.5 hr	7×10^8	15 hr	8.2×10^6	120 days	3.6×10^8	5.3 years	4×10^8		
Cu †.....	4,370	2.5 hr	1×10^9	13 hr	4.2×10^9	> 100 days	2×10^6				
Zr ‡.....	4,700	2.5 hr	3×10^8	20 hr	8×10^7	60 days	4×10^8				
Graphite:											
GBF.....	1,360	2.5 hr	None	15 hr	1×10^5	100 days	8×10^2	5.3 years	1.2×10^4		
C-18.....	15,400	2.5 hr	None	15 hr	7×10^5	70 days	1.3×10^5	5.3 years	8.3×10^4		

* C. D. Bopp, "Gamma Radiation Induced in Engineering Materials," ORNL-1371, May 6, 1953.

† For thin specimens, hence no self-absorption.

‡ Ion chamber calibrated with Co^{60} , two photons per disintegration, 1.25-Mev average energy.

§ Source and analysis not known, probably commercial electrical copper.

¶ AEC source.

ing press appropriately serviced and controlled. *Grinding* may be done in two general ways: (1) changeable, graded papers on a rotating wheel against which the mounted specimen is moved by a mechanical arm or (2) a lapping machine on which the specimens, properly weighted, are ground. *Polishing* may be carried out either electrolytically or mechanically, depending upon the material and desired data. Electro-polishing is readily accomplished in a commercial unit or a homemade device, but each must provide for changing reagents and current control. Mechanical polishing is technically difficult but has been successfully done on standard polishing wheels. The wheels are modified to allow changing of cloths remotely and accurate alignment with a mechanically moved specimen holder. *Cleaning* in a solvent bath agitated ultrasonically has proved successful. The equipment is commercially available and needs little modification. The specimen is held with the general-purpose manipulators or by a fixed manipulator. *Etching* with standard techniques is easy and requires only provisions for handling, introducing, and disposing of reagents. Cathodic etching is much more difficult, and no commercial equipment is available. *Photomicrography* is accomplished using a standard metallograph either mounted inside the cell with all controls operated remotely and the image brought outside optically or mounted outside with shielded stage, some controls operated remotely, and standard optics. Both methods involve expensive instrument modification, and the choice is usually dictated by cell-wall thickness and the activities involved.

2.44 Microhardness can be measured through the use of a commercially available instrument* that is adapted for remote operation by the factory. Only the optics need be modified, as all other adjustments are electrically actuated. The instrument may be inside or outside the cell, as in the case of the metallograph.

2.45 Testing. Materials testing procedures employ the standard test instruments that are easily adaptable to remote operation by the use of elongated controls through the cell wall, motorizing, or general-purpose manipulators. Some instruments, such as tensile machines, may be purchased directly as remotely operable units. Wherever possible, the test specimens should be machined prior to irradiation in order to avoid the expensive and slow process of remote machining.

2.46 Machining may be done with standard machine tools whose controls are made remote in the usual manner. For some cases these tools must be modified to suit special requirements through addition of air chucks and other screw-machine actuating devices, turrets, hydraulic or air table traveling devices, etc. Lathes, milling machines, drill presses, hydraulic hack saws, grinders, shears, etc., have all been successfully modified and remotely controlled at a relatively low cost.

2.5 Decontamination

Decontamination of equipment, specimens, and hot cells often follows the completion of a study. It is important to confine contamination to as small an area as possible and to cover all exposed surfaces of the equipment with a disposable material. Chips from machine tools, grindings, dissolved material, aerosols, lubricating fluids, etc., should be caught in disposable or easily cleanable containers. These procedures lessen the hazard and difficulty of decontamination and permit reuse of equipment that does not require drastic decontamination.

Disposal of radioactivated materials must be planned in advance. Procedures are described in Art. 10 of Sec. 11.

2.6 Reactor Safety

Coordination with reactor operations and safety is an extremely important aspect of the design of every in-pile experiment. If it is possible for the temperature of any given experiment to rise dangerously should the supply of cooling fluid fail, and if it is possible for this failure to occur, it is customary to interlock the temperature-control apparatus for the experiment with the control for the reactor so that the reactor is

* Wilson Mechanical Instrument Division of American Chain and Cable Company, Incorporated, 230 Park Avenue, New York 17, N. Y.

scrammed at a given temperature level. Some experiments require that the schedule of operation be controlled by, for example, the temperature rise in the experiment in question.

3 EXPERIMENTS USING CYCLOTRONS

Radiation-damage investigations have been carried out using charged particle beams, protons, deuterons, or α particles from cyclotrons.⁵ This method is particularly useful for fundamental studies of radiation effects on solids and for exploratory investigations preceding more elaborate reactor irradiations.

The merits of the cyclotron technique are principally:

1. Accurate knowledge of integrated exposure
2. Low induced activity in samples
3. Well-defined volume in which radiation is present, so that auxiliary apparatus is not activated
4. High radiation intensities available in large cyclotrons

The principal disadvantages of this type of experiment are:

1. Small cross-sectional area of cyclotron beam, permitting use of only very small samples
2. Restricted range of charged particles in solid materials, i.e., very small irradiated volume and high density of heat production
3. Nonuniform damage because of diminishing energy of impinging particle as it penetrates the sample

3.1 Dosage

Two principal means for measuring the integrated beam to which the sample has been exposed during an experiment are commonly used, the beam-current integrator and the activated foil counting.

The integrator circuit permits the beam current to be measured during the exposure. In the circuit generally used, the beam current charges a capacitor, the resulting voltage on which is amplified by a highly stable d-c amplifier and used to trigger a gas

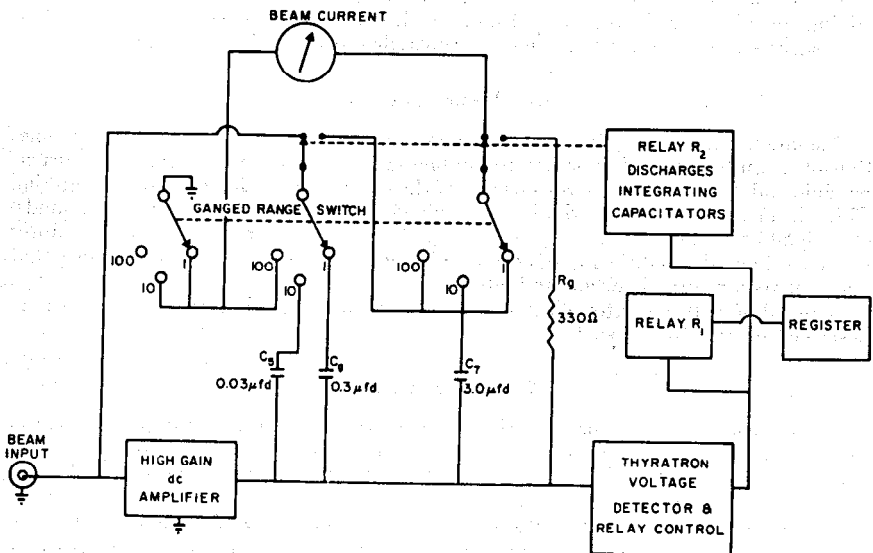


FIG. 3. Beam-current integrator.

discharge tube. The counting rate of this tube is then a measure of the current; the total number of discharges a measure of the integrated current. A circuit diagram of such an integrator is shown in Fig. 3.

The integrated beam intensity may also be measured, subsequent to the completion of an experiment, by activating a suitable thin foil placed in front of the sample. Copper foils 0.001 in. thick are conveniently used. The activity measured is due to β decay of Zn^{65} , which is produced in copper by protons, deuterons, or α particles.

The total sample exposure may be determined by counting the whole monitoring foil; in addition, sectioning the foil into strips permits the determination of the beam profile across the sample. Typical beam distributions are shown in Fig. 4a and b for an

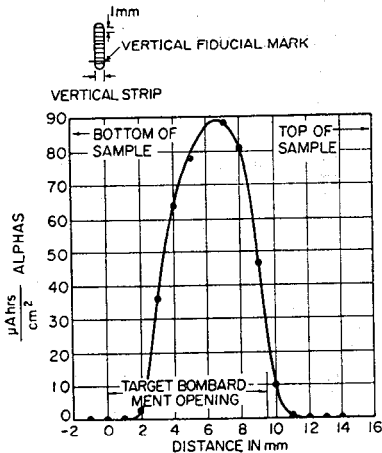


FIG. 4a. Vertical beam-distribution profile.

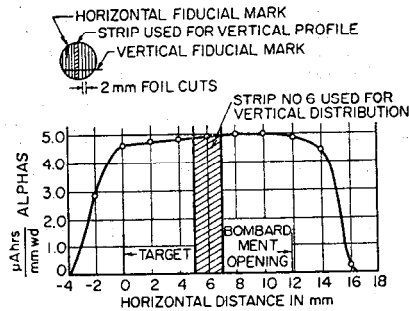


FIG. 4b. Horizontal beam-distribution profile.

irradiation with 37-Mev α particles. As is evident from these curves, the sample area which is uniformly irradiated is less than 1 cm^2 . With accompanying reduction in average intensity, this area may be increased by oscillating the beam across a layer area of the target or, vice versa, by suitably moving the target in the beam.

3.2 Experiments at Low Temperatures

Because of the short range of the charged particles in their passage through solids, the power density in the sample is quite large, several kilowatts per cubic centimeter. It is not generally possible to immerse the sample in a heat-transfer liquid because of the short particle range; a table of particle range vs. energy for different materials and different particles is given in Table 9.

The sample may be cooled and maintained at the desired low temperature by keeping it in close metallic contact with a support that is itself cooled by a suitable liquid, e.g., liquid nitrogen. This method allows the sample to be situated within the cyclotron vacuum systems, permitting the use of the undeflected beam, which may be larger in intensity and area than an external beam. However, the close metallic contact required for good conduction of the heat from the target to the cooled support may make it impossible to make measurements of various types, e.g., electrical conductivity, creep, etc., during the exposures.

The sample may also be maintained at a desired temperature by means of forced convection cooling with a cold gas, helium, cooled with liquid nitrogen. Very high gas velocities at the sample surface are required to obtain good cooling conditions with this method, and it is suitable only where it is desired to keep the sample as a whole below some given temperature rather than attempt to maintain it at some fixed temperature. The gas cooling method, however, permits greater flexibility in the type of measurement that can be made during the irradiation and can be more readily adapted to annealing experiments *in situ*.

Table 9. Particle Range vs. Energy
Alpha Particles

Pb $\rho = 11.3 \text{ g/cm}^3$	Ag $\rho = 10.5 \text{ g/cm}^3$	Cu $\rho = 8.96 \text{ g/cm}^3$	Al $\rho = 2.7 \text{ g/cm}^3$
10 Mev = $3.5 \times 10^{-3} \text{ cm}$	= $2.4 \times 10^{-3} \text{ cm}$	= $2.1 \times 10^{-3} \text{ cm}$	= $5.9 \times 10^{-3} \text{ cm}$
20 = 10.2	= 7.7	= 6.5	= 18.5
30 = 19.6	= 14.7	= 13	= 43
40 = 30.0	= 24.0	= 21	= 60
Deuterons			
Pb $\rho = 11.3 \text{ g/cm}^3$	Ag $\rho = 10.5 \text{ g/cm}^3$	Cu $\rho = 8.96 \text{ g/cm}^3$	Al $\rho = 2.7 \text{ g/cm}^3$
10 Mev = $20 \times 10^{-3} \text{ cm}$	= $17 \times 10^{-3} \text{ cm}$	= $10.3 \times 10^{-3} \text{ cm}$	= $37 \times 10^{-3} \text{ cm}$
20 = 60	= 50	= 42	= 120
30 = 115	= 95	= 85	= 250
40 = 185	= 155	= 140	= 390
Protons			
Pb $\rho = 11.3 \text{ g/cm}^3$	Ag $\rho = 10.5 \text{ g/cm}^3$	Cu $\rho = 8.96 \text{ g/cm}^3$	Al $\rho = 2.7 \text{ g/cm}^3$
10 Mev = $30 \times 10^{-3} \text{ cm}$	= $24 \times 10^{-3} \text{ cm}$	= $21 \times 10^{-3} \text{ cm}$	= $59 \times 10^{-3} \text{ cm}$
20 = 88	= 79	= 70	= 220
30 = 185	= 160	= 140	= 440
40 = 300	= 265	= 230	= 740

3.3 Experiments at High Temperatures

In studies where the sample must be kept at a controlled, elevated temperature during the exposure, it is generally necessary to establish a balance among three factors: (1) the heat generated by the beam, (2) any additional heat supplied to attain the desired high temperature, and (3) cooling losses to the ambient surroundings. At moderate temperatures, e.g., below 500°C , the tests can be carried out in a suitable inert atmosphere, but near 1000°C high vacuum is generally required to reduce the heat losses.

Rapid and erratic beam fluctuations, the high beam-power density in the target, and the small heat capacity of the targets generally used can result in temperature changes exceeding $125^\circ\text{C}/\text{sec}$. The control system for the additional heat supplied to the sample must be extremely rapid in response. For conductive materials, the best choice is electrical-resistance heating in the sample itself, electronically controlled by means of thermocouples attached to the sample. Special attention must be paid to problems peculiar to cyclotron irradiations. Forces on the sample due to the fluctuating current through it in the presence of the cyclotron magnetic field may disturb the experiment. Also, proper beam integration requires a high resistance between the sample and electrical ground, and this complicates the control circuits.

3.4 Induced Radioactivity

This may be estimated crudely, using the principal elements in the target materials, the tabulated reactions and cross sections for those materials, and the decay constants for the activated products produced. Because of the small size of the specimen, handling is a simple problem compared with that for experiments with reactors. Cooling times of a few hours permit handling of specimens with short tongs. Health-physics monitoring must accompany the work, however.

3.5 Use of Electrons

The comparatively low momentum of electrons having energies even in the several Mev range results in only minor changes in the physical properties of solids, except for molecular materials in which ionization is of primary importance. The principal application of electron irradiation has been in the determination of the threshold energy for atomic displacements and in irradiations of molecular materials. In the former case, an accurately known, stable, and well-defined value for the electron accelerating energy is of primary importance. Such conditions are well satisfied with a belt-charged type of electrostatic generator, the Van de Graaff machine, which can readily supply beam currents of 100 μ a at energies in the 1- to 2-Mev range.

Radioactivity of specimens is customarily no problem, since only a few nucleides are activated by electrons.

4 ELEMENTARY PROCESSES FOR DAMAGE IN SOLIDS

Damage to ionic, metallic, and valence crystals is due to processes that displace one or more atoms at a time from their normal sites in the solid, producing structural changes. Primary defects produced by radiation may rearrange themselves, returning the original or equivalent structure or combining with themselves and with other defects. In conducting solids, atoms are displaced as recoils or knock-on atoms by close collisions with energetic particles. In nonconducting solids, similar knock-on events occur and in addition defects are produced by ionization and excitation.

4.1 Atom Displacements

4.11 Threshold Energy. A threshold energy ϵ_0 imparted to an atom (in a collision process) will move it sufficiently far from its original site that return is impossible, provided the temperature is sufficiently low. Threshold energies have been determined by fast-electron irradiation for a few solids and are given in Table 10. It is to be expected that this threshold energy is a function of direction of displacement of the atom and possibly, to some extent, the temperature.

4.12 Single atom displacements occur if the energy given to the primary knock-on is between ϵ_0 and $3\epsilon_0$.

4.13 Multiple Atom Displacements. If the energy imparted to a primary knock-on atom exceeds three times the threshold energy, the probability of its producing secondary displacements becomes significant and will increase with energy. The average number of total displacements produced by a given primary, including the primary itself, has been worked out.⁶ The results, also given by Seitz and Koehler,⁷ are shown in Fig. 5. The expressions, if $x \equiv \epsilon/\epsilon_0 - 1$, are

$$g(x) = 1, 0 \leq x \leq 1; g(x) = 1 + \ln x, 1 \leq x \leq 2; g(x) = 0.56(1 + x), x > 2$$

where $g(x)$ is the number of displacements by given primary knock-on of energy ϵ (including itself).

4.14 The total number of displacements produced by each type of primary particle may be estimated using the methods of collision theory.

Fast Electrons. The cross section σ for a collision in which the atom receives more energy than ϵ_0 , when the electron energy is E , is as follows: Define

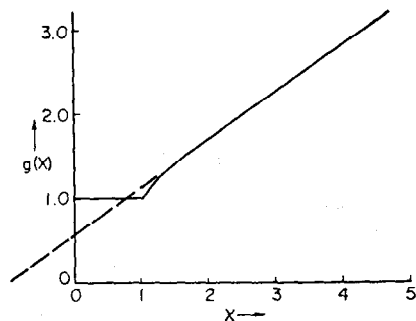


FIG. 5. Number of atom displacements, $g(x)$, as a function of $x = (\text{energy in excess of threshold})/(\text{threshold energy})$.

$$\epsilon_m = \frac{4m_0M}{(m + M)^2}$$

$$y = \frac{\epsilon_m}{\epsilon_0} 4 \frac{m_0}{M} \frac{E}{\epsilon_0} \left(1 + \frac{E}{2m_0c^2} \right)$$

$$\lambda = 1 - \beta^2 = \left(\frac{m_0c^2}{W} \right)^2$$

$$W = E + m_0c^2$$

where m_0 = rest mass of electron
 c = velocity of light
 β = velocity of electron/ c

Table 10. Threshold Displacement Energies

Solid	ϵ_0 , ev	Electron energy, Mev
Graphite	24.7 ± 0.9	0.12 ± 0.005*
Ni	34 ± 1	0.58†
Cu	25 ± 1	0.49‡
Ge	30	0.63¶

* D. T. Eggen, "Energy Required for Atomic Displacements in Graphite Determined by Electron Bombardment," NAA-SR-69, Apr. 10, 1950 (secret as of September, 1950).

† H. W. Kenworthy, NAA-SR-report, to be issued.

‡ D. T. Eggen and M. J. Laubenstein, Displacement Energy for Radiation Damage in Copper, *Phys. Rev.*, **91**: 238(A) (1953).

¶ E. E. Klontz, AECU-2267, 1952.

For convenience in use and for purposes of illustration, assume that $M = 2.25Z$ atomic mass units and $\epsilon_0 = 25$ ev. Deviations from these values may be interpolated linearly within the accuracy of the estimates. Then

$$\sigma = 2.5 \times 10^{-25} Z^2 \frac{\lambda}{\beta^4} \{ (y - 1) - \beta^2 \ln y + 0.023Z\beta[2(y^{1/2} - 1) - \ln y] \}$$

Since an irradiation of 10^{17} particles/cm² = 4.44 μ a-hr/cm² is a convenient dose, let

$$F = 10^{17} \sigma$$

The fraction F of the atoms displaced by 10^{17} particles/cm² in the target of a solid of atomic number Z is shown in Fig. 6. Secondary displacements do not occur in the range considered.

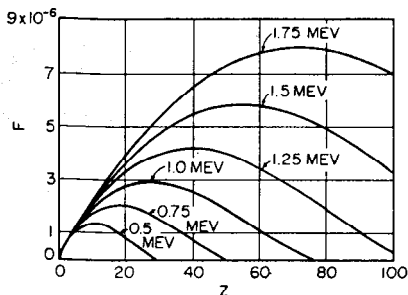


FIG. 6. Fractions of atoms displaced per fast electron.

Cyclotron Particles. Using the definitions and assumptions given above, the cross section for all collisions of a charged particle with an atom in a solid in which an atom receives energy in excess of 25 ev is

$$\sigma = \frac{11.5Z_1^2Z_2m}{E} \times 10^{-16} \text{ cm}^2$$

where Z_1 , m , and E are the atomic number, mass in atomic mass units, and energy in electron volts of the incident particle and Z_2 is the atomic number of the atom in the solid. For 10-Mev protons at a dose of 10^{17} particles/cm², the fraction of primary displacements is

$$F = 1.15 \times 10^{-5} Z_2$$

Interpolation or extrapolation of the cross sections to selected values of the particle mass, charge, or energy may be made by means of the following functions where k is a scale factor for each of the variables as given.

$$\begin{aligned}\sigma(m, Z_1, Z_2, E) &= k\sigma(m, Z_1, Z_2, kE) = \frac{1}{k} \sigma(km, Z_1, Z_2, E) \\ &= \frac{1}{k^2} \sigma(m, kZ_1, Z_2, E) \simeq \frac{1}{k} \sigma(m, Z_1, kZ_2, E)\end{aligned}$$

The energy given atoms by cyclotron particles will often exceed $3\epsilon_0$. The energy spectrum of the primary knock-ons or displacements is

$$\begin{aligned}\frac{dn}{d\epsilon} &= \frac{6.55 \times 10^{-14} N_0 Q Z_1^2 Z_2^2 m}{ME\epsilon^2} & \epsilon_0 \leq \epsilon \leq \epsilon_m \\ &= 0 & \epsilon < \epsilon_0 \quad \text{and} \quad \epsilon > \epsilon_m\end{aligned}$$

where ϵ = energy given to the primary knock-on

$\epsilon_m = 4mM/(m+M)^2$ = maximum energy of a knock-on

Q = total incident particles per cm^2

and the energy units are in electron volts. Using this spectrum, the average total number of displacements per primary collision is as given by Seitz,⁷

$$\bar{\nu} = 0.885 + 0.561 \ln \frac{\epsilon + 1}{4}$$

The fraction of all atoms displaced may be estimated by combining this number with the fraction of primary displacements above. The limitations on these estimates are discussed by Seitz.

Fast Neutrons. The cross section for displacement collisions of fast neutrons is just the experimentally determined scattering cross section σ_s . The energy spectrum is

$$\begin{aligned}\frac{dn}{d\epsilon} &= \frac{QN_0\sigma_s}{\epsilon_m} & \epsilon_0 \leq \epsilon \leq \epsilon_m \\ &= 0 & \epsilon < \epsilon_0 \quad \text{and} \quad \epsilon > \epsilon_m\end{aligned}$$

Using this together with the $g(x)$ above, the total fraction of atoms displaced by 10^{17} 1-Mev neutrons is

$$\begin{aligned}F_{tot} &= Fg(x_{avg}) \\ F_{tot} &= 4.5 \times 10^{13} \sigma_s \frac{mM}{(m+M)^2}\end{aligned}$$

4.15 The mean free path between collisions of the primary knock-on with stationary atoms depends on the interaction potential between two atoms. The potential function used by Seitz* gives several atom distances. Another expression for the interaction potential chosen by Brinkman,⁸ which gives reasonable numerical values of the potential at distances of approach about the size of an atom, leads to a much smaller mean free path, equal approximately to one lattice spacing in most solids from energies of the order of the displacement energy up to another threshold energy, the magnitude of which depends on the properties of the atoms in the solid in question.

4.2 Models of Structural Changes Produced by Displacements

4.21 Interstitial-vacancy pairs are thought to be the structural defect resulting from the displacement of the single atom with energy $\epsilon_0 \leq \epsilon \leq 3\epsilon_0$. It is reasonably well established that the vacant site with some relaxation of neighboring atoms

* Manuscript reviewed by private communication.

represents physical reality. However, the arrangement of atoms in the neighborhood of the displaced atom is less clear.⁹ In open structures it may occupy a true interstitial site and thus be correctly described by its term. For all crystals the location of the displaced atom will be called an interstitial in spite of this question. If the mean free path of several atom distances is correct, the displacements estimated above are nearly independent and remain at low temperatures as interstitial-vacancy pairs except for those removed by radiation thermal spikes and other recovery processes.¹⁰ Graphite provides a good example of the case in which single displacements predominate. A count of displaced atoms by neutron diffraction¹¹ agrees with the calculation on this basis.

4.22 Closely spaced collisions produce atomic rearrangements that differ in important ways from those produced by the widely separated collisions. Since collision of the primary knock-on with its immediate neighbor is highly probable, double, triple, or multiple vacancies are produced with high probability, with the appropriate number of interstitial atoms more or less surrounding the region of the vacancies. Moreover, Brinkman⁸ shows that at some critical value of the number of secondary displacements produced by a primary knock-on the region becomes unstable.

Displacement spikes result from the above instability promoted by the quasi-thermal excitation of the region as a result of the collision processes, which will induce regions above a critical size to collapse. Thus, mixing and disordering of a small region result directly from the displacements. In this picture the number of permanently displaced atoms that are produced by the collision processes involving neutrons with medium and high mass number solids is less than that in the picture employing the longer mean free path. Cyclotron particles produce a significant number of displacement spikes, but these do not affect the estimate of the total point defects very greatly. Brinkman gives relationships that permit estimating the type and number of multiple displacements.

Replacement Spikes. Kinchin and Pease¹² estimate that a large number of secondary collisions are sufficiently energetic to push an atom out of the site while the colliding atom merely occupies the vacancy. This process, analogous to interstitialcy migration, can play an important role in the rearrangement of atoms in some multicomponent systems, where the atoms are about the same size and mass.

Thermal spike is a term describing the situation in a small region in which a rapidly moving particle is slowed down and stopped. Brooks¹³ has shown that the large amount of the energy of the particle which is dissipated to the electrons flows away by electronic conduction without achieving equilibrium with the lattice for at least 100 atom distances. A smaller fraction of the energy, that which produced knock-ons discussed above, is dissipated directly to the lattice and is conducted away by lattice waves or by moving atoms. A small fraction of the energy is stored by displacing atoms from their normal lattice sites. Although the duration of the spike is too short to permit equilibrium to be established in any given region, it is nevertheless a useful approximation to think of the region as having a high temperature and to use the picture that thermally activated processes take place to the extent permitted by the time. A theoretical description of the thermal spike has been given by Brooks.

4.23 Fission Recoil Effects. Because of their mass and energy, fission recoils displace a large number of atoms from their normal sites in the solid. Probably few of these displaced atoms are interstitial-vacancy pairs. The thermal-spike and displacement-spike pictures mentioned above are probably most suitable for describing changes induced by fission recoils.

4.24 Foreign atoms introduced at the end of the fission recoil range produce another type of damage. Table 11 lists most of the fission-product elements, their yield, and volume. Changes in density may be estimated (1) on the oversimplified assumption that the volume of the atoms is additive or (2) on the assumption that elasticity theory may be used to compute crystal lattice distortions around foreign atoms. Lattice stresses around atoms as large as krypton, xenon, and cesium (the daughter of Xe¹³⁵) are probably relieved by the association of lattice vacancies with the region.

Table 11. Fission-product Yields and Atomic Volumes

Element	Fission yield Y_i , %	Atomic volume V_i , cm ³ /mole	$Y_i V_i/100$
Se	0.4	18.5	0.71
Kr	4.1	28	1.15
Rb	2.1	55.8	1.17
Sr	8.5	33.7	2.86
Y	10.5	16.1	1.69
Zr	29.4	14.2	4.18
Nb			
Mo	18.4	9.4	1.73
Tc	6.2	8.6	0.53
Ru	12.4	8.4	1.04
Rh	3.7	8.5	0.31
Pd	1.7	9.0	0.15
Sb			
Te	2.0	20.4	0.41
I	1.2	25.8	0.31
Xe	20.5	37.6	7.70
Ca	18.7	70	13.10
Ba	6.6	39.3	2.59
Ia	6.2	22.6	1.40
Ce	17.0	20.4	3.48
Pr	5.7	21.6	1.23
Nd	17.3	21.0	3.64
Pm	2.6	21	0.55
Sm	2.7	21.5	0.58
Eu	0.2	21.8	0.04
Br	0.2	27.6	0.06
$\Sigma Y_i = 198.3$	Vol of fission product from 1 mole of U = $\Sigma Y_i V_i/100 = 49.97$ cm ³		
U ²³⁵	Vol of 1 mole of U = 12.35 cm ³		

Table 12

Vacancies

	Cu	Ag	Au
$\Delta\rho^*$	1.3	1.5	1.5
Interstitials			
$\Delta\rho^*$	1.4† 5.0‡		

* Microhm-cm per atom per cent defect.

† Blatt.

‡ Jongenburger.

4.25 Changes in properties that result from the processes and structures mentioned above are given in following articles. Some of the elementary relations between structures and properties may be summarized as follows: *Electrical resistivity* increments due to scattering of conduction electrons by interstitials and vacancies have been calculated by Jongenburger and by Blatt (see Table 12). The changes in residual resistivity estimated from these values together with the cross sections given for cyclotron particles or electrons are five to fifteen times greater than the observed changes. Qualitative descriptions of other property changes may be given in terms of the structural defects: *energy stored*, due to interstitial-vacancy pairs; *changes in mechanical properties*, due to tying down or evolution of motion of dislocations by defects; *disordering*, by displacement and thermal spikes and by motion of vacancies; other reactions, activated in the region of the spike.

4.3 Mechanisms for Removal of Damage, Recovery

Thermally activated movement of defects permits their removal. It has been estimated on theoretical grounds¹⁴ that the activation energy for motion of *interstitials* is between 0.1 and 0.2 ev in a typical face-centered-cubic crystalline solid, copper. The activation energy for motion of a *vacancy* is significantly higher in most solids. An unequivocal assignment of activation energy and frequency factors for movement of these primary defects in solids is impossible at the present time. In Table 13 are

Table 13. Temperature Ranges for Recovery

Solid	Type of irradiation	Temperature of irradiation	Temperature range for significant recovery of electric resistivity
Graphite	Electron*	10°K	80-110°K; 150-300°K; no studies at higher temperatures
		103°K	150-300°K; no studies at higher temperatures
		20°C	180-330°C; 1000-1400°C; 1800°C
	Proton†	150°C	180-330°C; 1000-1400°C; 1800°C
		120°K†	150-300°K
Al	Fast neutron‡	30°C	180-330°C; 1000-1400°C; 1800°C
		80°K	213°K
Ni	Fast neutron§	10°K	33°K; 273°K
Cu	Electron**	80°K	20°C; 200°C
		10°K	33°K; 40-280°K (very gradual); 200°C
	Deuteron††	80°K	243°K; 200°C
		10°K	30°K (sharp); 30-200°K (gradual); 200-230°K
	Ag	Deuteron††	10°K
Au	Deuteron††	10°K	

* S. B. Austerman and J. E. Hove, Irradiation of Graphite at Liquid Helium Temperatures, *Phys. Rev.*, **100**: 1214-1215 (1955).

† G. Hennig and J. E. Hove, Interpretation of Radiation Damage to Graphite, P/751, *Proc. Intern. Conf. on Peaceful Uses of Atomic Energy*, August, 1955.

‡ W. P. Eatherly, *Bull. Am. Phys. Soc.*, **30**: 8 (1955); also T. J. Newbert, *ibid.*

§ W. K. Woods, L. P. Bupp, and J. F. Fletcher, "Irradiation Damage to Artificial Graphite," P/746. Effects in Cu and Al at 80°K, *Phys. Rev.*, **98**: 418-425 (1955).

** C. J. Meechan and J. A. Brinkman, Electrical Resistivity Study of Lattice Defects Introduced in Copper by 1.25 Mev Electron Irradiation at 80°K, *Phys. Rev.*, **103**: 1193 (1956).

J. W. Corbett, J. M. Denny, M. D. Fiske, R. M. Walker, Electrical Irradiation of Copper Near 10°K, *Phys. Rev.*, **108**: 954-964 (1957).

A. Sosin, C. J. Meechan, Defect Production and Migration in Copper and Nickel, NAA-SR-2062, Nov. 15, 1957.

†† F. Seitz and J. S. Koehler, "The Theory of Lattice Displacements Produced During Irradiation," P/749.

given the temperature ranges in which recovery of changes in electrical resistivity occurs and which must be related to thermally activated motion of primary defects observed in several solids studied to date. It may be noted that complete recovery requires heating to temperatures associated with the usual annealing of metals.

The case of graphite may be somewhat clearer than that for metals in that single interstitial atoms lie between the planes and move at approximately 80 to 100°K. Vacant sites move near 1800°C. The possible reactions of the primary defects in graphite are discussed later.

After apparently complete removal of interstitial-vacancy pairs, defects remain that increase the resistance of metals to flow. These defects are thought to be either jogs in dislocations or aggregates of interstitials or vacancies forming the equivalent of stacking faults or both.

Fission-fragment damage anneals only partially at temperatures below those at which atomic diffusion occurs. Depending on the activation energy for diffusion in the material in which the fission products find themselves, there will be a temperature range in which the atoms are sufficiently mobile that further diffusion to metastable or stable configurations is possible. Certain of the fission-product atoms, particularly the inert gases, are far too large to fit in ordinary metallic lattice. The

initial lattice strains are probably relieved by diffusion of vacancies to the region of the inert-gas atom; subsequently, the region of vacant sites along with the gas atom may diffuse out of the crystal, first to grain boundaries and then along or with grain boundaries out of the solid. While this is proceeding, if the concentration of fission-product atoms is sufficiently high, agglomeration and bubble formation are possible. At temperatures too low for diffusion, fission-product atoms will influence the physical and mechanical properties of solids in all the ways generally pictured for the effects of impurities. Because of the large mismatch in atom size, large effects at very low concentration may be expected.

4.4 Ionic Crystals

Displacements occur in ionic crystals in the way described above. In addition, two other sources of point defects exist.

Vacancies may evaporate from jogs in dislocations,¹⁵ the energy being supplied by excitons¹⁶ or by thermal activation.

Interstitial atoms may be produced¹⁷ by ionization of an anion by γ radiation or fast electrons followed by movement of the anion itself under coulomb repulsion or of a cation pushed by the anion. The cross section for the process is approximately $10^{-(15+n)}$ cm², where n is the number of electrons removed.

The interaction of crystal defects with one another and with electrons and holes is covered in the references cited.^{14,15}

5 CHANGES PRODUCED IN MACROSCOPIC PROPERTIES OF MATERIALS

5.1 Nonfissionable Metals

The effects of radiation on nonfissionable metals are generally relatively small as far as the engineering applications of the materials are concerned. The results observed, however, are of considerable interest in basic studies on the properties of imperfect materials.

5.11 Mechanical Properties. The effects on mechanical properties require some consideration in the practical application of metals to structures in a strong radiation field. The changes in electrical properties have been extensively explored also but are probably of lesser engineering significance.

The mechanical properties investigated have been of considerable variety. Table 14 summarizes the results on numerous metals.*¹⁸

5.12 Electrical Properties. The changes in electrical properties of metals have been studied primarily as a tool for the fundamental investigation of radiation-damage phenomena. In general, the resistivity near room temperature in samples exposed at such temperatures changes very little, less than 1 per cent. At lower temperatures of exposure and measurement, significant changes are observed, and the study of these changes and their annealing behavior at higher temperatures has been of considerable importance to the subject. Other electrical or magnetic properties have been investigated in special instances, including magnetic permeability and thermoelectric power. Table 15 summarizes results on the electrical resistivity changes observed in various metals.

The thermal conductivity of metals generally follows the behavior of the electrical conductivity. Measurements have been made in a few materials, e.g., Inconel and stainless steels, at elevated temperatures in the range 300 to 800°C with no changes observed.

The thermoelectric power of several materials has been studied¹⁹ as a function of irradiation. The data appear in Table 16.

5.13 Effects of Radiation on Reactions in Solid Metals (Metallurgical Processes). Several major types of reactions in solid metals (metallurgical processes) induced or

* These data have been collected from numerous unpublished AEC reports. A useful summary is given in Ref. 18.

Table 14. Change in Mechanical Properties of Metals and Alloys

Metal	Property*	Exposure†	Change observed	Remarks‡
Aluminum, high-purity annealed	Offset yield strength	$2 \times 10^{20}/\text{cm}^2$ thermal neutrons, $5 \times 10^{19}/\text{cm}^2$ fast neutrons	+100%	Exposed at about 50°C for all properties given
	Ultimate strength Fractional elongation		+60% -67%	
Aluminum, high-purity half hard	Offset yield strength	$2 \times 10^{20}/\text{cm}^2$ thermal neutrons, $5 \times 10^{19}/\text{cm}^2$ fast neutrons	+10%	Exposed at about 50°C for all properties given
	Ultimate strength Fractional elongation		+6% 0	
Aluminum	Creep rate	$\sim 10^{13}/(\text{cm}^2)(\text{sec})$ thermal neutrons	Negligible	Tested at 450°C, 27 kg/cm ²
Aluminum	Creep rate	$\sim 10^{13}/(\text{cm}^2)(\text{sec})$ 9-Mev protons	Negligible	Tested between 170-335°C, 45-180 kg/cm ²
Aluminum alloys:		$10^{20}/\text{cm}^2$ fast neutrons		Exposed at 70°C for all properties given
Type 6180	Yield strength Tensile strength		+290% +150%	
Type A54S	Yield strength Tensile strength		+6% +6%	
Type 5280, 61ST6	See above		$\sim 50-100\%$ for both Y.S and T.S	
Beryllium	Various	$\sim 3 \times 10^{20}/\text{cm}^2$ fast neutrons	Negligible	Exposed at $\sim 30^\circ\text{C}$
Copper Ann. OFHC	Hardness	$2 \times 10^{18}/\text{cm}^2$ fast neutrons	41 → 57 DPH	Exposed at 60°C
		$6 \times 10^{19}/\text{cm}^2$ fast neutrons	+53 Brinell numbers	Exposed at 80°C
Copper, single crystals	Critical shearing stress	$2 \times 10^{18}/\text{cm}^2$ fast neutrons	0.4 → 2.0 kg/mm ²	Exposed at 40°C, measured at 20°C
	Creep	$10^{13}/(\text{cm}^2)(\text{sec})$, 16-Mev deuterons	Negligible	At 260°C, 700 kg/cm ²
Copper-2% Be alloy:	Hardness—Rockwell G	9×10^{19} neutrons/cm ² thermal neutrons, 2×10^{19} neutrons/cm ² fast neutrons	R _G 18 → R _G 80	Exposed at 30°C, alloy originally in solution-annealed state
Quenched from 800°C			R _G 100 → R _G 103	Exposed at $\sim 30^\circ\text{C}$, alloy near maximum hardness originally
Quenched for 2 hr at 285°C			R _G 67 → R _G 85	Exposed at $\sim 30^\circ\text{C}$, alloy originally overaged thermally
Quenched for 18 hr at 400°C				
Copper-manganese:	DPH hardness	$1.4 \times 10^{18}/\text{cm}^2$ fast neutrons		All exposed at $\sim 30^\circ\text{C}$
1.0% Mn 5.8% Mn			+13.7 DPH numbers +16.8 DPH numbers	
17.4% Mn			+11.6 DPH numbers	
Copper-zinc:	Hardness	$1.5 \times 10^{18}/\text{cm}^2$ fast neutrons		Exposed at $\sim 30^\circ\text{C}$ Exposed at 30°C, annealed 1 hr at 750°C before exposure
1.35% Zn 34% Zn			26 → 60 R _F 64 → 71 R _F	

Table 14. Change in Mechanical Properties of Metals and Alloys. (Continued)

Metal	Property*	Exposure†	Change observed	Remarks‡
34% Zn (Cont.)	Hardness (Cont.)	$1.5 \times 10^{18}/\text{cm}^2$ fast neutrons (Cont.)	100 → 101 R _F	Exposed at 30°C, cold-rolled before exposure
Iron	Hardness	$2 \times 10^{17}/\text{cm}^2$ fast neutrons	84 → 90 R _B	Exposed at 40°C
Iron alloys: Type 304 SS	Hardness	$1.3 \times 10^{19}/\text{cm}^2$ thermal neutrons, $10^{18}/\text{cm}^2$ fast neutrons	Negligible	200°C during exposure
	Fatigue strength	$2 \times 10^{19}/\text{cm}^2$ fast neutrons	Insignificant	Irradiated at 100°C, tested at 1,700 cpm
Type 316 SS	Hardness	$5 \times 10^{19}/\text{cm}^2$ fast neutrons	83 → 98 R _B	Exposed at 25°C
	Ultimate strength Elongation at rupture		+90% -15%	
Type 347 SS	Hardness	$6 \times 10^{19}/\text{cm}^2$ fast neutrons	75 → 93 R _B	Exposed at 160°C
	Yield point		2300 → 5400 kg/cm ²	
	Ultimate tensile strength		600 → 7300 kg/cm ²	
	Hardness	$1.1 \times 10^{17}/\text{cm}^2$ 36-Mev α particles	190 → 230 DPH	Exposed at -70°C, measured at 20°C
	Hardness	$6.7 \times 10^{17}/\text{cm}^2$ 36-Mev α particles	190 → 260 DPH	
	Elongation at rupture	$6 \times 10^{19}/\text{cm}^2$ fast neutrons	57 → 34%	Exposed at 160°C
	Elongation at rupture	$7 \times 10^{18}/\text{cm}^2$ fast neutrons	Negligible	Exposed at 280°C
	Creep rate	$\sim 10^{12}/(\text{cm}^2)(\text{sec})$ fast neutrons	Decreased 25%	Tested in reactor at $\sim 700^\circ\text{C}$ under 8,000-psi stress
SA-212 pressure vessel steel	Fatigue endurance limit	$1 \times 10^{19}/\text{cm}^2$ fast neutrons	48,000 → 42,000 psi	Sample without notch exposed at 40°C
SA-285 pressure vessel steel	Tensile strength (2% offset)	$4 \times 10^{19}/\text{cm}^2$ fast neutrons	+60%	Exposed under load of 1,000 kg/cm ²
	Elongation at rupture		12 → 3%	
Molybdenum	Hardness	$10^{20}/\text{cm}^2$ fast neutrons	+35 Brinell numbers	Exposed at 80°C
	Yield strength (2% offset)		100,000 → 140,000 psi	
	Fracture strength		220,000 → 160,000 psi	
	Ductile-to-brittle transition temperature		-30 → +70°C	
Nickel	Hardness	$10^{20}/\text{cm}^2$ fast neutrons	43 → 96 R _B	Exposed at 30°C
	Ultimate strength		4400 → 6600 kg/cm ²	
	Elongation at rupture		47 → 26%	
Zirconium	Hardness	$2 \times 10^{20}/\text{cm}^2$ fast neutrons	+10 DPH numbers	Exposed at 260°C
	Yield strength (2% offset)		17,000 → 24,000 psi	
	Elongation		Negligible change	
	Creep rate	$\sim 10^{12}/(\text{cm}^2)(\text{sec})$ thermal and fast neutrons	Rate decreased by factor of 20	Tested in reactor at 260°C in stress range 1,000-2,500 kg/cm ²

* Creep rates are "in-beam" or "in-pile"; other properties are before-and-after measurements.

† In "Exposure" and "Remarks" columns conditions are not repeated. Initial conditions govern all entries for a given metal in "Metal," "Property," and "Change observed" columns until a changed condition is indicated by a new entry.

Table 15. Electrical Resistivity

Metal	Exposure	Change observed	Remarks
Aluminum, high-purity annealed.....	$2.2 \times 10^{17}/\text{cm}^2$ (36-Mev α particles)	+40 %	Exposed at $\sim -100^\circ\text{C}$, measured at $\sim -170^\circ\text{C}$
Aluminum, 2S.....	$4 \times 10^{19}/\text{cm}^2$ fast neutrons	+10 % +0.7 %	Exposed at 50°C , measured at -190°C Exposed at 50°C , measured at $+20^\circ\text{C}$
AlSi alloy (2.3 % Si, in solution).....	$4.8 \times 10^{18}/\text{cm}^2$ fast neutrons	Negligible	Exposed at 50°C
Copper OFHC.....	$2.2 \times 10^{17}/\text{cm}^2$ (36-Mev α particles) $1.5 \times 10^{18}/\text{cm}^2$ fast neutrons	+30 % +0.2 %	Exposed at -100°C , measured at -170°C Exposed at 60°C , measured at 20°C
CuSn alloys:			
1 % Sn.....	$1.7 \times 10^{18}/\text{cm}^2$ fast neutrons	+0.39 %	Exposed at $\sim 50^\circ\text{C}$
5.4 % Sn.....	$1.7 \times 10^{18}/\text{cm}^2$ fast neutrons	+0.01 %	Exposed at $\sim 50^\circ\text{C}$
CuZn alloys:			
1.35 % Zn.....	$1.5 \times 10^{18}/\text{cm}^2$ fast neutrons	+0.3 %	Exposed at $\sim 50^\circ\text{C}$
6.3 % Zn.....	$1.5 \times 10^{18}/\text{cm}^2$ fast neutrons	-0.65 %	Exposed at $\sim 50^\circ\text{C}$
12.6 % Zn.....	$1.5 \times 10^{18}/\text{cm}^2$ fast neutrons	-1.8 %	Exposed at $\sim 50^\circ\text{C}$
Iron.....	$1.7 \times 10^{18}/\text{cm}^2$ fast neutrons	Negligible	Exposed at $\sim 50^\circ\text{C}$
Iron alloys:			
Type 304 SS.....	$4 \times 10^{19}/\text{cm}^2$ fast neutrons	+5 %	Exposed at 280°C , measured at $\sim 20^\circ\text{C}$
Type 347 SS.....	$7 \times 10^{17}/\text{cm}^2$ (18-Mev deuterons)	+4 %	Exposed and measured near -150°C
Type 347 SS.....	$25 \times 10^{19}/\text{cm}^2$ fast neutrons	-1 %	Exposed at 260°C , measured at 25°C
Type 322W SS.....	$25 \times 10^{19}/\text{cm}^2$ fast neutrons	-7 %	Exposed at 260°C , measured at 25°C
Nickel, type A.....	$2 \times 10^{19}/\text{cm}^2$ fast neutrons	Negligible	Exposed at $\sim 50^\circ\text{C}$
Zirconium.....	$2.2 \times 10^{17}/\text{cm}^2$ (36-Mev particles) $1.4 \times 10^{20}/\text{cm}^2$ thermal neutrons ($\sim 2 \times 10^{19}/\text{cm}^2$ fast) $25 \times 10^{19}/\text{cm}^2$ fast neutrons	+60 % +6 % Negligible	Exposed at $\sim -100^\circ\text{C}$, measured at -170°C Exposed at $\sim 30^\circ\text{C}$, measured at 20°C Exposed at 260°C , measured at 25°C

Table 16. Thermoelectric Power

Metal	Exposure	Thermoelectric power vs. unirradiated metal	Remarks
Copper.....	$1.7 \times 10^{17}/\text{cm}^2$ 35-Mev α particles	$-0.03 \mu\text{V}/^\circ\text{C}$	Exposed, measured at -120°C
Iron.....	$2 \times 10^{18}/\text{cm}^2$ 9-Mev protons	$-0.3 \mu\text{V}/^\circ\text{C}$	Measured near 30°C
Chromel vs. Alumel.....	6×10^{13} neutrons/ cm^2 fast-neutron flux	Negligible	Exposed, measured near 100°C

affected by radiation have been studied extensively: order-disorder transformations, precipitation from solid solution, phase change from austenitic to ferritic structure, and diffusion.

Order-Disorder. In the alloy Cu_3Au , neutron exposures have been observed to disorder initially well-ordered specimens at temperatures near 50°C .²⁰ In a somewhat higher temperature range, radiation has been observed to accelerate the ordering of initially disordered specimens.²¹

Similar disordering effects have been observed in Ni_3Mn from measurements of changes in the magnetic properties.²²

In the alloy β brass, which normally exists only in the ordered states below its transition temperatures, exposure to $4 \times 10^{17}/\text{cm}^2$ of 36-Mev α particles at -150°C produced a 100 per cent increase in resistivity.²³ This is much greater than is observed in other brasses and anneals out rapidly below room temperature. This change has been interpreted as disordering of the β -brass structure at low temperatures.

All these results can be described qualitatively in terms of enhanced local diffusion on a microscale. The exact mechanism required to account for the rapidity of the effects is not yet clear. Several hypotheses, described as "thermal," "displacement," or "replacement" spikes, have been proposed.*²⁴

Precipitation from Solid Solution. The system that has been studied most extensively is copper containing about 2 per cent beryllium.²⁵ The changes in electrical resistance during and subsequent to exposure, the changes in hardness after varying exposures, and the subsequent alteration of these changes during annealing were investigated. In summary, a correspondence between effects produced by neutron irradiation and by low-temperature ($\sim 100^\circ\text{C}$) aging was observed. The results suggest that radiation can produce precipitate nuclei and that these form because of the accelerated microdiffusion which takes place in the presence of radiation.

The decrease in resistivity observed in type 322W stainless steel (Table 15) has also been attributed to precipitation induced by radiation.

Phase Transformation. Austenitic stainless steels, alloys of iron, chromium, and nickel, are metastable only at ordinary temperatures; the stable state is a mixture of austenitic and ferritic. The ferritic phase is ferromagnetic, and magnetic measurements have been used as a sensitive means for detecting the presence of transformed material. A slight increase in ferritic content after neutron bombardment of type 347 stainless steel has been observed,²⁶ but of a magnitude probably below practical significance.

Diffusion. The effects of radiation on the several processes discussed in earlier paragraphs suggest that microdiffusion is accelerated in metals when they are exposed to particle radiation. Direct experiments on this phenomenon have not yielded positive results, however.

Detailed experiments on the effect of radiation on the diffusion rate in the copper-gold, copper-nickel, and lead-tin systems and on self-diffusion in silver have been made.

Copper-gold and copper-nickel samples were exposed in a fast-neutron flux of $\sim 5 \times 10^{12}$ neutrons/ $(\text{cm}^2)(\text{sec})$ in the temperature range 280 to 380°C , with no observable change in diffusion rate compared with control samples at the same temperature.²⁷

Lead-tin samples, exposed in a much lower flux, also gave negative results.

Silver self-diffusion was studied using cyclotron beams of 3×10^{13} neutrons/ $(\text{cm}^2)(\text{sec})$ of 10-Mev protons. The temperature range was 700 to 850°C . No detectable change was observed.²⁸

5.2 Moderator Materials

5.21 Graphite. Information concerning changes in the following properties of graphite is of direct use in the design and operation of reactors: (1) linear dimensions, (2) thermal conductivity, (3) enthalpy (stored energy), and (4) Young's modulus. Of engineering importance but not of direct use are changes in (1) strength and (2)

*Revised by D. S. Billington in Ref. 24.

machinability. Studies aimed at understanding and describing radiation damage have made use of measurements of the following quantities, in addition to those above, as a function of irradiation dose and temperature and of temperature and time after irradiation: (1) lattice parameters; (2) electromagnetic coefficients, (a) electrical resistivity, (b) thermoelectric power, (c) Hall coefficient, (d) magneto-resistivity, (e) magnetic susceptibility, (f) paramagnetic resonance; and (3) diffusion of radioactive tracers. A self-consistent and nearly complete description of the observed changes in terms of elementary processes is given by Hennig and Hove.²⁹

In this article only the properties of reasonably direct use will be summarized. The references cited give nearly all available information.

Table 17. Nomenclature of Graphites

Designation	Filler	Binder	Manufacturing process
CSF	Cleves*	Standard§	Acheson
CS-GBF	Cleves	Standard	GBF
KC	Kendall†	Chicago**	Acheson
KS	Kendall	Standard	Acheson
WSF	Whiting‡	Standard	Acheson
WS-GBF	Whiting	Standard	GBF
TS-GBF	Texas¶	Standard	GBF

* Petroleum coke (mid-continent crudes) from the Gulf Oil Company refinery at Cleves, Ohio.

† Petroleum coke (Pennsylvania crudes) from the Kendall Oil Company refinery at Bradford, Pa.

‡ Petroleum coke (mid-continent crudes) from the Standard Oil Company (Indiana) refinery at Whiting, Ind.

§ No. 2 medium-hard coal-tar manufactured by the Barrett Company.

¶ Petroleum coke (mid-continent crudes) from the Texas Company refinery at Lockport, Ill.

** Barret-Chicago No. 7HO coal-tar pitch manufactured by the Barrett Company.

Table 18. Thermal Conductivity of Unirradiated Graphite Parallel and Transverse to Direction of Extrusion

Grade	Parallel conductivity, cal/(cm)(sec)(°C)	Transverse conductivity, cal/(cm)(sec)(°C)
KC	0.43	0.27
CSF	0.40	0.26
TS-GBF	0.20	0.18

Graphite Types. Table 17³⁰ lists the trade designation of several types of graphite used and studied in connection with reactors. Methods of blending, forming, baking, graphitizing, and purification are given by Currie.³¹ The properties of a graphite body appear to be controlled largely by (1) crystallite size, influenced by source material and graphitizing temperature; (2) crystallite orientation, determined largely by forming methods; (3) amount and nature of intercrystalline binder material, probably governed by the source material used for binder, by temperature, and by time of graphitization; and (4) density. These factors may vary somewhat throughout a body.

Dimensional changes arise primarily because graphite crystallites expand along their *c* axis ([001] direction) and are influenced secondarily by preferred orientation. Figures 7 and 8³⁰ show length changes of several graphites in directions parallel and perpendicular to the forming direction. *The temperature variation* of the physical expansion during irradiation is shown in Fig. 9.³⁰

Thermal conductivity and its reciprocal, thermal resistivity, are shown in Table 18³⁰ and Figs. 10, 11, and 12 for three types of graphite.

Stored energy or the increase in enthalpy in irradiated graphite has been measured by two methods: (1) determination of specific heat by comparison in a differential calorimeter with unirradiated specimens and (2) accurate determination of heat of

combustion. The first method gives data of the type shown in Fig. 13, which are typical of well-graphitized material.

This method supplemented by the second gives the data shown in Fig. 14.

Increasing the *temperature of irradiation* lowers the amount of energy stored at constant irradiation as shown in Fig. 15.

Young's modulus varies with irradiation in the manner shown in Fig. 16.

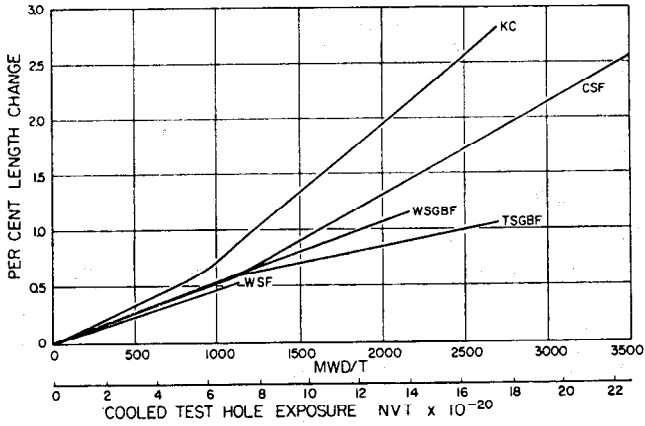


Fig. 7. Length increase of several graphites in directions parallel to forming direction.

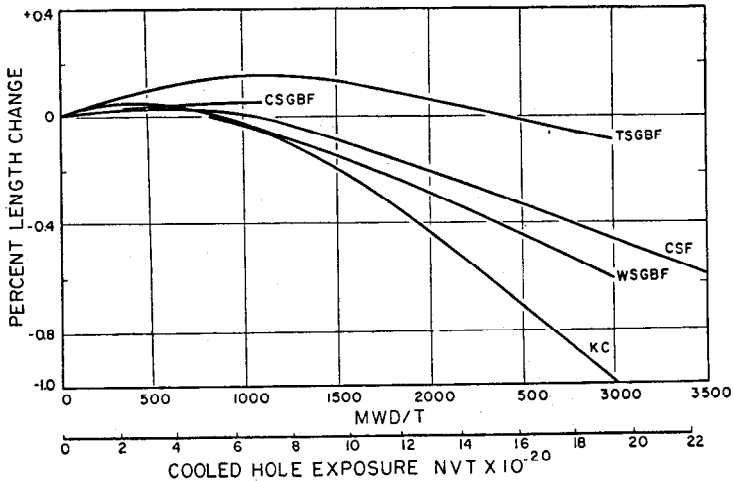


Fig. 8. Length changes of several graphites in directions perpendicular to forming direction.

The *recovery* of the above properties upon heating is illustrated by the data on dimensions plotted in Fig. 17. Complete restoration of properties does not occur short of 1800 to 2000°C. *Radiation recovery* of all properties can also occur. Figure 18 shows the behavior of the dimensions of graphite specimens that may be taken as illustrative of other properties.

The *mechanisms* concerned in the radiation damage of graphite and a model of damaged graphite involve the following points: (1) Carbon atoms are displaced predominantly one at a time by primary and secondary collisions; a few collisions may displace pairs of atoms. The fraction of displaced atoms per megawatt-day per ton is 3.5 to 7×10^{-3} . (2) A number of displaced atoms remain relatively close to a

vacancy and are called *close pairs*. (3) Displaced atoms occupy interplanar positions and cause the extension of crystallites in the *c* direction. (4) Well-separated interstitial-vacancy pairs accept electrons and serve as scatterers for electrical conduction. As electrons are trapped, holes are created. At first electrical conductivity is lowered,

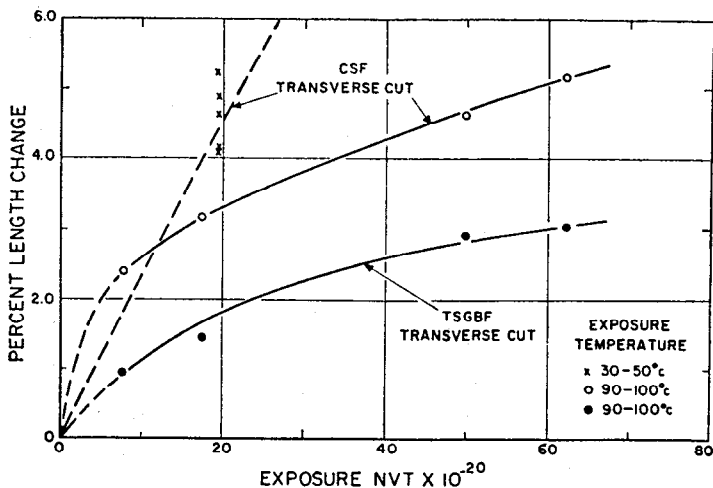


FIG. 9. Temperature variation of the physical expansion of graphite during irradiation.

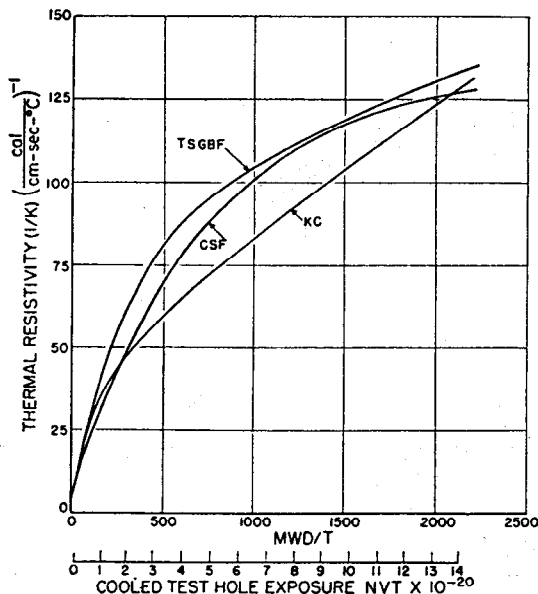


FIG. 10. Thermal resistivity of graphite parallel to the axis of extrusion as a function of exposure.

but finally the increase in carriers balances the increase in scattering. Close pairs do not become charged. (5) Interstitial atoms are immobile below 80°K, but above this temperature (a) close pairs may recombine and (b) charged interstitials may separate because of coulomb repulsion. Paramagnetic resonance, which is due to unpaired electrons on these interstitials, sharpens as a result of this separation. (6)

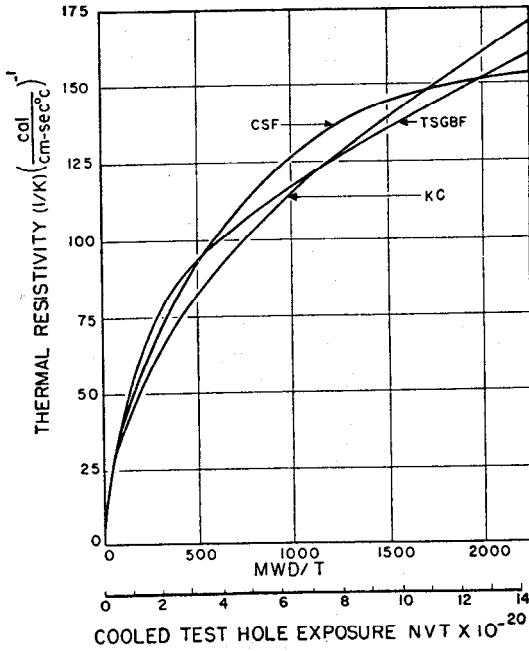


FIG. 11. Thermal resistivity of graphite transverse to the axis of extrusion as a function of exposure.

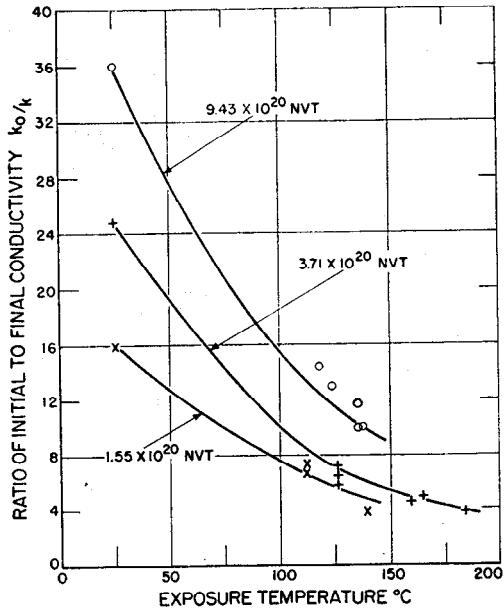


FIG. 12. Effect of exposure temperature on conductivity of graphite.

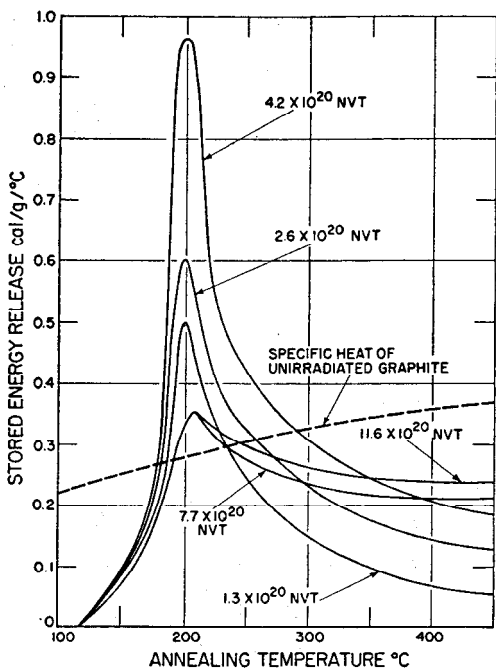


Fig. 13. Effect of annealing temperature on stored energy in graphite.

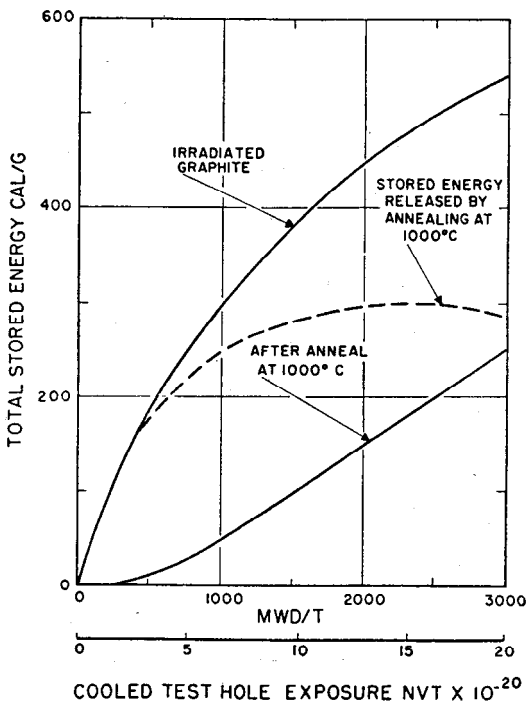


Fig. 14. Stored energy remaining in graphite after annealing as a function of exposure.

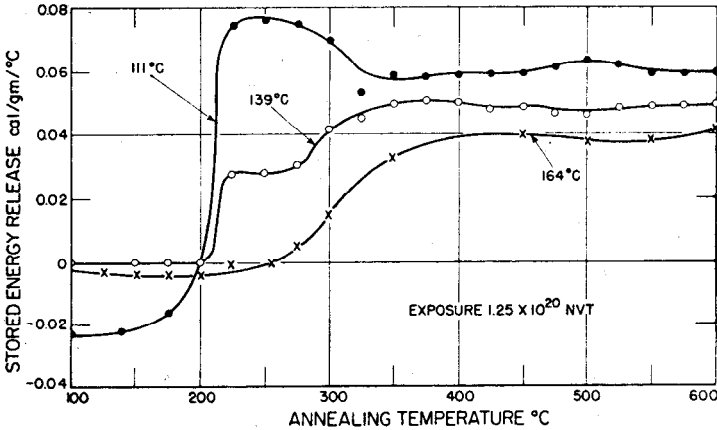


FIG. 15. Release of stored energy in graphite by annealing.

Above room temperature single, charged interstitials may combine to form C_2 molecules or ions releasing energy. (7) Hot atoms also may combine with vacancies before loosing their recoil energy and acquiring a charge. (8) Arrays of charged interstitials, C_2 ions, and clumps of atoms bend the graphite planar layers and scatter the lattice waves that conduct heat, thus reducing thermal conductivity progressively. (9) At higher temperature, reintegration and migration of interstitial complexes into planes and to crystalline boundaries and discontinuities, respectively, take place. (10) Only at temperatures above $1800^\circ C$ do vacancies diffuse to boundaries.

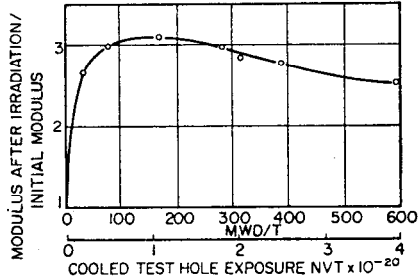


FIG. 16. Effect of irradiation on Young's modulus of elasticity of graphite.

5.22 Beryllium Oxide. *Mechanical properties* of beryllia do not change more than 10 per cent after irradiation up to about 220 Mwd/ton.

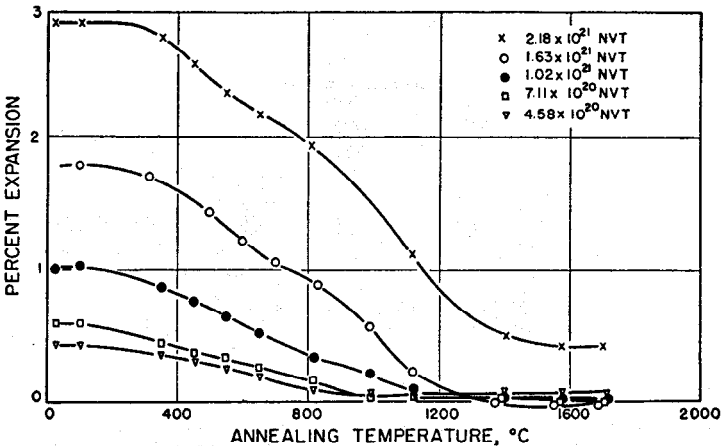


FIG. 17. Restoration or recovery of graphite dimensions by annealing.

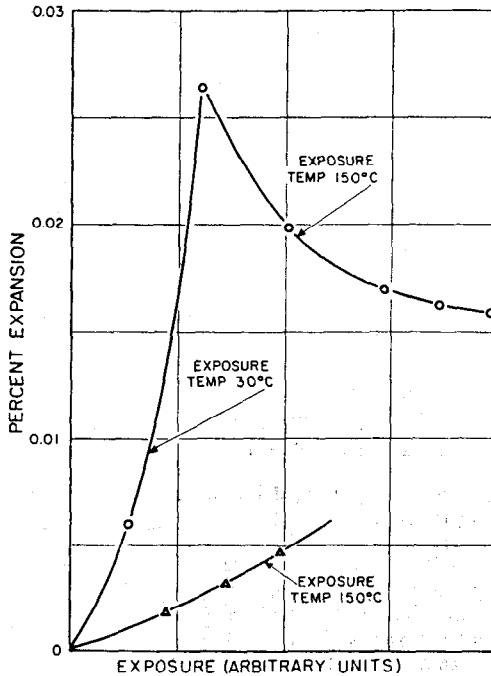


Fig. 18. Recovery due to additional radiation at increased temperature.

Table 19. Thermal Resistivity of Beryllium Oxide
Transient Flow of Heat
(Ratio of thermal resistivity after irradiation to that before)

Mwd/ton	Density, 2.7 g/cm ³	
	2.7 g/cm ³	2.9 g/cm ³
54	1.19	1.33
109	1.54	1.46
219	1.51	1.62

Steady-state Flow of Heat

Temperature of irradiation, °C	Thermal resistivity, (°C)(cm)/watt	
	Unirradiated	Irradiated 54 Mwd/ton
200	0.82	0.61
300	0.65	0.51
350	0.59	0.47

The thermal conductivity falls off slightly as shown in Table 19.

Recovery of the change of thermal resistivity is complete after annealing at about 800°C for 1 hr.

5.3 Reactor Fuels

Solid fuel materials for nuclear reactors may be discussed conveniently and characteristically under the following headings: (1) metallic-uranium-base materials, (2)

dispersions of uranium or uranium compounds in ductile metallic matrices, (3) ceramic materials. Materials on which information is available will be listed under these headings.

5.31 Units of Dose or Exposure. The chief effects of radiation in fuel materials are a function of the number of fissions, other variables being held constant. The per cent of all atoms fissioned in the materials is called burnup, *bu*. It is related approximately to other units of exposure as follows:

$$1\% \text{ bu} \approx 8.8 \times 10^3 \text{ Mwd/ton (metric uranium)}$$

$$1 \text{ Mwd/Ct}^* \approx \text{an } \textit{wt} \text{ of } 3.44 \times 10^{17} \text{ (BNL graphite-moderated reactor)}$$

5.32 Uranium-base Fuels—Unalloyed α Uranium. Dimensional changes often termed *growth* accompany burnup in *single crystals* of α uranium. At constant temperature the growth rate appears to obey the relation

$$\frac{1}{l} \frac{dl}{d(bu)} = G$$

Values of *G* are listed in Table 20.

Table 20. Radiation Growth of Alpha Uranium Crystals*

Crystallographic direction	Growth coefficient <i>G</i>
[100]	-420 ± 20
[010]	+420 ± 20
[001]	0 ± 20

Temperature: 100°C approximately
Range of applicability: 0 to ~0.1% bu

* S. H. Paine and J. H. Kittle, Irradiation Effects in Uranium and Its Alloys, P/745, *Proc. Intern. Conf. on Peaceful Uses of Atomic Energy*; also, "Progress in Nuclear Energy," vol. 4, part 1, Pergamon Press, London (to be published).

Polycrystalline α uranium grows at rates that increase with preferred orientation (actually the detailed texture) and decrease slightly with increasing grain size. Since highly textured specimens grow as much as twice as fast as single crystals under identical conditions, the phenomena cannot be merely growth of individual grains subject to the restraints imposed by adjacent grains. The *dominant variable, texture*, is a highly complex quantity. Figure 19 shows how the growth coefficient varies with the textures produced by rolling at 300°C. Textures produced by the above rolling are discussed by Foote.³⁵ A dominant component of the texture places the pole for the (010) plane, i.e., the [010] direction, in the rolling direction. *Recrystallization* at approximately 600°C leaves the (010) pole concentration about the same but shifts the high (110) pole concentrations from the rolling direction and near 60° from the rolling direction to more random orientations. The distribution of (100) poles is also shifted. These changes plus the change in grain boundaries result in lower growth coefficients. Table 21 shows the effect of recrystallization on the growth coefficient as well.

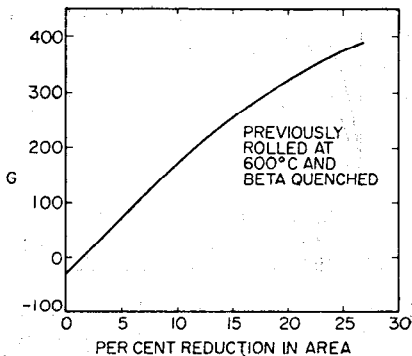


FIG. 19. Effect on *G* of rolling beta quenched alpha uranium at 300°C.

Thermal cycling textured uranium between, for example, $T_u = 500^\circ\text{C}$ and $T_l = 100^\circ\text{C}$

also causes growth in the direction in which the metal was worked (for example,

* Central metric ton.

Table 21. G for Round-rolled Uranium Rods Worked and Heat-treated as Shown

Rolling temperature, °C	Subsequent heat treatment	G
300	As rolled	
	2 hr at 630°C	
400	As rolled	475
	2 hr at 600°C	204
500	As rolled	321
	2 hr at 600°C	163
600	As rolled	4
	2 hr at 575°C	6
640	As rolled	-22
	2 hr at 575°C	

rolled). This growth varies with grain size and texture in ways analogous to those given above.

Changes in length follow the relation

$$\frac{1}{l} \frac{dl}{dn} = G_T \left(T_w, T_l, t_w, t_l, \frac{dT}{dt} \right)$$

where n is the number of cycles and t refers to time; G_T and G are both plotted in Fig. 20 for cold-worked and recrystallized uranium.

The temperature variation of radiation growth G is known qualitatively, is approximately zero at 500°C,³⁶ appears to be a maximum near 150 to 200°C,^{33,34} and has perhaps 20 per cent of the 100°C value at -100 to -120°C.³⁷

Surface roughening occurs in coarse-grained uranium upon either irradiation or thermal cycling because of the relative displacement of adjacent grains.

Mechanisms for radiation growth have been suggested along the following two lines:

1. Microscopic deformation^{33,34,36} in and around a thermal spike, the known laws for macroscopic deformation governing and leading to flow as given above. A difficulty with the mechanism is that dislocations cannot move the requisite distance during the lifetime of a thermal spike, 10^{-11} sec.

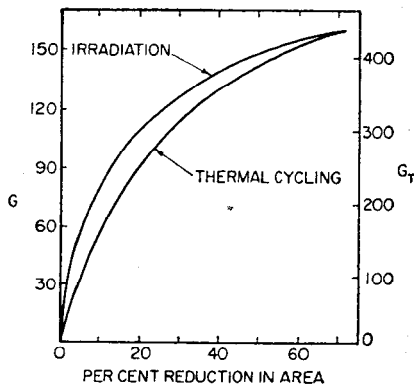


FIG. 20. Comparison of thermal cycling and irradiation on growth of uranium.

2. Anisotropic diffusion of vacancies and interstitials produced by displacements, the interstitials moving predominantly between the somewhat loosely spaced corrugated planes parallel to (010) and aggregating to form platelets, thus causing growth in the [010] with concomitant diffusion of vacancies predominantly in the [100] causing shrinkage in this direction. The nature of coupling between grains to enhance growth in textured uncrystallized specimens is not known.

Mechanisms for thermal cycling growth involve the following:

1. The differential thermal expansion of adjacent grains. The expansion coefficients in the three crystallographic directions are:

Direction	Coefficient of thermal expansion $\times 10^6$, 25-650°C
[100]	36.7
[010]	-9.3
[010]	34.2

2. Flow and relaxation of stresses at grain boundaries in the temperature range above 350°C.

3. Yield by slip (assisted by twinning) under the stresses due to differential expansion in the temperature range in which grain boundaries are rigid.

4. The existence of two major components of the texture in worked uranium.

Other pairs of deformation mechanisms may take part,³⁸ but their existence has not been demonstrated experimentally as has the above pair.^{38,39}

Density Changes. In the article on elementary processes, it was shown that changes in density should be about 2.5 to 3.5 times the burnup. Figure 21 shows the results of measurements that fall in the band shown. It may be noted that the minimum amount found corresponds reasonably well to the volume taken up by fission products. Some void formation evidently occurs in some specimens due (1) probably to cracks at grain boundaries and occlusions formed as the crystals deform and strain one another, (2) to diffusion of vacancies into the stress fields caused by the large fission products. Data on agglomeration of fission gases and bubble formation are not available as yet.

Mechanical properties of α uranium change drastically after small burnup. Measurements are illustrated in Table 22.

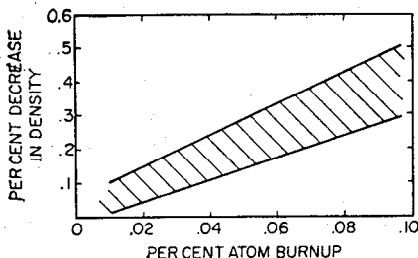


FIG. 21. Decrease in density of uranium with burnup.

Table 22. Effect of Burnup on Some of the Mechanical Properties of α Uranium

Conditions	Ultimate strength		Yield strength		% elongation		Young's modulus, $\text{psi} \times 10^{-6}$
	$\text{Psi} \times 10^{-3}$	% change	$\text{Psi} \times 10^{-3}$	% change	1-in. gauge	% change	
Control*. ³⁸	104	33	...	17	25
0.035 % burnup at 120°C..	76	- 27	71.5	117	0.36	- 97.9	28
Same irradiated, annealed 15 hr at 400°C in <i>vacuo</i> .	65	- 38	52	58	0.54	- 96.8	
Same irradiated, tension tested at 285°C.....	71	- 32	70	112	0.7	- 95.9	12
Cast uranium ³⁸ high carbon:							
Before.....	78.2						
After.....	29.8	- 62					

* Standard tension test specimens of 1/4-in. diameter prepared from material quenched from the β range.

Electrical Resistivity. Konobeevsky, Provdyuk, and Kutaitsev⁴⁰ report a 4 per cent increase in the resistivity of rolled foil at exposures to $nvt = 10^{20}$ at 80°C. Activation energies for recovery are given in Table 23. Royal⁴¹ reports a 1 per cent change after 2×10^{-4} per cent *bu*.

Table 23. Activation Energy for Recovery of Electrical Resistivity of Irradiated Uranium

Temperature, °C	Activation energy, kcal
171	45.3
209	52.5
218	62.7

5.33 Uranium-base Fuels—Alloyed α Uranium. A number of elements have been added to uranium in small quantities up to approximately 4 atom per cent in order to modify its properties.³⁵

The most interesting systems are provided by those addition elements which show some solubility in the β and/or γ phases but lower solubility in the α phase and hence modify the transformations on cooling. The completely stable room-temperature state produced by annealing, aging, or tempering is α uranium containing a rejected phase. Only a few data are available on the properties of these alloys after irradiation.

Uranium-Zirconium. As in the case of α uranium, *dimensional changes* depend on preferred orientation. Quantitative comparison with pure α uranium is not possible at the present time. If properly heat-treated, these alloys contain little or no preferred orientation and hence do not change dimensions to any great extent. *Density changes* correspond to the lower line of the band shown in Fig. 21. *Thermal conductivity* changes approximately 5 per cent at 0.1 per cent burnup.

Uranium-Chromium. *Dimensional* and *density* changes in these alloys appear to be similar to the uranium-zirconium alloys in the range of a few hundredths of a per cent burnup.

Uranium-Aluminum. Englander⁴² reports that a 3 per cent uranium-aluminum alloy solution heat-treated around 1090°C, quenched to room temperature, and tempered at 480°C shows little or no dimensional changes under irradiation or thermal cycling.

5.34 Uranium-base Fuels—Alloyed β Uranium. Chromium and molybdenum have been used to make metastable β -

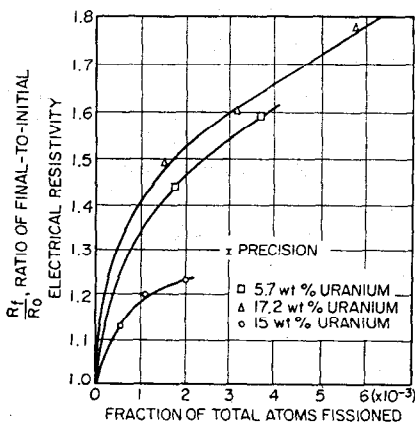


FIG. 22. Change of electrical resistivity of aluminum-uranium alloys with burnup.

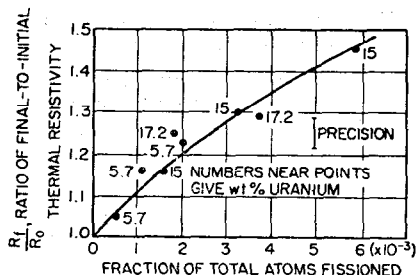


FIG. 23. Change of thermal resistivity of aluminum-uranium alloys with burnup.

uranium alloys by quenching the β field to room temperature. Tucker and Senio* have shown that the metastable alloy does not change to α uranium under irradiation.

5.35 Uranium-base Fuels—Alloyed γ Uranium. As may be seen from Ref. 41, alloys containing in the neighborhood of 8 weight per cent molybdenum or niobium may be quenched from the γ field to room temperature without transformation. On tempering or aging at 350°C or above in the α field, the γ phase decomposes into α uranium and an ϵ prime phase. Konobeevsky, Provdyuk, and Kutaitsev⁴⁰ show that such an alloy containing 9 per cent molybdenum is transformed to the γ structure by an irradiation of the order of 10^{19} *nut* at 50°C.

5.36 Dispersions of Uranium and Uranium Compounds in Ductile Metallic Matrices. If fissile materials are dispersed as discrete particles throughout a metallic matrix, damage by fission recoils and atoms may be confined to the region of the particle. The damage to the matrix then becomes primarily that due to fast neutrons discussed in foregoing articles.

Aluminum-Uranium Alloys. Research reactors utilize alloys containing approximately 2 atomic per cent uranium in the form of intermetallic compound UAl_3 dispersed in commercial aluminum. Measurements of the properties of several alloys containing 5 to 17 weight per cent uranium have been determined by Siegel and Billington⁴¹ and are shown in Figs. 22 to 25. Density changes in uranium-aluminum

* Page 11 of Ref. 41.

alloys are approximately $2\frac{1}{2}$ per cent at 1 per cent burnup and within experimental error are linear with burnup.

Aluminum-UO₂ Mixtures.^{43,44} Bodies consisting of aluminum in which particles of UO₂ are dispersed behave in a fashion analogous to the aluminum-uranium alloy mentioned above. Effects on the aluminum itself decrease with increasing particle size of the UO₂.

Beryllium-Uranium Alloys.⁴⁰ Beryllium containing 0.5, 1.0, and 3 per cent uranium dispersed throughout the beryllium as UBe₁₃ showed changes in electrical

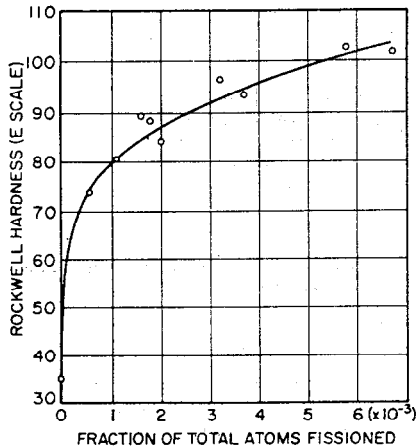


FIG. 24. Change of hardness of aluminum-uranium alloys with burnup.

resistivity from 1.5 to 9 per cent after 0.06 per cent burnup, the change being approximately linear in uranium concentration. Changes in dimension and density were not outside experimental error of measurement.

Zirconium-Uranium Alloys. Dilute al-

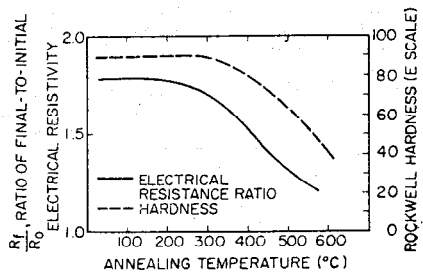


FIG. 25. Effect of annealing on electrical resistivity and hardness of irradiated aluminum-uranium alloys.

loys of uranium in zirconium consist of the two phases nearly pure zirconium in which is dispersed nearly pure uranium. In the range of a few hundredths of a per cent burnup, little or no change occurs in physical properties, and density changes proceed linearly with burnup at approximately the theoretical rate.

Steel-UO₂ Mixtures. Weber⁴⁴ gives the following changes in hardness dispersions of UO₂ in austenitic stainless steel:

Volume % UO ₂	Hardness before irradiation, DPH	Hardness after irradiation, DPH	Particle size UO ₂ , μ
24	225-250	475-500	3
24	175-260	330-440	15-44

5.37 Ceramic Materials. Beryllium Oxide-Uranium Oxide. After burnup of 5×10^{-4} per cent, the following changes were noted in beryllia bodies containing 2 per cent UO₂ mixed with BeO, density 2.4 to 2.8 g/cm³, UO₂ particle size approximately 2μ : (1) thermal resistivity increases by a factor of 5 to 6; (2) linear dimensions, +1 per cent; (3) elastic modulus, -30 per cent; (4) compressive strength, -30 per cent.

Uranium Oxide. The broadening of X-ray diffraction lines from U₃O₈⁴¹ shows that fragmentation of the crystal occurs at a burnup of approximately 3×10^{-6} per cent. UO₂ is relatively unaffected.

Graphite-Uranium Oxide. Test bodies have been made by (1) impregnating graphite with a uranium salt and baking to give U₃O₈, (2) mixing UO₂ with graphite and a resin and baking at 1370 to 1400°C. The results of irradiation are shown in Tables 24 and 25.

Table 24. Effect of Irradiation on the Properties of Impregnated Graphite-U₃O₈ Bodies (Hanford Irradiation Facility)

Mg of U ²³⁵ /g of graphite	Dose, Mwd/t*	Fractional change in property		
		Diameter	Length	Electrical resistivity
0	27.3	+2.93
12	27.3	+0.021	-0.007	+2.79
0	56.6	+3.14
11	56.6	+0.040	-0.025	+2.83
0	186.3	+0.003	-0.0008	+4.07
115	186.3	+0.080	-0.045	+3.21

Temperature of unimpregnated < temperature impregnated ≤ 100°C.

AGOT-KC graphite cut parallel to direction of extrusion.

* Equivalent to $not = 8.21 \times 10^{18}$ thermal neutrons/cm².

Table 25. Effect of Irradiation on the Properties of Molded Graphite-UO₂ Bodies
Dosage: $1.85 \pm 0.05 \times 10^{18}$ neutrons/cm²
Temperature: 66-88°C

Type sample	UO ₂ particle size	Fractional change in property		
		Young's modulus	Electrical resistivity	Thermal conductivity
Transverse cut AGOT.....	No U	+0.44	+0.39	-0.22
Molded.....	No U	+0.37	+0.28	-0.11
Molded, natural U.....	586	+0.34	+0.30	-0.8
Molded, natural U.....	334	+0.38	+0.32	-0.14
Molded, natural U.....	94	+0.41	+0.34	-0.10
Molded, 90% enriched U.....	486	+0.35	+0.21	-0.09
Molded, 90% enriched U.....	334	+0.33	+0.21	-0.13
Molded, 90% enriched U.....	94	+0.30	+0.28	-0.13

Annealing of specimens used to obtain data for Table 25 was done for as long as 22 hr at 800°C with little change.

5.4 Semiconductors⁴⁵

These materials are of special importance because of their increasing use in solid-state electronic devices, as rectifiers and amplifiers. The electronic properties of semiconductors are dependent on the concentration of carriers, which arise from the presence of impurities or lattice defects. Radiation with massive particles thus produces very large and very rapid changes in the electrical properties of this class of materials.

In *n*-type germanium the conductivity decreases from 0.27 to 0.004 (ohm-cm)⁻¹ after 1.5×10^{16} /cm² of fast neutrons. The conductivity, after passing this minimum value equivalent to the intrinsic conductivity of the semiconductor, then increases with further irradiation, reaching 0.03 (ohm-cm)⁻¹ at 3×10^{16} /cm².

In *p*-type germanium the conductivity increases monotonically, changing from 0.04 to 0.06 (ohm-cm)⁻¹ after 3×10^{14} /cm² fast neutrons.

The behavior of germanium is quite complex, depending on the exposure temperature and the initial state of the material.

In silicon, the conductivity decreases with irradiation in both *n*- and *p*-type material. The rate of decrease is much greater in *p* type than in *n* type, however.

Data for *p*- and *n*-type samples appear below:

Electrical Resistance of Silicon Specimen

Exposure.....	0	3×10^{16}	1.5×10^{16}	3×10^{16}	4.5×10^{16}
<i>p</i> type, ohms.....	30	50	190	16,000	68,000
<i>n</i> type, ohms.....	23	25	31	32	37

These data are typical, but since the properties of semiconductors depend so markedly on their initial state of purity and heat treatment, their applicability to particular samples is questionable. For this reason, practical devices such as diodes and transistors must be individually investigated at the present state of knowledge.

5.5 Ionic Crystals

In these materials, of which the alkali halides are most typical, the principal changes that have been investigated are the optical properties and the ionic conductivity.

The increase in optical absorption is produced by both γ -ray and particle radiation. The data on this phenomenon are very extensive and have been reviewed by Seitz.¹⁵ These optical effects are electronic in origin; electrons are excited by the incident radiation and are trapped near lattice defects that already exist in the crystal. Such trapped electrons or combinations of them have characteristic absorption spectra and annealing or bleaching behavior.

The data on ionic conductivity changes are meager and ambiguous. The conductivity of KCl was lower subsequent to irradiations with γ rays and short exposures in a reactor.^{46,47} The conductivity of NaCl was similarly decreased by a factor of 30, subsequent to exposure to $10^{15}/\text{cm}^2$ of 350-Mev protons at 50°C. Prolonged exposure in a reactor, however, produces an increase in conductivity in these materials by a factor of 10.

5.6 Covalent Crystals

Quartz, zircon, and diamond are typical examples of covalent crystals and have been investigated extensively.⁴⁷ The most striking effect in these crystals is the decrease in density produced by radiation.

At an exposure of $2 \times 10^{20}/\text{cm}^2$ of fast neutrons in a reactor, the density of quartz decreases by 15 per cent. At about $5 \times 10^{19}/\text{cm}^2$, the material is no longer crystalline, hence is optically isotropic and nonpiezoelectric. In spite of these large changes in density, macroscopic defects, e.g., cracks or bubbles, were not observed.

On annealing at 950°C, the sample reverts from the amorphous to a polycrystalline α quartz structure; in addition, macroscopic channels about 0.05 mm in diameter, 5 mm long, are formed.

In the case of zircon, exposure to $3 \times 10^{20}/\text{cm}^2$ produces a density decrease of 4.2 per cent. In these crystals long-range structural order is preserved, but mosaic crystalline blocks are created. The annealing of those changes barely begins at 1000°C and is incomplete even at 1600°C.

In the case of diamond, the lattice expansion observed is tabulated below:

Exposure, cm^2 fast neutrons	Density decrease, %
5×10^{19}	1.5
1×10^{20}	2.5
1.5×10^{20}	3.0
2.0×10^{20}	3.2
4×10^{20}	3.7
6×10^{20}	3.7

A high degree of long-range order persists in these heavily exposed crystals. X-ray diffraction patterns continue to indicate a well-ordered lattice. The crystals become opaque after $10^{17}/\text{cm}^2$, and annealing at 1600°C, which produces a 70 per cent recovery in the density decrease, does not appreciably affect this opacity.

5.7 Glasses⁴⁸

The principal effect of radiation on glass is the increase in optical absorption. This is of practical importance for windows and optical devices.

The darkening is due to the same phenomenon observed in ionic crystals; the radiation excites electrons, which are trapped in vacancies and thus have typical absorption spectra. Special glasses containing cerium have been developed that are radiation resistant. The cerium ion serves as an electron trap, preventing the trapping in vacancies and the formation of F' centers.

Typical data on darkening of glass protected by the addition of cerium and unprotected glass, having an index of refraction 1.517 and a dispersion of 64.5, are as follows:

Per Cent Transmission

Exposure, τ	Protected			Unprotected	
	0	10^6	4.7×10^8	0	10^6
$\lambda = 450 \text{ m}\mu$	89	85	58	91	3.4
500	91	88	68	91	15
550	91	89	71	92	31
600	91	89	74	92	44
700	92	91	...	92	68

Acknowledgments

Sincere thanks are due J. Brinkman for indispensable suggestions on methods of displaying the fundamental processes of radiation effects, J. Douic for collecting information on methods of examining radioactive materials, and J. Bastion for checking manuscript and proof.

REFERENCES

- Gilbert, F. W.: *Nucleonics*, **10**: 6 (1952).
- Richardson, D. M.: "Calorimetric Measurement of Radiation Energy Dissipated by Various Materials Placed in the Oak Ridge Pile," ORNL-129, Oct. 1, 1949.
- Proctor, B. E., and S. A. Goldblith: "Dosimetry Research of the Cobalt-60 Source," AEC-NYO-3339, Sept. 1, 1952. D. V. Cormack, R. W. Hummel, H. E. Johns, and J. W. T. Spinks: Irradiation of Ferrous Ammonium Sulfate Solutions: Energy Absorption and Ionization Calculations for Cobalt-60 and Betatron Radiation, *J. Chem. Phys.*, **22**: 6-12 (1954). C. S. Hochanadel and J. A. Ghormley: A Calorimetric Calibration of Gamma Ray Actinometers, *J. Chem. Phys.*, **21**: 880-885 (1953).
- Pearsall, C. S., and P. K. Zingesser: "Metal to Nonmetallic Brazing," NP-841, Apr. 5, 1949.
- Yockey, H. P., et al.: Cyclotron Techniques for Radiation Damage Studies, *Rev. Sci. Instr.*, **24** (10): 1011-1019 (October, 1954).
- Snyder, W. L., and J. Neufeld: *Phys. Rev.*, **97**: 1636 (1955).
- Seitz, F., and J. S. Koehler: The Theory of Lattice Displacements Produced during Irradiation, *Proc. Intern. Conf. on Peaceful Uses of Atomic Energy*, August, 1955.
- Brinkman, J. A.: "The Production of Atomic Displacements by High Energy Particles," NAA-SR-1459, September, 1955; On the Nature of Radiation Damage in Metals, *J. Appl. Phys.*, **25**: 961-970 (1954).
- Lomer, W. M., and A. H. Cottrell: Annealing of Point Defects in Metals and Alloys, *Phil. Mag.*, **46**: 711-719 (1955).
- Cooper, H. G., J. S. Koehler, and J. W. Marx: Irradiation Effects in Cu, Ag, and Au Near 10°K, *Phys. Rev.*, **97**: 599 (1955).
- Dienes, G. J.: Theoretical Aspects of Radiation Damage in Metals, *Proc. Intern. Conf. on Peaceful Uses of Atomic Energy*, P/750, August, 1955.
- Kinchin, G. H., and R. S. Pease: *J. Nuclear Energy*, **1**: 200 (1955).
- Brooks, Harvey: TID 10633, The Thermal Spike Picture of Radiation Damage, Knolls Atomic Power Laboratory Report.

14. Seitz, F.: *Revs. Mod. Phys.*, **18**: 384 (1946).
15. Seitz, F.: Color Centers in Alkali Halide Crystals, *Revs. Mod. Phys.*, **26**: 7 (1954).
16. Kittle, Charles: "Introduction to Solid State Physics," pp. 319-320, John Wiley & Sons, Inc., New York, 1953.
17. Varley, J. H. O.: A New Interpretation of Irradiation Induced Phenomena in Alkali Halides, *J. Nuclear Energy*, **1**: 130-143 (1954).
18. Sutton, C. R., and D. O. Lesser: *Iron Age*, **174**: 97, 128 (1954).
19. Andrew, A., and C. R. Davidson: Induced Thermoelectric Potential from Radiation Damage, *Phys. Rev.*, **89** (4): 876-877 (1953).
20. Siegel, S.: *Phys. Rev.*, **75**: 1823 (1949).
21. Blewitt, T. H., and R. R. Coltmann: *Acta Met.*, **2**: 549 (1954).
22. Aronin, L. R.: *J. Appl. Phys.*, **35**: 344 (1954).
23. Bowman, F. E., and R. R. Eggleston: *J. Appl. Phys.*, **24**: 229 (1953).
24. Billington, D. S.: *Proc. Intern. Conf. on Peaceful Uses of Atomic Energy*, P/744, August, 1955.
25. Murray, G. T., and W. E. Taylor: *Acta Met.*, **2**: 52 (1954). J. W. Cleland et al.: *Phys. Rev.*, **91**: 238 (1953).
26. Reynolds, M. B., et al.: *J. Metals*, **7**: 555 (1955).
27. Martin, A. B., R. D. Johnson, and F. Asaro: Diffusion of Gold into Copper, *J. Appl. Phys.*, **25** (3): 364-369 (1954). P. Duwez and R. D. Johnson: "The Effect of Irradiation on Diffusion in Copper-Gold and Copper-Nickel Powder Techniques," NAA-SR-168, March, 1952.
28. Martin, A. B., and R. D. Johnson: The Effect of Cyclotron Bombardment on Self-diffusion in Silver, *J. Appl. Phys.*, **23** (11): 1245-1254 (1952).
29. Hennig, G., and J. E. Hove: "Interpretation of Radiation Damage to Graphite," *Proc. Intern. Conf. on Peaceful Uses of Atomic Energy*, P/751, August, 1955.
30. Woods, W. K., L. P. Bupp, and J. F. Fletcher: "Irradiation Damage to Artificial Graphite," *Proc. Intern. Conf. on Peaceful Uses of Atomic Energy*, P/746, August, 1955.
31. Currie, L. M., V. C. Hamister, and H. G. McPherson: "The Production and Properties of Graphite for Reactors," *Proc. Intern. Conf. on Peaceful Uses of Atomic Energy*, P/534, 1955.
32. Eatherly, W. P.: *Bull. Am. Phys. Soc.*, **30**: 8 (1955). T. J. Newbert, *ibid.*
33. Paine, S. H., and J. H. Kittel: Irradiation Effects in Uranium and Its Alloys, *Proc. Intern. Conf. on Peaceful Uses of Atomic Energy*, P/745, August, 1955.
34. "Progress in Nuclear Energy," vol. 1, part 1, Pergamon Press, London (to be published).
35. Foote, F. G.: Physical Metallurgy of Uranium, *Proc. Intern. Conf. on Peaceful Uses of Atomic Energy*, P/555, August, 1955.
36. Pugh, S. F.: Damage Occurring in Uranium during Burnup, *Proc. Intern. Conf. on Peaceful Uses of Atomic Energy*, P/443, August, 1955.
37. a. TID 7502, "Growth of Irradiated Uranium," pp. 564-571.
b. AERE M/R 2004, The Effects of Radiation of Some Enriched Fuels.
38. Chiswick, H. H., and L. R. Kelman: *Proc. Intern. Conf. on Peaceful Uses of Atomic Energy*, August, 1955.
39. Burke, J. E., and A. M. Turkalo: *J. Metals*, **4**: 651-656 (1952).
40. Konobeevsky, S. T., N. F. Provdyuk, and V. I. Kutaitsev: Effects of Irradiation on Structure and Properties of Fissionable Materials, *Proc. Intern. Conf. on Peaceful Uses of Atomic Energy*, August, 1955.
41. Billington, D. S.: Radiation Damage in Reactor Materials, *Proc. Intern. Conf. on Peaceful Uses of Atomic Energy*, August, 1955.
42. Englander: Private communication August, 1955.
43. Cunningham, J. E., and E. J. Boyle: MTR Type Fuel Elements, *Proc. Intern. Conf. on Peaceful Uses of Atomic Energy*, P/953, August, 1955.
44. Weber, C. E.: Dispersion Type Fuel Elements, *Proc. Intern. Conf. on Peaceful Uses of Atomic Energy*, P/561, August, 1955.
45. "Semiconducting Materials," Academic Press, Inc., New York, 1951. J. W. Cleland and J. H. Crawford: *Phys. Rev.*, **95**: 1177 (1954).
46. Nelson, C. M., et al.: *Phys. Rev.*, **90**: 364 (1953).
47. Crawford, J. H., and M. C. Wittels: *Proc. Intern. Conf. on Peaceful Uses of Atomic Energy*, P/753, August, 1955.
48. Kreidl, N. J., and J. R. Hensler: NYO-3780, Bausch and Lomb Optical Company, Rochester, N.Y., 1954.

10-5 RADIATION DAMAGE TO LIQUIDS AND ORGANIC MATERIALS

BY

Vincent P. Calkins

Radiation damage can be defined as any adverse change occurring in the physical or chemical properties of a material or system as a result of exposure to radiation. "Radiation damage" is a relative term: What is damage to a material or system as far as one person is concerned could constitute an improvement in properties and be very beneficial from the viewpoint of a second person. For example, the evolution of a gaseous hydrocarbon from an organic fluid being irradiated could represent an explosive hazard, an unwanted change in the viscosity of the liquid, or a new and very desirable method for synthesizing this hydrocarbon. However, changes in the properties of a material or system associated with a power plant are viewed with suspicion and are considered generally to be possible sources of damage.

Experimental radiation-damage data on the following general classes of material are compiled and evaluated: water, aqueous solutions, fused salts, organic fluids, and organic solids in the form of elastomers and plastics. These data are then used as a basis for evaluating radiation damage to various electrical, electronic, and mechanical systems as a function of the specific materials these systems employ.

1 MECHANISM AND NATURE OF RADIATION DAMAGE

Although the fundamentals of the ionizing properties of radiation and the mechanism of radiation absorption are discussed elsewhere, a summary statement of the effects of various types of radiation on liquids and organic materials is pertinent at this point.

1.1 Fast Neutrons

Fast neutrons react with the nuclei of the atoms of an irradiated medium, and an appreciable fraction of the energy of the neutron is transferred to each struck nucleus. The nucleus is ejected as a recoil ion, the neutron being scattered or reflected to strike other nuclei until it is degraded to a thermal-energy state. The ejected nuclei in the form of recoil ions traverse the medium and interact with orbital electrons, thus producing molecular excitation and ionization. Eventually, the recoil ions become neutralized, although they still possess energies considerably above the thermal level. As fast-moving neutral particles, they are thermalized in two ways: (1) by still losing an important part of their remaining energy by causing electronic excitation and (2) by losing the other part of this energy by undergoing elastic collisions with other atoms of the medium, thereby suffering losses in momentum. About 95 to 98 per cent of the energy of a fast neutron is transferred to a medium via electronic excitation and ionization, and only 2 to 5 per cent by loss in momentum.

Thus, since organic compounds and covalent materials are not already ionized and are usually highly susceptible to electronic excitation and ionization, the main bulk (95 to 98 per cent) of the deposited energy of the fast neutrons is instrumental in causing considerable damage to these materials by excitation and ionization. The 2 to 5 per cent energy of the fast neutrons deposited by momentum losses also causes damage in these nonionic materials by dislocation of atoms; this is commonly called

Wigner-type damage.* Conversely, since ionic materials such as many inorganic compounds are already ionized and since metals can be considered as being in an ionized state, these materials are not very susceptible to further electronic excitation and ionization, and the bulk of the energy deposited by fast neutrons in these materials, therefore, has little effect.† Some Wigner-type damage does occur, but since this damage can be caused by only a very small fraction of the total fast-neutron energy deposited, only slight damage to metals and ionic materials frequently occurs at fast-neutron dosages one thousand-fold and more greater than those dosages at which considerable damage occurs to nonionic materials such as organics.

1.2 Gamma Radiation

Gamma radiation reacts with matter primarily by the photoelectric effect, Compton effect, and pair production—depending upon the atomic number of the constituents of the irradiated medium and upon the energy of the attendant γ radiation. For materials containing elements of low atomic number (27 or less) such as hydrogen, carbon, or aluminum, the photoelectric effect predominates for γ energies below 0.1 Mev, the Compton effect for energies from 0.1 to 10 Mev, and pair production above 10 Mev. For materials containing elements of high atomic number (82 or greater) such as lead, the photoelectric effect predominates for γ energies below 0.5 Mev, the Compton effect from 1.0 to 4.0 Mev, and pair production above 4 Mev.

In the photoelectric effect, the γ ray interacts with the entire atom and transfers all the energy of the photon in one encounter. This energy is received by a single atomic electron, which is usually in the *K* or *L* shell, and this electron is ejected from the atom with an energy of $E = h\nu - \beta$, the energy of the incident photon minus the binding energy of the electron in the atom. In contrast to the photoelectric effect, the γ -ray photon in the Compton effect collides elastically with a single electron, the incident photon giving up a portion of its energy to the electron, which recoils and flies off at an angle to the direction of the incident γ photon. In accordance with current theory, pair production is caused by the complete absorption of a γ in the region of the nuclear coulomb field with the resulting formation of a positron-electron pair (e^+, e^-).

In brief, the net result of the photoelectric effect, Compton effect, and pair production is to produce either an ejected electron or an electron pair that traverses the medium, interacts with orbital electrons, and causes damage by electron excitation and ionization. Since the subsequent loss in charge of the ejected electrons and electron pairs does not result in a heavy neutralized recoil ion, no transfer of energy by loss in momentum occurs. Therefore, in general, γ radiation will cause very little damage to ionic compounds but can cause considerable damage to nonionic or covalent compounds.

1.3 Thermal Neutrons

Thermal neutrons are captured by nuclei, and damage to the surrounding material is due primarily to the secondary radiation evolved. The main damage to organic materials by slow or thermal neutrons is due to ionization of the organic media by the 2.2-Mev γ rays that are given off when the neutrons are captured by hydrogen atoms. With chloro-organics such as neoprene, the $n-\beta$ reaction is also an important factor due to the high thermal-neutron absorption cross section of chlorine. For organics possessing a high nitrogen content, a major portion of the damage produced by

* "Covalent compounds—which include the common gases and liquids and organic materials—consist of molecules each of which is formed from a group of individual atoms held together by shared electron bonds which give rise to strong exchange forces. The molecules themselves are bound together by relatively weak van der Waals forces, i.e., by the attraction due to electric fields."

† Ionic compounds—which include salts and oxides—consist of a combination of highly electro-positive and electronegative elements in the forms of ions held in a crystal lattice. The lattice of ions is held together by electrostatic forces in accordance with Coulomb's law, and there is no actual union in the crystal to give molecules, although all crystals can be considered as consisting of huge molecules the size of which is limited only by the capacity of the crystal for growth.

Metals can be considered as consisting of positive ions in a crystal lattice with the ions being immersed in an electron gas.

thermal neutrons may be due to the $N^{14}(n,p)C^{14}$ reaction, the damage being caused by ionization of the media by the ejected proton. For organic or other covalent materials containing lithium or boron, the primary damage should result from dense ionization due to the α particles given off by capture of thermal neutrons by either lithium or boron.

For ionic compounds and metals, the extent of the $n-\gamma$ reaction in any material will depend upon the capture cross section of the constituents of the material, but the ionization produced by the generated γ s would cause very little damage in this type of material. For those metals and ionic compounds containing lithium and boron, very little damage would be caused by ionization by the generated α particles, but once the α particles have lost their charge, some Wigner-type damage would be caused by the neutralized but energetic α particles.* The degree of such damage would depend upon the lithium or boron content and the degree of orientation or order in the crystal lattice of the matrix material, but generally, the degree of such damage would be small even at considerably high thermal-neutron dosages.

1.4 Fission Products

Fission products are generated as ions and are usually contained by the fuel matrix of a nuclear reactor. Since the fuel matrix is ordinarily ionic in nature, damage by fission ions would not be caused by ionization but by displacements or dislocations of the matrix atoms by collision with the neutralized fission ions. Exposure of covalent or organic materials to fission products would result in considerable damage caused by direct electronic excitation and ionization of the organic media by the fission ions. Also, a build-up of fission-product impurities in the fuel matrix due to prolonged fissioning could eventually affect the physical and mechanical properties of the fuel system by ordinary metallurgical contamination.

1.5 Other Particles

1.51 Beta radiation consists of electrons emitted from nuclei, and damage is caused by the same general mechanism as the recoil (Compton) electrons produced by γ radiation.

1.52 Protons, deuterons, and α particles are often produced for irradiation testing purposes by the use of particle accelerators such as the cyclotron or Van de Graaff. Protons cause damage in organic and ionic materials by the same mechanism as fast neutrons and also thermal neutrons in certain reactions such as the $N^{14}(n,p)C^{14}$ reaction. Deuterons, being essentially heavy protons, cause damage by a similar mechanism. The highly energetic α particles produced in the cyclotron cause damage by the same mechanism as that for thermal neutrons involving neutron α reactions.

1.53 High-energy electrons and X rays are readily produced by the betatron and the Van de Graaff, and the mechanism of damage is similar to that for β and γ radiation.

1.6 Damage as a Function of Energy Absorption

The amount of radiation damage suffered by any material as a result of exposure to radiation should be some function of the actual energy absorbed or deposited per unit

* As in the case of the recoil ions ejected as a result of the collisions of fast neutrons with the nuclei of atoms of the irradiated material, α particles and fission ions are positively charged and lose most of their energy by interaction with the orbital electrons of the atoms of a nonmetallic medium or by interaction with the so-called free electrons of a metallic medium, thereby causing excitation and ionization. As positively charged ions, these particles do not cause many primary displacements of the atoms in the lattice of an irradiated medium by collision with the nuclei of these atoms because of the coulombic repulsion forces between the charged ion and the charged atomic nuclei.

As these ionic particles approach the end of their trajectory, they lose their charge and become neutralized, although they still possess energies considerably above the thermal level of the medium. Therefore, as fast-moving neutralized particles they are not subject to coulombic repulsion forces, and even though in this state they still lose an important portion of their energy by causing electronic excitation and ionization of the medium, they can now cause and do cause actual displacement of the atoms in the lattices of the irradiated material by billiard-ball-type collisions.

mass of material.*¹ Since γ rays, X rays, electrons, β rays, and slow neutrons in the case of the n - γ reaction produce damage by the same general mechanism, equivalent damage to the materials might be anticipated for the same energy deposition. Fast neutrons, protons, α rays, fission products, and slow neutrons in both the n - p and the n - α reactions produce damage by other mechanisms, and hence a different damage vs. energy relationship might be expected.

The difference in damage to water by X rays and electrons and to water by α rays has received considerable attention.² A considerably higher concentration of hydrogen and hydrogen peroxide has been formed with α rays than with X rays or electrons. Many different mechanisms of reactions have been postulated to account for this phenomenon. It has also been found (see Table 1) that, on an equivalent energy basis, irradiation of borated water by a pile flux of fast neutrons, slow neutrons, and γ rays produced considerably more hydrogen than irradiation of nonborated water by the same pile flux.

Despite the difference in results obtained by irradiating water either directly or indirectly with α rays from the results obtained by irradiation of water with X rays and electrons, an analytical survey of a large variety of experimental data reveals that γ rays, electrons, and combined pile radiation on an equivalent energy basis do produce equivalent damage to materials such as organics, even though damage is produced by different mechanisms.

Certainly, for covalent materials such as organics, the generalization that equivalent damage is produced for equivalent energy absorption is a good rule of thumb, and for data examined to date for these materials, this rule has been found to be good within a factor of 2. For those cases where pile fluxes are most accurately known; this rule has been found to apply even closer than within a factor of 2.

Recent unpublished and preliminary results on the effects of radiation on organic materials containing boron indicate that the gross damage occurring for γ irradiation and for pile irradiation is equivalent—within a factor of 2—for equivalent energy absorption, although a more quantitative analysis of the products of each irradiation seems to indicate that there is a difference in their composition.

2 CALCULATION OF RADIATION ENERGY ABSORPTION

To relate radiation damage to energy deposition or absorption, a definition of an absorbed dose of ionizing radiation is needed. This need has been satisfied by the recommendation of the International Commission on Radiological Units at the Seventh International Congress of Radiology, Copenhagen, Denmark, July, 1953.³ This Commission recommended that the absorbed dose of any ionizing radiation be defined as the amount of energy imparted to matter by ionizing particles per unit mass of irradiated material at the place of interest, and this dose should be expressed in rads. The rad is the unit of an absorbed dose and is equivalent to 100 ergs per gram of material.

Since it is frequently easier to measure the absorption of ionizing energy in air rather than in the material actually being irradiated, a general relationship between roentgen and rad is very convenient. Therefore, although it is not strictly valid, 1 rad can be considered as being roughly equivalent to 1.2 roentgens.

Accurate calculations of the 95 to 98 per cent energy transferred to a medium from radiative particles through the mechanism of electron excitation and ionization can be made only with considerable difficulty, but approximately calculations of this energy transfer can usually be readily made. It is nearly impossible, even with involved mathematical equations, to make either very accurate or approximate calculations of the 2 to 5 per cent energy transferred from neutralized heavy particles to a medium through the mechanism of loss in momentum. Since covalent materials such as the organics are highly susceptible to molecular electron excitation and ionization, and since radiative particles lose most of their energy in this manner, methods for approximate calculations of this type of absorbing energy for these materials are of considerable importance. Listed below are methods for making

* Superscript numbers refer to References at end of subsection.

approximate calculations of the energy absorbed by a material from each of the principal components of a normal pile radiation, namely, fast neutrons, γ 's, and thermal neutrons.

2.1 Absorption Energy from Fast Neutrons

The amount of energy E_o absorbed per gram of an organic material from a fast-neutron dosage ϕ_n with an average neutron energy E_n is

$$E_o = \phi_n \frac{\Sigma_s}{\rho} \frac{1}{2} E_n$$

where ρ is the density of material, $\frac{1}{2}$ is the fraction of the initial energy of the neutron transferred to the hydrogen* atom per collision, and Σ_s is the macroscopic scattering cross section of hydrogen in the material being considered; Σ_s is equal to $\sigma_s N_H$ where σ_s is the microscopic scattering cross section for hydrogen, and N_H is equal to the number of hydrogen atoms per cubic centimeter of material. To determine more exactly, but still not rigorously, the total energy absorbed from a fast-neutron dosage, the energies absorbed from neutrons over each small incremental energy range would have to be calculated, using the dose and scattering cross section corresponding to each energy range. These energies would then need to be summed to obtain the total energy E_o^{total} . On the basis that 0.01-Mev neutrons are the lowest energetic neutrons above thermal that contribute any appreciable energy to the medium through the scattering process, the total energy absorbed would be

$$E_o^{\text{total}} = \sum_{0.01}^{8.0} E_o^{0.01-1.0} + E_o^{1.0-1.5} + E_o^{1.5-2.0} + \dots$$

where

$$E_o^{0.01-1.0} = \phi_n^{0.01-1.0} \sigma_s^{0.01-1.0} \frac{N_H}{\rho} \frac{1}{2} E_n^{0.01-1.0}$$

2.2 Absorption Energy from γ Radiation

The energy absorption from a γ photon dosage ϕ_γ can be approximated by the following equation:

$$E_o^\gamma = \phi_\gamma \mu_\gamma E_\gamma$$

where E_o^γ is the energy absorbed per gram of material from γ radiation and E_γ is the average energy of the γ photons. The term μ_γ is the energy absorption coefficient (in square centimeters per gram) of the material for γ radiation of energy E_γ , and it is the fraction of energy dissipated by a narrow beam of γ rays in traversing an absorber. It is obtained by multiplying the probability of each interaction process by the probable fraction of the photon energy actually dissipated in the absorber as a result of the process.

The energy-absorption coefficients of various materials are given as μ_a/ρ in Table 2 of Sec. 7-3. In many cases where the μ_γ value for a particular material being considered cannot be found, the μ_γ value for an analogous material can be readily substituted. The value for water can generally be used for ordinary organic materials.

2.3 Absorption Energy from Thermal Neutrons

For the $H(n,\gamma)D$ reaction, which is the main source of energy deposition in organics by thermal neutrons, the energy absorbed per gram can be crudely approximated by the following equation:

* The deposition of energy in an ordinary organic compound by fast neutrons and thermal neutrons is due primarily to its hydrogen content, since hydrogen has a much larger scattering and absorption cross section than carbon.

$$\begin{aligned}
 E_a^{\text{th.n.}} &= \phi_n \frac{\Sigma_a}{\rho \mu_\gamma} \mu_\gamma E_\gamma \\
 &= \phi_n \frac{\Sigma_a}{\rho} E_\gamma
 \end{aligned}$$

where ϕ_n is the thermal-neutron dose, ρ is the density of the material, E_γ is the average energy of the photons generated by the n - γ reaction, and Σ_a is the macroscopic absorption cross section of hydrogen in the material being considered; Σ_a is equal to $\sigma_a N_H$, where σ_a is the microscopic absorption cross section for hydrogen and N_H is the number of hydrogen atoms per cubic centimeter.

2.4 Average Energy in Breaking a Bond

The average energy required to break a chemical bond is approximately 25 ev, and the average energy difference between successive electronic levels is about 5 ev. It is obvious that the Mev energies possessed by ordinary pile fast neutrons and γ photons constitute large sources of energy that can be transferred via secondary processes and cause extensive electronic excitation and ionization in a chemical compound. Although the average energy of a thermal neutron at normal temperatures is 0.025 ev and is insufficient to cause electronic excitation or ionization, the capture of these low-energy neutrons by matrix nuclei results in secondary radiation from n - γ , n - p , and n - α reactions which involves energy in the Mev range.

Two different methods have been frequently used in the past to relate the rate of reaction of liquids and gases as a function of the irradiation energy involved. In gases, the ion-pair yield has been used as a reaction rate measure, the energy required to produce an ion pair varying in different gases from approximately 28 to 38 ev. This energy range is approximately 18 to 22 ev greater than the ionization potential range of the gases, and this difference represents the energy necessary for the formation of electronically excited states.

In liquids, since it is difficult to measure the number of ions produced by radiation, it has been frequently customary to determine the rate of reaction by the amount of material reacting for a given energy input. The term G has been used for this purpose, and it is defined as the number of molecules reacting per 100 ev of energy absorbed. For general covalent materials, it is useful to remember that the normal value of G is approximately 4.

In this article, the changes in physical and chemical properties of the various materials listed have been related to the amount of energy absorbed per gram weight of irradiated material.

3 CALCULATION OF RADIATION DAMAGE

3.1 Radiation Damage to Water, Aqueous Solutions, and Fused Salts

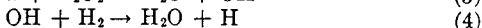
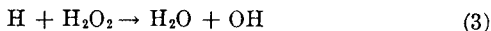
Excellent reviews of the effects of radiation on water and aqueous solutions and many other materials have been written. These reviews have appeared under the general title of Radiation Chemistry in the "Annual Reviews of Physical Chemistry" from 1950 through 1954⁴ and in the same "Annual Review" for 1955 under the title of Radiation and Hot Atom Chemistry. These reviews are concerned with the fundamental aspects of the effects of radiation on various materials.

The general mechanism of the effects of radiation on water has received rather exhaustive treatment in these reviews. It is generally agreed that the decomposition of pure water proceeds to a limited extent and then comes to a standstill because of the back reaction. The main initial decomposition reactions of irradiation are



Although the H_2O_2 formed decomposes to oxygen in a secondary reaction, the back

reaction involving the combination of the reaction products to re-form water can be formulated as follows:



The decomposition of irradiated aqueous solutions proceeds according to Eqs. (1) and (2), but the presence of solutes protects the initial decomposition products by destroying the free radicals by oxidation-reduction reactions. Thus, hydrogen can evolve and the hydrogen peroxide can decompose. Since solute molecules vary considerably in specificity of reaction, appreciable differences in results can be obtained when various aqueous solutions are irradiated.

The data in Table 1 are concerned primarily with the engineering aspects of the radiation damage to water, aqueous solutions, and fused salts. As can be seen from this table, the reaction of water with pile radiation is reversible, and relatively low equilibrium pressures are obtained. However, when borated water is irradiated, an irreversible reaction occurs and the gas evolution is a linear function of the combined energy absorption from neutron scattering and neutron capture minus the γ -energy absorption. In other words, the γ -energy absorption appears to favor the back reaction, whereas the energy absorbed from neutron scattering and the n - α reaction with boron appears to favor the forward reaction.

Even without the presence of boron, antifreeze solutions will tend to decompose extensively under radiation; the presence of boron simply accelerates this effect. As would be expected from the mechanism of reaction, fused salts are not detectably affected by the pile radiation. In the liquid state, they are not even affected by that portion of the fast-neutron energy (2 to 5 per cent) deposited in the liquid by momentum losses, since the ions are then in a less ordered state than they would be in the solid form.

A fairly extensive review of the unclassified data available on the decomposition of water by radiation has been made.⁵ This review is divided into four main parts: (1) General Considerations—an approximate picture of the gross process of radiation-induced decomposition of water, (2) The Mechanism—the role of ionization and the principal chemical reactions involved, (3) Major Factors—the major variables and their effects upon decomposition, and (4) Practical Considerations—general observations on decomposition that are of interest to the reactor designer, general rules for minimizing decomposition, and specific decomposition data obtained from in-reactor experiments and from full-sized reactors are presented.

Four major conclusions have been made in this review:

1. "Under the average neutron-gamma flux levels existing in cooling water or moderating water of present reactors, both the instantaneous decomposition rates and the maximum concentrations of decomposition products are very close to zero for initially gas-free, relatively pure water." Relatively pure water is defined in Monson's review in a very approximate manner as having a minimum specific resistance of 200,000 ohm-cm and a maximum gas content of 0.1 ml/liter.

2. "In general, increased temperature results in reduced decomposition rates and equilibrium concentrations of decomposition products." Above 300°F, the recombination rate is high and essentially independent of temperature.

3. "In general, the presence of ionic impurities results in increased decomposition rates and equilibrium concentrations of decomposition products, some impurities producing slight increases and others producing very large increases." At low temperatures, solutions of some ionic impurities such as KBr, KI, and CuSO_4 may produce partial pressures of 1,500 psi under radiation conditions that produce only a partial pressure of less than 10 psi for relatively pure water. At high temperature, i.e., above 400°F, exploratory work has shown that certain impurities strongly catalyze the backward reaction. Such impurities are copper, rhodium, palladium, platinum, silver, and iodine; and tin, iron, and titanium to a lesser extent.

4. "At low temperature, decomposition is so repressed by excess hydrogen that virtually no decomposition occurs at average neutron and gamma irradiation levels

Table 1. Radiation Damage to Water, Aqueous Solutions, and Fused Salts

No.	Class of material	Specific material tested	Temperature of irradiation, °F	Irradiation source ^a	Type of reaction ^b	Gas evolution, ml/ml (STP)	Dosage, 10 ⁹ rads	Particle dosages each equivalent to 10 ⁹ rads				Container	Remarks
								Thermal ^c neutrons, 10 ¹⁹ neutrons/cm ²	Fast ^d neutrons, 10 ¹⁷ neutrons/cm ²	Gamma energy			
										Photons ^e , 10 ¹⁸ γ/cm ²	Roentgens, 10 ⁹ r		
1	Water	Demineralized	220-250	WR	Rev., equil. pressure: 1.27 psi H ₂	None	20	3.37	2.78	2.01	1.06	Al, series 300 Stainless steel	Terminated ad libitum. Equilibrium should continue with increasing dosage.
2		Distilled	220-250	WR	Rev., equil. pressure: 0.25 psi O ₂	None	30	3.37	2.78	2.01	1.06	Al, series 300 Stainless steel	Same as above
3	Antifreeze solutions	60% Prestone in 4% H ₂ BO ₃ water solution	200-220	GR	Irrev. pressure: 6 psi H ₂	Not measured	0.0002	0.016	2.92	2.03	1.06	Al	No change in freezing point (-80 to -85°F)
4		60% Prestone in 4% H ₂ BO ₃ water solution	220-275	GR	Irrev. pressure: 2 psi O ₂	Not measured	0.2	0.016	2.92	2.03	1.06	Al	Completely carbonized; solid and black
5	Aqueous acid solutions	0.095% boron ^f	220	WR	Irrev.	0.30 ^g	0.011	0.059	2.78	2.02	1.06	Al, series 300 Stainless steel	The system was operated at pressures up to 60 psi. No indication of equilibrium conditions was observed
6		1.90% boron ^f	220	WR	Irrev.	1.98 ^g	0.040	0.0032	2.84	2.02	1.06	Al, series 300 Stainless steel	Same as above
7		Ortho-phosphoric	77-330	VG	Irrev.	Extensive	1.8	4.18 ^h	0.72	2.16	1.13	Series 300 Stainless steel	Extensive decomposition, darkening, and heavy frothing
8	Fused salts	Sodium hydroxide	1300	GR	Rev.	Not detected (<1%)	.22	0.62	10.2	2.22	1.17	Ni	No evidence of damage. No change in freezing point, determined in situ.
9		Sodium hydroxide	1800	VG	Rev.	Not detected (<1%)	20	0.62	10.2	2.22	1.17	Ni	No pressure was detected. Same as above

^a WR—water reactor, GR—graphite reactor, VG—van de Graaff—2-Mev electrons.

^b Rev.—reversible, Irrev.—irreversible.

^c Thermal-neutron dosage equivalents calculations based on geometric configuration of a 1.25-cm radius cylinder.

^d Fast neutrons ≥ 1.0 Mev.

^e Gamma photon average energy—1.0 Mev.

^f USP boric acid in demineralized water.

^g A series of tests using concentrations of 0.095, 0.59, 0.94, and 1.90 per cent boron was run. The gas evolution was found to be a linear function of the rad dosage calculated as $E_n - E_\gamma$ where

E_n is the combined energy absorption from neutron moderation and the neutron- α reaction with boron and E_γ is the γ energy absorption.

^h This dosage includes not only the energy absorbed from the H(n, γ)D reaction but that absorbed from the P(n, β)S. The energy from the P(n, β)S reaction was calculated from average disintegrations per second with a build-up of five half-lives.

in present reactors if hydrogen equivalent to 5 to 10 psi partial pressure is initially dissolved (and maintained) in otherwise relatively pure water." The same statement is essentially true for water used at high temperature.

In general, the reactor designer should consider the following steps in attempting to minimize water decomposition: (1) Initially remove all the oxygen economically feasible, and dissolve a small amount of hydrogen in the water before subjecting it to irradiation; (2) maintain a partial pressure of a few pounds per square inch of hydrogen (or deuterium for heavy water) in the system; and (3) maintain the water relatively pure (10^6 ohm-cm or higher) by installation of a bypass, mixed-bed, ion-exchange system.

3.2 Radiation Damage to Organic Fluids

In a nuclear power plant, organic liquids, in general, can be used in many different ways, such as for greases, lubricants, coolants or heat-transfer media, moderating materials, and allied usages. Two of the most striking effects occurring in an organic liquid as the result of exposure to radiation are gas evolution and changes in viscosity. The viscosity usually increases upon continual exposure to radiation until the liquid has polymerized into a solid form.

Several broad generalizations can be made regarding the effect of radiation on organic fluids. The gas evolution is not dependent upon the dosage rate, but it is a linear function of the total dose of energy applied. The per cent viscosity increase is also a function of the radiation dosage rather than the dosage rate, and a marked threshold of reaction appears to exist. The viscosity gradually increases initially with radiation dosage until a definite amount of radiation has been absorbed; at this point there is an exponential increase in viscosity with small incremental amounts of radiation energy. Generally, there is considerable difference between the behavior of aromatic compounds and other organic compounds under radiation. Aromatics are far more resistant to radiation damage than aliphatics, the radiative energy absorbed presumably being taken up primarily by excitation of the shielded system of π electrons in the aromatic nucleus.*

In a more definitive manner, the difference in susceptibility of various aromatic structures to radiation damage can be considered and explained on the basis of their ability to assume several different electronic configurations, that is, on their ability to resonate. The higher the resonance energy of the aromatic structure, the more resistant it should be to radiation. The resonance energy of a compound being defined as the difference between the experimentally determined energy of formation and the calculated energy of formation as determined by adding up the individual bond energies, the following values in terms of kilocalories per mole are obtained in order of decreasing resonance energy for various organic materials: anthracene, 105; naphthalene, 75; quinoline, 69; stilbene, 54; indole, 54; diphenyl, 47; styrene, 46; pyridine, 43; and benzene, 39. The values given for diphenyl, styrene, and stilbene include 8, 7, and 15 kcal/mole of resonance energy, respectively, in addition to the 39 kcal/mole for the benzene ring. The experimental radiation-damage data obtained to date on various homologues of benzene, naphthalene, and diphenyl are in good general agreement with the rule that "the higher the resonance energy of the aromatic structure being tested, the greater the resistance to radiation damage." This is a good general rule to remember in predicting the effects of radiation on a new aromatic-type material, and this rule should be of assistance in synthesizing or developing a new material to meet certain radiation-resistant requirements.

By using the general law that equivalent damage to organic materials is obtained for equivalent energy absorption, the engineer can utilize the experimental data presented in Table 2 (also Tables 3 and 4) to estimate the radiation stability of a given material under any mixed pile flux. For example, the life of a material such as

* If the symbol sigma (σ) is used to represent the pair of electrons that goes to make up the single bond between the carbon-to-carbon atoms and the carbon-to-hydrogen atoms of an aromatic nucleus, then pi (π) can be arbitrarily used to represent the pair of electrons that goes to make up the second bond between the carbon to carbon atoms. However, each pair of these pi (π) electrons should be considered as being distributed over the entire aromatic ring structure and should not be considered as belonging to any particular carbon-to-carbon atoms.